

See discussions, stats, and author profiles for this publication at: <https://www.researchgate.net/publication/382141695>

# Unraveling the Degradation Mechanisms of Lithium-Ion Batteries

Article in *Energies* · July 2024

DOI: 10.3390/en17143372

CITATIONS

2

READS

285

10 authors, including:



**Carlos Antônio Rufino Júnior**  
Technische Hochschule Ingolstadt

32 PUBLICATIONS 149 CITATIONS

SEE PROFILE



**Eleonora Riva Sanseverino**  
University of Palermo

401 PUBLICATIONS 6,712 CITATIONS

SEE PROFILE



**Pierluigi Gallo**  
University of Palermo

99 PUBLICATIONS 1,402 CITATIONS

SEE PROFILE



**Murilo Amaral**  
State University of Campinas (UNICAMP)

8 PUBLICATIONS 131 CITATIONS

SEE PROFILE

# Unraveling the Degradation Mechanisms of Lithium-Ion Batteries

Carlos Antônio Rufino Júnior <sup>1,2,3</sup>, Eleonora Riva Sanseverino <sup>4</sup>, Pierluigi Gallo <sup>4,5</sup>, Murilo Machado Amaral <sup>1</sup>, Daniel Koch <sup>3</sup>, Yash Kotak <sup>3</sup>, Sergej Diel <sup>3</sup>, Gero Walter <sup>3</sup>, Hans-Georg Schweiger <sup>3</sup> and Hudson Zanin <sup>2,\*</sup>

- <sup>1</sup> School of Electrical and Computer Engineering, University of Campinas (UNICAMP), Campinas 13083-852, Brazil; carlos.rufino@carissma.eu (C.A.R.J.); m228835@dac.unicamp.br (M.M.A.)  
<sup>2</sup> Interinstitutional Graduate Program in Bioenergy (USP/UNICAMP/UNESP), 330 Cora Coralina Street, Cidade Universitária, Campinas 13083-896, Brazil  
<sup>3</sup> CARISSMA Institute of Electric, Connected and Secure Mobility (C-ECOS), Technische Hochschule Ingolstadt, 85049 Ingolstadt, Germany; daniel.koch@carissma.eu (D.K.); yash.kotak@carissma.eu (Y.K.); sergej.diel@thi.de (S.D.); gero.walter@carissma.eu (G.W.); hans-georg.schweiger@thi.de (H.-G.S.)  
<sup>4</sup> Engineering Department, University of Palermo (UNIPA), 90128 Palermo, Italy; eleonora.rivasanseverino@community.unipa.it (E.R.S.); pierluigi.gallo@unipa.it (P.G.)  
<sup>5</sup> Consorzio Nazionale Interuniversitario per le Telecomunicazioni (CNIT), 43124 Parma, Italy  
\* Correspondence: hzanin@unicamp.br

**Abstract:** Lithium-Ion Batteries (LIBs) usually present several degradation processes, which include their complex Solid-Electrolyte Interphase (SEI) formation process, which can result in mechanical, thermal, and chemical failures. The SEI layer is a protective layer that forms on the anode surface. The SEI layer allows the movement of lithium ions while blocking electrons, which is necessary to prevent short circuits in the battery and ensure safe operation. However, the SEI formation mechanisms reduce battery capacity and power as they consume electrolyte species, resulting in irreversible material loss. Furthermore, it is important to understand the degradation reactions of the LIBs used in Electric Vehicles (EVs), aiming to establish the battery lifespan, predict and minimise material losses, and establish an adequate time for replacement. Moreover, LIBs applied in EVs suffer from two main categories of degradation, which are, specifically, calendar degradation and cycling degradation. There are several studies about battery degradation available in the literature, including different degradation phenomena, but the degradation mechanisms of large-format LIBs have rarely been investigated. Therefore, this review aims to present a systematic review of the existing literature about LIB degradation, providing insight into the complex parameters that affect battery degradation mechanisms. Furthermore, this review has investigated the influence of time, C-rate, depth of discharge, working voltage window, thermal and mechanical stresses, and side reactions in the degradation of LIBs.

**Keywords:** lithium-ion batteries; electric vehicles' batteries; degradation; ageing; failure

**Citation:** Rufino Júnior, C.A.; Sanseverino, E.R.; Gallo, P.; Amaral, M.M.; Koch, D.; Kotak, Y.; Diel, S.; Walter, G.; Schweiger, H.-G.; Zanin, H. Unraveling the Degradation Mechanisms of Lithium-Ion Batteries. *Energies* **2024**, *17*, 3372. <https://doi.org/10.3390/en17143372>

Academic Editor: Massimo Guarnieri

Received: 22 February 2024  
Revised: 22 June 2024  
Accepted: 3 July 2024  
Published: 9 July 2024



**Copyright:** © 2024 by the authors. Licensee MDPI, Basel, Switzerland. This article is an open access article distributed under the terms and conditions of the Creative Commons Attribution (CC BY) license (<https://creativecommons.org/licenses/by/4.0/>).

## 1. Introduction

Global interest in reducing the consumption of fossil fuels as an energy source has led to a search for renewable energy sources. In this scenario, the development of Electric Vehicles (EVs), which can be supplied by batteries, is a major contribution. However, as most of the sustainable energy sources are intermittent, the available energy and user consumption present temporal gaps. Therefore, the design of energy storage systems to supply stationary applications, such as power grids, can contribute to the application of energy storage devices and overcome this drawback [1].

Furthermore, as EVs use energy storage devices (i.e., batteries) as their source, they are an interesting alternative to replace the usage of fossil fuels [2], as they present significant advantages, particularly the considerable decrease in carbon dioxide (CO<sub>2</sub>)

emissions, which is one of the main responsible gases that contribute to global warming [3]. Furthermore, quantitative assessments have indicated that the transportation sector accounts for approximately 24% of global CO<sub>2</sub> emissions, while road, rail, and off-road vehicles account for 75% of these emissions [4–7].

Several public policies have been proposed to decarbonise the transport sector, which includes Regulation 2019/631, created by the European Union Parliament on 17 April 2019, that established strict CO<sub>2</sub> emission regulations for light commercial automobiles from 2020 onwards. This regulatory policy requires CO<sub>2</sub> emissions from the transportation field to decrease to 15% in 2025 and 37.5% in 2030 compared to 2021 [7,8]. Globally, many governments have passed transportation CO<sub>2</sub> emission reduction laws [7,9–13]. Although EVs are an alternative to decarbonise the transport sector, several challenges still need to be overcome, such as the price of battery modules. Although battery module prices have fallen in recent years, it is estimated that battery modules make up approximately 2/3 of the total EV cost [7].

Regarding the battery systems applied to EVs, LIBs are the most used because of their advantages, including high specific energy, low self-discharge, extended lifespan, safety, and cost [14–17]. During the operation of EVs, the batteries suffer from various degradation mechanisms that depend on numerous factors (e.g., road conditions, driver behaviour, ambient temperature, and cabin temperature) [3]. These degradation mechanisms can reduce battery capacity and power, resulting in a shorter EV range, which may cause range anxiety in customers. Furthermore, accelerated battery degradation also reduces charging and discharging efficiency, increasing internal resistance and shortening the battery's lifetime [18].

A deeper understanding of the degradation processes of batteries will allow companies to determine the best time to replace EV batteries, optimise their design (i.e., maximise their efficiency), accelerate the product development cycle, and ensure battery safety for an adequate performance to operate EVs and other secondary applications. In this context, vehicle manufacturers expect to replace batteries when they reach 70 to 80% of the initial charge range [19]. This limit is still uncertain, and many studies have reported that batteries will be used below this limit. On the other hand, early battery replacement will be recommended if the battery's degradation mechanisms are not adequately mitigated [20].

In terms of economic aspects, it is possible to estimate and reduce the return on the investment, identify new ways to capture the value, and maximise the value captured during the operation of batteries based on the degradation mechanisms. These systems can extend battery life and establish a market for second-life batteries [21,22]. From a research perspective, it is possible to identify the factors that accelerate batteries' degradation, predict the moment of battery failure, identify new viable applications, and identify possible defects. Thus, it is possible to design new models and solutions to overcome the existing issues [20]. Automating battery disassembly and categorisation requires an in-depth understanding and accurate models of secondary-life battery degradation. Therefore, a clearer understanding of battery degradation will enable the development of technologies focused on reducing the time and cost associated with battery disassembly and sorting [23]. This method reduces or eliminates the need for exhaustive battery testing, thereby enhancing the overall efficacy of battery lifecycle management [24].

Moreover, predictive maintenance is also essential to ensure battery safety, and most battery manufacturers provide predictive maintenance services based on vehicle distance travelled and lifetime. However, this process has high costs, low efficiency, and is time-consuming. Therefore, understanding battery degradation is essential for the manufacturer to provide the maintenance service at the ideal moment, avoid unscheduled maintenance, and reduce costs and maintenance time. Hopefully, predictive maintenance can be optimised using machine-learning algorithms to define the optimal time to provide intelligent service based on previous maintenance history and battery operation data [25].

Battery degradation mechanisms are complex, and the understanding of them is not trivial once they are influenced by numerous factors. However, identifying the optimal

operating range of temperature, current, and potential for an Energy Storage System (ESS) is crucial for the diagnosing and prognosis of battery failures and for predicting and extending battery life. A systematic literature review is needed to understand battery behaviour in critical situations, predict failures and lifespan, and implement safety functions in the Battery Management System (BMS).

The non-linear characteristics of the Solid-Electrolyte Interphase (SEI), lithium coating, and active material loss hinder the comprehension, modelling, and management of battery degradation mechanisms. Numerous events coexist and impact one another, making the simulation of each degradation mechanism difficult. Therefore, more research is necessary to comprehend the battery deterioration mechanism in order to develop dependable novel monitoring and diagnostic technologies.

Usually, the degradation mechanisms are investigated in analyses carried out after batteries reach their lifespan, known as post-mortem analyses. In these analyses, aged cells are disassembled, and their components are carefully separated and individually analysed. The advantage of post-mortem analyses is that they enable the identification of the degradation effects in each cell's components. However, one of the main disadvantages is the need to carry out stress tests on the cell to evaluate the degradation mechanisms, making this analysis time-consuming and costly [26]. Beyond this point, post-cycling analyses have restrictions, as they cannot directly track structural changes during intermediate lithiation/delithiation processes, as well as heating conditions. In this scenario, a plausible alternative is to conduct *in situ/operando* techniques, which can provide information about the SEI layer formation, lithium dendrites formation, redox mechanism, parasitic reactions, and morphological and structural changes under operating conditions. However, *in situ* analyses can be challenging, as they require the design of specific spectro-electrochemical cells, as well as the *in situ* set-up [27].

Battery degradation comprises complex phenomena that need to be modelled and controlled by systems capable of keeping battery operation within operating limits, increasing battery life in EVs and other applications. Several reviews are available in the literature, such as the study conducted by Braithwaite et al. [28], which investigated the current collector's ageing mechanism for power reduction and increased battery impedance. Furthermore, the effects of active material loss in the irreversible capacity loss of LIBs have been investigated in a work conducted by Christensen and Newman [29]. Moreover, a study conducted by Vetter et al. [30] reviewed ageing mechanisms for LIBs, focusing on diagnosing battery degradation, and the authors offered prognoses, understanding the effects of cycling conditions on degradation, and understanding how the degradation mechanisms are interrelated.

Despite the studies available in the literature that have investigated battery degradation processes, certain issues still need to be clarified, such as the formation of the Cathode–Electrolyte Interface (CEI) layer. The CEI layer significantly influences the performance of LIBs, despite being less investigated than the SEI, formed on the anode–electrolyte interface, which significantly affects the storage and release of  $\text{Li}^+$  during the lithiation and delithiation processes. Therefore, this review aims to clarify the mechanisms of LIB degradation, focusing on comprehensively explaining how cycle and calendar effects affect degradation processes and how diagnosing and predicting these degradation mechanisms can contribute to battery safety and lifespan. Unlike most studies available in the literature, this work provides a systematic review of battery degradation mechanisms, the causes of battery failure, and ways to mitigate these effects.

In summary, this work presents the working principles of LIBs and their main degradation mechanisms simply and directly. Section 2 presents the motivation for this work. The goal of Section 3 is to answer the following questions: How do LIBs work? What are the main components of LIBs? Which LIB chemicals are most used in EVs? Which cell types are most used in EVs? What is the degradation behaviour of these cells? Furthermore, Section 3 aims to introduce the degradation of LIBs applied in EVs, including large-format cell degradation modes. Then, Section 4 presents the degradation mechanisms of

LIBs, Section 5 discusses the results found in the literature, and Section 6 presents the conclusions of this review article.

## 2. Diagnostic Methods

The volume of data derived from batteries has increased because of technological advancements, particularly in Internet of Things (IoT) and smart sensor systems. This information is vital for the enhanced monitoring of batteries in EVs, facilitating their remanufacturing, reuse, and recycling, and enhancing automated disassembly procedures. Additionally, it contributes to accurately estimating battery residual value, thereby informing strategic decisions regarding battery lifecycle management [24].

The digitalisation of batteries is crucial for conducting fault diagnoses, identifying fundamental causes, and facilitating the efficient collection, classification, and determination of environmental implications. It facilitates detailed digital characterisation, reducing the need for repeated and overlapping battery supply chain examinations and significantly optimising time and cost parameters. Recent research has shown significant advancements in the development of models to predict the State of Health (SOH) of batteries. These models can be categorised as electrochemical models, empirical models, equivalent circuit models, physical-based models, semi-empirical models, and data-driven models, and different classifications of models can be developed to predict battery parameters, as shown in Figure 1 [31–33].

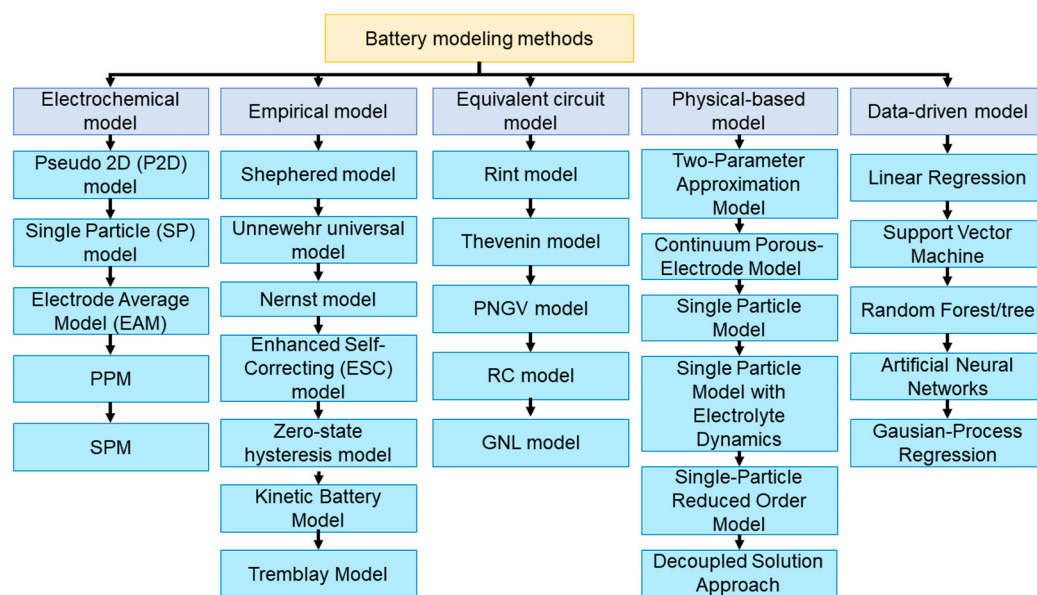


**Figure 1.** Battery classification models. Adapted from [33], under terms of CC-BY license.

### 2.1. Electrochemical Models

Electrochemical models are used to simulate the behaviour of cells, which are accurate once they are based on mathematical equations describing the chemical characteristics of the cell's materials. The main disadvantage of these models is the difficulty of describing mathematical equations. The chemical behaviour of cells and their degradation mechanisms are complex once many of these phenomena co-occur; they depend on numerous external factors and have non-linear characteristics. From a computational perspective, these complex mathematical equations require a high computational cost to be solved, which can take a long time to model and predict. From a practical point of view, this model usually requires cell disassembly and the exposure of its operator to high voltages, making the procedure too slow and challenging to be scalable [20,34].

Electrochemical models can be divided into three main categories: Pseudo Two-Dimensional (P2D) model, Single Particle (SP) model, and extended SP model [35]. The P2D

model utilizes the principles of porous electrode theory and lumped solution theory to accurately represent the terminal voltage of lithium-ion batteries [36]. This model describes battery reactions more comprehensively through complete order equations, and the main disadvantage is the iterative solution, which makes the model highly computationally expensive. The SP model simplifies some chemical reactions to reduce the computational cost of the model. To simplify the model, the electrode is depicted as a solitary spherical particle, and the electrolyte is assumed to possess a consistent lithium-ion concentration and potential. An additional approach to simplify the model involves minimizing the number of variables by focusing on the sparsity and configuration of the governing equations. Nevertheless, the SP model exhibits a diminished accuracy in comparison to the P2D model [36]. Finally, the extended SP model uses simplified electrochemical equations to approximate the solution using a mathematical method and find a balance between mathematical complexity and model accuracy.

The Electrode Average Model (EAM) battery model accurately estimates the average electrode voltage by integrating spatial information and atomic composition [37]. This model applies attention-based graph convolutional neural network methodologies, integrating chemical compositions and atomic coordinates in three-dimensional space. Consequently, it achieves a 17% enhancement in accuracy for predicting voltage compared to machine-learning models based on composition [37].

The EAM model directly gathers knowledge of the chemical interactions between electrodes and metal ions to predict their average voltage [37]. It may also include the predicted formation energy to enhance accuracy and enable transferability across various metal ions [37,38]. This advanced model is crucial for optimizing battery performance and exploring new electrode designs in the evolving field of battery technology.

The Polynomial Model (PPM) using porous electrodes is a significant advancement in battery modelling, especially for applications such as lithium-ion batteries (LIBs) [1]. Porous electrodes are essential in determining battery performance, and the PPM model provides a complete framework for understanding how battery performance is related to the intrinsic physical and chemical processes occurring inside these electrodes [39]. The PPM model enables the examination of several internal characteristics of the battery, including  $\text{Li}^+$  content, electrical potential, reaction rate distribution, overpotential, and impedance [3]. The PPM model utilizes thermal, mechanical, and aging models to mimic battery temperature and voltage distribution and anticipate degradation throughout operation [4]. When coupled with state observers, this model enables real-time monitoring of battery states for effective battery management systems [5].

The Single Particle Model (SPM) is a popular battery model in battery simulation [40,41]. It provides precise low current-level results with minimal computational effort [42]. SPM has been improved through the development of a Self-Correcting Single Particle Model (SC-SPM) using a Multipopulation Genetic Algorithm (MPGA) [42]. The SC-SPM has the ability to adjust measured values by taking into account changes in terminal voltage. This leads to more precise observations of the solid-phase diffusion process in batteries [43]. Furthermore, SPM has been experimentally identified for high-power  $\text{LiFePO}_4$  cells, showing its effectiveness in modelling battery behaviour under dynamic current profiles. SPM performance remains acceptable, even at high discharge peaks, outperforming other models such as the Equivalent Circuit Model (ECM). Table 1 compares the different electrochemical models for batteries.

**Table 1.** Comparison of various electrochemical battery models.

Model	Assumption	Advantages	Remarks
P2D model	<ul style="list-style-type: none"> <li>• Solid phase composed of multiple identical spherical particles.</li> <li>• Potentials and concentrations in the electrolyte phase vary in the x direction.</li> <li>• Diffusion considered in the radial direction (r).</li> </ul>	<ul style="list-style-type: none"> <li>• Describes the entire electrochemical process during battery operation.</li> <li>• Provides detailed battery dynamics over both space and time.</li> <li>• High accuracy in estimating the SOH of the battery.</li> </ul>	<ul style="list-style-type: none"> <li>• Requires a large number of parameters for accurate modeling.</li> <li>• Computationally intensive due to the model's complexity.</li> </ul>
Electrode Average Model (EAM)	<ul style="list-style-type: none"> <li>• Neglects concentration variations in the solid phase.</li> <li>• Considers only the concentration in the electrolyte phase.</li> <li>• Electrolyte phase concentration is directly correlated with the SOC of the battery.</li> </ul>	<ul style="list-style-type: none"> <li>• Very simple to set up with few parameters needed.</li> <li>• High accuracy in estimating the SOC of the battery.</li> </ul>	<ul style="list-style-type: none"> <li>• High error in voltage prediction due to excessive simplifications.</li> <li>• Significant loss of information regarding solid phase dynamics.</li> <li>• Parameter identification is challenging for real-time applications.</li> </ul>
Porous electrode with Polynomial Model (PPM)	<ul style="list-style-type: none"> <li>• Parabolic profile describes each spherical particle</li> <li>• Incorporates the parabolic approximation with the P2D model.</li> </ul>	<ul style="list-style-type: none"> <li>• Estimates the battery voltage at higher discharge rates (<math>\geq 1C</math>).</li> <li>• Voltage prediction error <math>\in 0.013\text{--}0.135\%</math> <math>\rightarrow</math> discharge rate = <math>2C</math>.</li> </ul>	<ul style="list-style-type: none"> <li>• Similar complexity to other porous electrode models.</li> <li>• Requires detailed knowledge of material properties and reaction kinetics.</li> </ul>
Single Particle Model (SPM)	<ul style="list-style-type: none"> <li>• Each electrode is represented by a single spherical particle.</li> <li>• Neglects concentration variations in the electrolyte phase.</li> <li>• PDEs of solid phase concentration are simplified to ODEs.</li> </ul>	<ul style="list-style-type: none"> <li>• Battery's voltage estimation accuracy is high at low discharge rates (<math>&lt; 1C</math>).</li> <li>• Voltage prediction error <math>\in 3.404\text{--}6.70\%</math> <math>\rightarrow</math> discharge rate = <math>1C</math>.</li> </ul>	<ul style="list-style-type: none"> <li>• Inaccurate at high discharge rates (<math>\geq 1C</math>).</li> <li>• Voltage prediction error ranges from 59.37% to 67.34% at a discharge rate of <math>2C</math>.</li> </ul>
SPM	<ul style="list-style-type: none"> <li>• Similar assumptions to the traditional SPM.</li> <li>• Considers concentration variations in the electrolyte phase.</li> </ul>	<ul style="list-style-type: none"> <li>• More accurate at high discharge rates.</li> <li>• Voltage prediction error <math>\in 19\text{ mV}</math> <math>\rightarrow</math> discharge rate = <math>5C</math>.</li> </ul>	<ul style="list-style-type: none"> <li>• More complex compared to the traditional SPM.</li> <li>• Involves additional parameters for electrolyte phase concentration.</li> </ul>

Note: SPM is widely recognized as the most dependable method for forecasting battery voltage. Therefore, significant research efforts are concentrated on improving the precision of the system by integrating degradation mechanisms and thermal dynamics in different charge/discharge scenarios, including mechanical stress. Source: Adapted from [44], under terms of CC-BY license. Copyright (2022), IEEE Xplore.

## 2.2. Empirical Models

Empirical models can be considered as a simplified electrochemical model and are constructed from direct measurements of battery observables [33]. Although empirical models do not require battery disassembly, their major drawback is performing cycle tests to measure the model's variables, which can be expensive and take a long time. Empirical models are built for a specific scenario, e.g., batteries employed in EVs and, consequently, they cannot be used to forecast battery ageing mechanisms in a different scenario, such as

the batteries used in a second application [45]. Empirical modelling techniques are mostly open-loop within the context of control theory, avoiding the feedback mechanisms that are essential to closed-loop systems. With this design, the computational cost is significantly reduced due to the simplification of the computational architecture [46].

The empirical models that are developed to estimate the SOC of batteries describe the SOC as a function of current through mathematical equations [33]. Table 2 shows the main empirical model equations that are used to predict battery SOC. In the equations shown in Table 2,  $y_k$  represents the terminal voltage,  $E_0$  represents the open circuit voltage when the battery is fully charged,  $R_i$  is the internal resistance,  $K_1$  is the polarization resistance,  $i_k$  is the instantaneous current,  $z_k$  is the battery charge state,  $dq/dt$  is the charge variation rate,  $k_f$  is the flow constant between the compartments,  $q_t$  is the total amount of charge,  $q_b$  is the available charge,  $k_r$  is the recharge constant, and  $V$  is the battery voltage.

**Table 2.** Comparison of empirical models applied to batteries.

Model Type	Assumptions	Advantages	Disadvantages	Limitations	Equations	Applications	Reference
Shepherd Model	Linearity under certain loading/unloading conditions	Simplicity of implementation, performs well on lead–acid batteries	Does not capture non-linear dynamics	Requires frequent calibration	$y_k = E_0 - R \cdot i_k - \frac{K_1}{z_k}$	SOC forecast, load capacity forecast	[47]
Unnewehr universal model	Empirical relationship based on charge/discharge profile	Versatile for different charging and discharging states	Moderate computational complexity	Less accurate for extreme charge/discharge rates	$y_k = E_0 - R \cdot i_k - K_1 \cdot z_k$	SOC forecast, SOH forecast	[48,49]
Nernst Model	Relationship between electro motive force and ion concentration	Accurate physicochemical model for SOC prediction	Requires detailed knowledge of electrochemical properties	Difficult to obtain accurate parameters for each battery	$y_k = E_0 - R \cdot i_k - K_2 \cdot \ln(z_k) + K_3 \cdot \ln(1 - z_k)$	SOC forecast, load capacity forecast	[50]
KiBaM (Kinetic Battery Model)	The model concept is derived from the kinetic model of charge and discharge	Considers the effect of discharge rate for lithium-ion	Complexity to define the parameters	Limitations in representing modern batteries	$\frac{dq}{dt} = k_f(q_t - q_b) - k_r \cdot q$	SOC forecast, load capacity forecast	[51]
Tremblay Model	Empirical dynamic response model, adjustable	Easy to implement for lithium-ion batteries	Variable accuracy for different types of batteries	Requires specific performance tests for calibration	$V = E_0 - R_i \cdot i_k$	SOC forecast, SOH forecast	[52–54]

Source: Adapted from [33], under terms of CC-BY license.

Researchers have enhanced conventional models to enhance their accuracy. When used in real-time applications, the Shepherd model experiences algebraic loops and simulation instability. To overcome this limitation, the model proposed in [48] replaces the internal resistance voltage with the polarization voltage term. Subsequently, a new method was proposed considering the OCV-SOC relationship and a polarization voltage term. Additionally, novel proposals were made to decrease the relative error to less than 0.5% in FTP72 cycles, with execution times ranging from 2.35  $\mu$ s to 4.35  $\mu$ s. Another way to improve the Nernst model is to add two constants,  $\tau_1$  and  $\tau_2$ , to increase the model's ability to describe the dynamic terminal voltage [33]. The main limitation of existing empirical methods is that they present limitations during the relaxation time because they do not consider the hysteresis effect of the battery voltage [33]. To overcome this limitation, the Nernst equation incorporates the term  $s \cdot M$  to account for the hysteresis effect, with  $M$

representing the correction factor that needs to be determined [55]. Furthermore, a more advanced self-correction model that takes into account voltage hysteresis is suggested in [56]. This model incorporates the gradual hysteresis voltage based on the SOC and the instantaneous hysteresis voltage that varies with the direction of the current. Table 3 shows the main equations of the modified traditional empirical models.

**Table 3.** Modified empirical models.

Model Equation	Reference
$y_k = E_0 - K \cdot \frac{Q}{Q - i_k \cdot T} + A \cdot e^{-B \cdot i_k \cdot T}$ <p><math>Q</math> represents the battery capacity, <math>A</math> represents the amplitude of the exponential zone, <math>B</math> represents the inverse of the time constant of the exponential zone, and <math>K</math> represents the polarization voltage.</p>	[53]
<p>Discharge: <math>y_k = E_0 - R \cdot i_k - K \cdot \frac{Q}{Q - i_k \cdot T} \cdot (i_k \cdot T + i^*) + A \cdot e^{-B \cdot i_k \cdot T}</math></p> <p>Charge: <math>y_k = E_0 - R \cdot i_k - K \cdot \frac{Q}{i_k \cdot T - 0.1 \cdot Q} \cdot i^* - K \cdot \frac{Q}{Q - i_k \cdot T} \cdot i_k \cdot T + A \cdot e^{-B \cdot i_k \cdot T}</math></p> <p><math>i^*</math> represents the current that has been filtered through the polarization resistance.</p>	[52]
$y_k = E_0 - R \cdot i_k - R_{pol} \cdot i_k^* - K \cdot Q \cdot \left( \frac{1}{z_k + z_0} - 1 \right) zA \cdot e^{-B \cdot (1-k)}$ $\tau \frac{di^*}{dt} + i^* = i$ $R_{pol} = \begin{cases} \frac{K}{z_k}, & \text{discharge} \\ \frac{K}{\lambda - z_k}, & \text{other conditions} \end{cases}$ <p><math>R_{pol}</math> is the filtered current through the polarization resistance.</p>	[57,58]
$y_k = E_0 - R \cdot i_k - K_2 \cdot \ln(\tau_1 + z_k) + K_3 \cdot \ln(\tau_2 + 1 - z_k)$ <p><math>\tau_1</math> and <math>\tau_2</math> are the two additional constants.</p>	[50]
$y_k = E_0 - R \cdot i_k - K_2 \cdot \ln(z_k) + K_3 \cdot \ln(1 - z_k) + s_k \cdot M$ $s_k = \begin{cases} 1 & i_k > \varepsilon \\ -1 & i_k < -\varepsilon \\ s_{k-1} &  i_k  \leq \varepsilon \end{cases}$ <p><math>\varepsilon</math> is a small positive number, <math>M</math> is the correction term.</p>	[55]
$y_k = OCV(z_k) + M_0 \cdot s_k + M \cdot h_k - R \cdot i_k$ $h_k = e^{\left( -\frac{ \eta \cdot t_{k-1} \cdot \gamma }{Q} \right)^T} \cdot h_{k-1} - \left( 1 - e^{\left( -\frac{ \eta \cdot t_{k-1} \cdot \gamma \cdot T}{Q} \right) \cdot \eta} \right) \cdot M \cdot \text{sign}(i_{k-1})$ $s_k = \begin{cases} \text{sign}(i_k) & i_k > 0 \\ s_{k-1} & \text{otherwise} \end{cases}$ <p><math>M</math> and <math>M_0</math> are the parameters estimated based on test data.</p>	[56,59]

Source: Adapted from [33], under terms of CC-BY license.

Semi-empirical models combine experimental data obtained from battery tests with aging mechanism analysis. Semi-empirical models have greater precision than empirical models. On the other hand, the computational cost of semi-empirical models is higher when compared to empirical models. Moreover, therefore, semi-empirical models are commonly used in offline applications [20,60].

The computational complexity can be observed by the implementation of sophisticated diagnostic methods, such as Electrochemical Impedance Spectroscopy (EIS). EIS is considered a non-invasive method for analysing a battery's increase in ohmic resistance. EIS provides detailed insights into the intrinsic electrochemical processes by employing alternating current perturbations across a range of frequencies and analysing the resulting impedance, making it an indispensable tool for real-time battery diagnostics [61]. This technique often identifies equivalent circuit model parameters that estimate battery states

such as internal impedance, Li-Ion diffusion dynamics, electrode contact impedance, SOC, and SOH [61]. Nevertheless, the majority of commercial BMSs do not currently gather EIS data directly on the vehicle because of the expensive nature of the required equipment. Furthermore, the outcomes are susceptible to fluctuations in temperature, and the examination is laborious. In addition, the results are subject to variations in temperature and the test is time-consuming [62]. Therefore, a methodology for modelling batteries to predict their Remaining Useful Life (RUL) is showed in Figure 2.

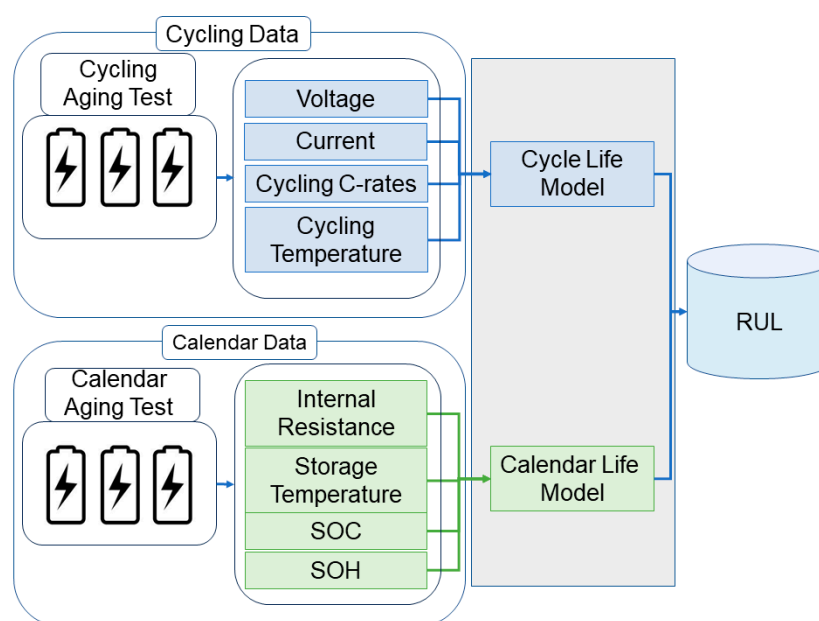


**Figure 2.** Example methodology for modelling batteries' RUL. Adapted from ref. [63] under terms of CC-BY license.

The most well-known empirical models are the ampere-hour counting method (also known as coulomb counting method) [64–72], and the event-driven ageing accumulation method. The ampere-hour method operates on the principle of determining the electric current's integral over time, which corresponds, in theory, to the change in a battery's SOC. Nonetheless, any inaccuracies in the current sensor or variations in the Coulombic Efficiency (CE), which consists of the ratio of ions extracted from the battery and the ions inserted into the battery during a complete discharge–charge cycle, can contribute to accumulated errors in estimating the SOC. In addition, the available battery capacity can fluctuate over time due to ageing, temperature, and discharge rate, which the ampere-hour method does not account for, compounding the estimation error. The ampere-hour method also has difficulties estimating the SOH in real applications with variable loads because the discharge cycles can be irregular, i.e., there are complete and incomplete cycles.

The use of high-precision sensors can substantially reduce the SOC estimation errors associated with the ampere-hour method to address these deficiencies. High-precision sensors provide a more precise reading of the electric current, reducing the possibility of errors in the integral calculation. The weighted ampere-hour method provides a sophisticated approach to estimating RUL. It considers the total charge/discharge, battery age, and temperature effects. Furthermore, high-precision sensors provide a more accurate estimation of the RUL by applying weighted factors to the current, considering the rate of battery deterioration and the impact of operating conditions, thereby reducing the errors inherent in the traditional ampere-hour method. This method improves the predictability of the remaining battery life, enhancing the dependability and efficacy of battery-dependent systems.

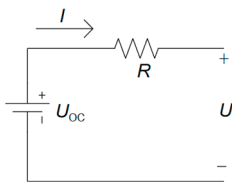
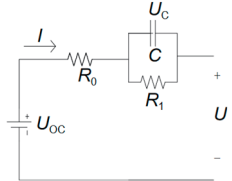
Incremental Capacitance Analysis (ICA) [73–75] and Differential Voltage Analysis (DVA) [76,77] consist of non-destructive techniques which provide accurate and reliable data on electrode degradation. These techniques can identify battery deterioration mechanisms with a high level of precision. Regarding ICA, it is an instrumental technique that converts voltage plateaus into observable charge differences to voltage. These differentials reveal the intercalation mechanisms that take place within biphasic regions under conditions that are comparable to those of potentiostats, which are frequently associated with phase transitions during charge/discharge processes. The singular characteristic of this configuration is the distinctive pattern of high and low points, which is used to identify electrode materials. In order to facilitate the examination of intercalation mechanisms and material modifications, this procedure is frequently executed at a low C-rate. Infrared thermography can enhance the accuracy of thermal models by verifying the calculated surface temperature of batteries, in addition to the use of ICA and DVA [61].

The Open-Circuit Voltage (OCV) methods have a very long measurement time and have margins of error. In the OCV method, the OCV curve of an LIB is obtained, and the SOC is estimated from the battery’s mathematical model. However, this method cannot be used in real-time and requires initial conditions that may not be known. Finally, the internal resistance method estimates the battery frequency response, aiming to establish its state; as this method usually requires generators and a separate testing period, it has a high cost and is challenging to implement.

### 2.3. Equivalent Circuit Model

Equivalent Circuit Models (ECM) are simple to comprehend and establish the SOH of the battery by initially defining changes in battery parameters using equivalent circuits that consist of capacitors, resistors, and voltage sources [23,33,78,79]. One of the key advantages of these models is the adaptability of the circuit design to a particular application. This circuit typically comprises a resistor that signifies self-discharge and a high-value capacitor or voltage source that indicates the battery’s OCV. The charge transfer and double-layer effect at the electrode, as well as the diffusion process in electrolytes and porous electrodes, are represented by the RC pairs with varying time constants. Table 4 shows the main equivalent circuit models:  $R_{int}$  model, resistance-capacitance model, Thevenin model, PNGV model, and second-order RC model, and discusses the main advantages and disadvantages of equivalent circuit models.

**Table 4.** Advantages and disadvantages of the best-known equivalent circuit models applied to batteries.

Battery Model	Equation	Features	Advantage	Drawbacks	Circuit Schematic
$R_{int}$	$U = U_{OC} - IR$	$U_{oc}$ is the open circuit voltage, $R$ is the internal ohmic resistance, $U$ is the terminal voltage, $I$ actual current.	Simple structure, Parameters easy to calculate.	Unable to describe the dynamic process, it will be fine when the current is too large. The temperature is relatively poor, which is particularly harmful to the battery.	
Thevenin	$U = U_{OC} - IR_0 - U_c$ $I = \frac{U_c}{R_1} + C \frac{dU_c}{dt}$	$R_1$ and $C$ are used to describe the polarization effect resistance and capacitance.	Takes into account the polarization of the battery effect on battery characteristics. Better simulation, in actual work.	Battery aging, temperature. Changes in the accuracy of the model have a greater impact.	

			Used more in engineering applications.	
PNGV	$U = U_{oc} - U_Q - U_c$ $U_Q = \frac{I}{C_Q}$	$- IR_0 U_Q$ is the equivalent capacitance.	It is easy for the model to consider the temperature degree of influence on the battery. Good applicability to different working conditions. Provides good accuracy.	
RC	$U = U_{oc} - IR_0 - \frac{U_{c1}}{R_1} + C_1 \frac{dU_{c1}}{dt} - U_{c2}$	$R_2$ and $C_2$ are rich, respectively. Differential impedance and concentration difference capacitance.	The level of computation is moderate. Enhanced accuracy, more closely resembling actual battery behaviour.	
GNL	$U = U_{oc} - U_Q - U_{c1} - U_{c2}$ $I_L R_0$	$R_s$ is self-discharge resistance.	Considering the effect of self-discharge, It considers the self-discharge effect and has high simulation accuracy.	

Source: Adapted from ref. [80], under terms of CC-BY license.

However, working conditions significantly affect these parameters, making them challenging to identify, limiting the method used to describe the batteries' dynamic and static characteristics [23,78,79].

### 2.4. Physical-Based Models

Physical model-based methods attempt to build a mathematical model that describes battery degradation behaviour. The application of this approach mostly depends on the influence on the battery's internal structure, considering the battery's ageing condition and degradation phenomena in detail. The decay mechanism model is mainly related to the chemical reaction, the formation of the SEI layer, and ion concentration [81–83].

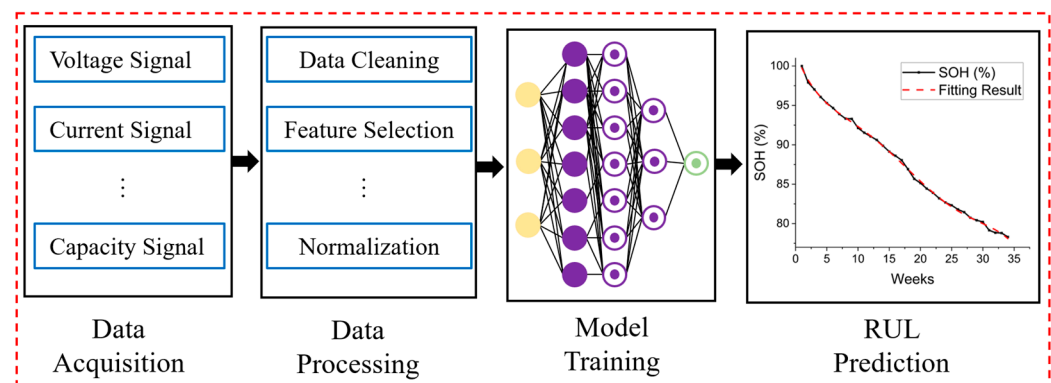
Physics-based approaches offer numerous benefits, including (i) the capacity for physical insights and contributing to a comprehensive understanding of the battery. Therefore, this method has good interpretability, facilitating the comprehension of the model's predictive behaviour. Another physics-based approach is (ii) good accuracy, including in scenarios beyond the operating region, with good extrapolation capability and transferability through chemistry. On the other hand, the high computational cost, over-parameterization, the need to identify several parameters, and the complexity of understanding the different degradation modes can limit the application of physics-based models in real applications [83]. Table 5 shows the trade-off between different the physics-based models applied to batteries.

**Table 5.** Comparison of physics-based models applied to batteries.

Model	Assumptions	Advantages	Disadvantages	Limitations	Application
Two-Parameter Approximation Model	Linear approximation of battery characteristics	Simplicity and ease of implementation	Does not capture complex dynamic characteristics	Requires frequent calibration	SOC and SOH forecast
Continuum Porous-Electrode Model	Continuous model for porous electrodes	Detailed physical approach	Computational complexity	Requires precise knowledge of system parameters	SOH forecast, remaining life forecast
Single Particle Model	Approximation of homogeneous electrodes	Good accuracy with less complexity	Limitations in modelling electrolyte diffusion	Not suitable for electrodes with significant non-homogeneity	SOH forecast, remaining life forecast
Single Particle Model with Electrolyte Dynamics	Includes electrolyte dynamics	Improved accuracy for predicting kinetics	Increased computational complexity	Assumptions about homogeneous electrode properties	Prediction of SOC, SOH, RUL
Single-Particle Reduced Order Model	Simplifying equations to reduce order	Good accuracy with lower computational cost	May not capture all dynamics	Requires adjustment to capture desired behaviour	SOC and SOH forecast
Decoupled Solution Approach	Separation of physical components for separate solution	More flexibility for different mechanisms	Simplified assumptions can impact the accuracy	Difficult to adapt to new systems with complex configurations	SOH forecast, RUL

### 2.5. Data-Driven Models

Data-based Models (DbMs) have become attractive due to the greater processing power of computers [62,84,85]. DbMs are increasingly being applied in the industry because they can reduce the design time, predict premature battery failures, and do not require the batteries to be disassembled to build these models. Furthermore, data from EIS [62,86] and OCV [87,88], among others, are employed to build models using pattern recognition and machine-learning techniques [17,20,86,89–91]. DbMs can be classified as empirical when parametric, i.e., built based on the battery's prior knowledge. On the other hand, DbMs can also be classified as non-empirical when built from real-time measurements, i.e., the model emits an output for each new sample measured [92]. Figure 3 shows a flowchart of data-driven models for batteries.

**Figure 3.** Flowchart of battery data-driven models.

The machine-learning algorithms that are widely used successfully in data-driven models include the time-series model [93,94], Artificial Neural Network (ANN) [95], Support Vector Machine (SVM) [96], and Gaussian Process Regression (GPR) [17].

### 2.5.1. Linear Regression

Time-series and linear-regression models map the non-linear relationships between resources and capacity or remaining battery life, and most relationships are non-linear, which makes non-linear mapping more popular. In battery studies, linear regression serves as a crucial tool for predicting critical parameters such as RUL and degradation over time. The basic mathematical model of linear regression can be expressed as shown in Equation (1):

$$y = m \cdot x + c, \quad (1)$$

where  $y$  is the dependent variable (e.g., the predicted RUL),  $x$  represents the independent variables (such as load cycles, voltage, and capacity),  $m$  is the vector of slope coefficients, and  $c$  is the intercept term. Applying techniques such as Singular Value Decomposition (SVD) can overcome problems related to singular solutions and obtain more robust models.

In the context of batteries, linear regression is not limited to linear relationships and can include quadratic or higher-order terms to capture non-linear behaviours. The simplicity and computational efficiency of linear regression allow for fast and accurate predictions in simple applications. However, this model type is limited to industrial applications with complex data.

### 2.5.2. Support Vector Machine

Support Vector Machines (SVMs) are powerful models for classification and regression, being very useful in analysing the performance of batteries for industrial applications. The SVM approach maps the input data to a high-dimensional space through a kernel function, such as the linear function or the Radial Basis Function (RBF), and finds the hyperplane that best separates different data classes, such as battery failure and health. The optimization problem can be described as shown in Equation (2):

$$\min_{w,b,\xi} \frac{1}{2} \|w\|^2 + C \sum_{i=1}^n \xi_i, \quad (2)$$

where  $w$  is the hyperplane weight vector,  $b$  is the bias,  $\xi_i$  are the slack variables for non-separable data, and  $C$  is the regularization parameter that controls the trade-off between maximizing the margin and minimizing the classification error.

SVM is efficient in processing large data sets and is able to deal with situations where there are multiple variables and classes. Compared to Artificial Neural Network (ANN) models, SVM has the advantage of being more interpretable, as it finds an explicit separation hyperplane. Furthermore, it tends to be more robust to overfitting, especially when the data set is relatively small, as the number of parameters to be adjusted is smaller.

On the other hand, the Relevance Vector Machine (RVM), an extension of the SVM, incorporates a probabilistic approach to the model. Instead of rigid margins, RVM provides a probabilistic rating prediction, which can be advantageous in industrial applications requiring a more detailed analysis of risk and uncertainty [97]. Compared to SVM, RVM can offer sparser and more efficient models, reducing prediction time [98,99].

### 2.5.3. Random Forest/Tree

The Random Forest method is widely used in machine-learning tasks for its ability to handle complex data and provide robust predictions. In the context of battery analysis, this method is often but not limited to predicting remaining battery life, SOC, and other parameters.

To effectively apply Random Forest to battery data, it is essential to understand the nature of the data and the variables involved. Data such as voltage, current, temperature, and charge/discharge cycles are often used.

Each tree is created from a random subset of the training data using the bootstrapping technique. The divisions within each tree are made using a random subset of the features, and the division criterion is chosen to maximize the reduction in variance. The tree prediction is made using an average of the predictions of all trees, as shown in Equation (3):

$$y = \frac{1}{T} \sum_{t=1}^T h_t(x), \quad (3)$$

where  $h_t(x)$  represents the prediction of tree  $t$  and  $T$  is the total number of trees.

Specifically for battery data, the Random Forest model can be trained to predict RUL based on observed patterns in charge and discharge cycles, changes in voltage, and other characteristics of the battery profile. The technique is robust against noise and outliers due to the aggregation process, which is essential for industrial environments, where data can be highly variable. Additionally, the importance of variables can be calculated by analysing the amount of reduction in variance provided by each variable across all trees, helping to identify which parameters are most critical to battery performance. Additionally, Random Forest can be combined with other techniques, such as dimensionality reduction and hyperparameter fine-tuning, to further improve model accuracy on battery data.

#### 2.5.4. Artificial Neural Networks (ANNs)

Artificial neural networks (ANNs) are widely used to predict the batteries' SOH and their RUL. The main types of artificial neural networks that are used are Modular Neural Networks (MNN), Feed-Forward Neural Networks (FFNN), Kohonen Self-Organizing Neural Networks (SONNs), RBF neural networks, HNNs, RNNs, LSTMs, etc.

ANNs are computational tools inspired by the form and function of the human brain and are made up of processing units known as artificial neurons. These units are arranged into three layers: input, hidden layer (or hidden layers in more complicated models), and output. In the context of battery performance prediction, the input layer receives and pre-processes essential operational data, such as voltage, current, temperature, and charge cycles, before sending it to the hidden layers.

This data is transformed and calculated non-linearly within the hidden layers, allowing the ANN to detect complicated patterns in variable relationships. Finally, the output layer generates forecasts such as Remaining Usable Life (RUL) and failure prediction. In the industrial setting, these properties make ANNs ideal for large-scale applications requiring real-time analysis of massive amounts of data.

In other words, neural networks learn the implicit rules of a pair of inputs and outputs during an offline training phase, forming a non-linear black box model to be utilized during the online operating phase. An appropriate ANN can differentiate between a battery system's normal and abnormal states. Despite strong self-learning from historical data, ANNs need huge historical data and have high training time, low generalization ability, and overfitting problems [97].

The first layer of the neural network involves pre-processing the data and filtering the data to reduce noise. Data preprocessing at the input layer is critical in eliminating noise and dealing with incomplete charge and discharge cycles. This preprocessing involves normalizing or standardizing the data to ensure all variables are on the same scale and to eliminate inconsistencies that could compromise the model's accuracy.

Each neuron is mathematically represented in the hidden layer by a weighted linear combination of inputs, followed by an activation function. Equation (4) describes the output calculation for a neuron:

$$z_j = f(\sum_i w_{ij}x_i + b_j), \quad (4)$$

where

- $z_j$  is the output of the neuron,
- $w_{ij}$  is the weight that connects the input  $x_i$  to neuron  $j$ ,
- $b_j$  is the bias associated with the neuron  $j$ , and
- $f$  is the activation function.

The output of the hidden layer is passed to the output layer, where the model makes predictions, such as on the battery's RUL. The final prediction calculation can be represented as described in Equation (5):

$$y = g(\sum_j w_{jo}z_j + b_o), \quad (5)$$

where

- $y$  is the final forecast, for example, the value of SOH or RUL,
- $w_{jo}$  are the weights that connect the hidden layer to the output layer,
- $b_o$  is the bias of the output layer, and
- $g$  is the final activation function.

However, more modern algorithms have been developed. Table 6 presents the main advantages, disadvantages, and limitations of the most well-known neural network algorithms.

**Table 6.** Comparison of machine-learning models applied to battery data analysis.

Model	Assumptions	Advantages	Disadvantages	Limitations
Multilayer Neural Network (MNN)	Battery data can be divided into sub-tasks	High efficiency for specific battery analysis tasks	High design complexity, requires specific training	Effective problem decomposition can be challenging for complex battery behaviour
FeedForward Neural Network (FFNN)	Battery data are static	Flexible, good for classification of battery faults	Prone to overfitting with limited battery data and black-box nature	Requires large battery data sets, challenging to interpret
SONNs	Battery data have meaningful clusters	Effective for clustering battery state-of-health data	Grid size determination can be difficult	Limited to clustering and visualization of battery data
RBF	Battery data are sensitive to local variances	Effective for capturing local variations in battery data	Sensitive to noisy battery data, requires radial centre tuning	Not scalable for high-dimensional battery data analysis
Hopfield Neural Network (HNN)	Symmetric weight matrix in battery data	Suitable for pattern recognition in battery diagnostics	Converges to local minima in training	Limited to small-scale pattern recognition in battery data
Recurrent Neural Network (RNN)	Battery data exhibit temporal dependencies	Effective for sequential battery data analysis	Gradient vanishing/expllosion, difficult training	Limited in capturing long-term dependencies in battery data
Long Short-Term Memory (LSTM)	Long-term dependence on battery data	Effective in retaining long-term dependencies in battery data	High computational complexity, prone to overfitting	Requires extensive training data, not easily interpretable

### 2.5.5. Gaussian-Process Regression

Gaussian Process Regression (GPR) is an advanced non-parametric machine-learning technique that effectively models the complex non-linear relationships observed in battery degradation profiles. GPR enables robust and accurate predictions by providing a probabilistic estimate of the uncertainty associated with predictions. This technique is particularly useful in industrial scenarios where accurate prediction of RUL and detection of failure patterns are critical.

Mathematically, GPR considers a multivariate Gaussian distribution over the data, defining a probabilistic distribution over functions parameterized by the mean and covariance matrix. Input data  $X$  and their respective outputs  $y$  are modelled as  $y \sim \mathcal{N}(\mu, K)$ , where  $\mu$  is the vector of means and  $K$  is the covariance matrix, defined by the chosen kernel. For a new data point  $x_*$ , the prediction is obtained using Equations (6) and (7):

$$\mu_* = K(x_*, X)^T K^{-1}y, \quad (6)$$

$$\sigma_*^2 = K(x_*, x_*) - K(x_*, X)^T K^{-1} K(x_*, X), \quad (7)$$

where  $K(x_*, X)$  represents the covariance between the new point and the training points, and  $K^{-1}$  is the inverse of the covariance matrix.

Compared to models such as Artificial Neural Networks (ANNs) and Support Vector Machines (SVMs), GPR takes a more explicit approach to estimating prediction uncertainty. While ANNs often require extensive tuning and SVMs are limited in quantifying uncertainty, GPR offers probabilistic predictions. However, its computational cost can be high due to the inversion of the covariance matrix, making it unsuitable for large data sets without optimizations. Thus, GPR is especially useful when quantifying uncertainty, which is useful in various battery scenarios.

### 2.6. Discussion on Battery Modelling

In the context of data-driven models applied to lithium-ion batteries, the models' fidelity, accuracy, and utility depend on factors such as data quality. Data quality is related to granularity, temporal resolution, noise level, and feature extraction and selection quality. Data granularity, which refers to the level of detail or resolution of measurements, is critical for capturing accurate information about battery performance. In scenarios where comparison between different cell designs is critical, the granularity needs to be high to identify slight variations in performance. Judicious feature extraction and selection are essential to distinguish nuances between different designs, while data filtering removes noise and provides a precise performance view [100–102].

On the other hand, for situations that require rapid identification of short-lived batteries, the granularity can be reduced to speed up data collection. However, feature extraction and selection must be more precise, as models must operate with limited data and quickly identify patterns that indicate possible failures [100–102].

The sampling period, or the interval between measurements, directly impacts the computational complexity and processing time of the models. For scenarios that require performance predictions, a broader and more varied sampling period is needed to adequately capture different cycling conditions. Filtering is critical to remove variability not indicative of the battery's long-term behaviour, while feature selection must be done to identify those that best represent degradation over time [100–102].

More complex forecasting models, such as those used to optimize charging protocols, require data granularity and adjusted sampling periods to capture both minute details and global trends. Data filtering is essential to ensure that only relevant information is used in the model, while feature extraction must identify parameters directly affecting loading efficiency [100–102].

When models need to be integrated into battery management systems (BMS), the data need to be highly granular and the sampling periods short, as it is necessary to capture the variability of usage conditions in real-time. Feature selection needs to focus on variables that directly indicate battery health, while data filtering must deal with significant noise [100–102].

Finally, the lack of historical data on battery reuse makes it essential to create models capable of identifying patterns from a few samples. In these cases, the granularity of the data can be moderate, but the selection of characteristics becomes critical, as it must focus on variables that can predict the future performance of the battery, even without available histories [100–102].

Extracting features from battery charge and discharge curves is the most common method used in battery management systems because these systems are developed to collect current and voltage data. However, new-generation BMS can obtain electrochemical impedance spectroscopy. Therefore, the new-generation BMSs can obtain impedance over a wide range of frequencies [103]. The challenge of methods that rely on EIS data characteristics is the identification of quantitative characteristics correlated with battery degradation [103].

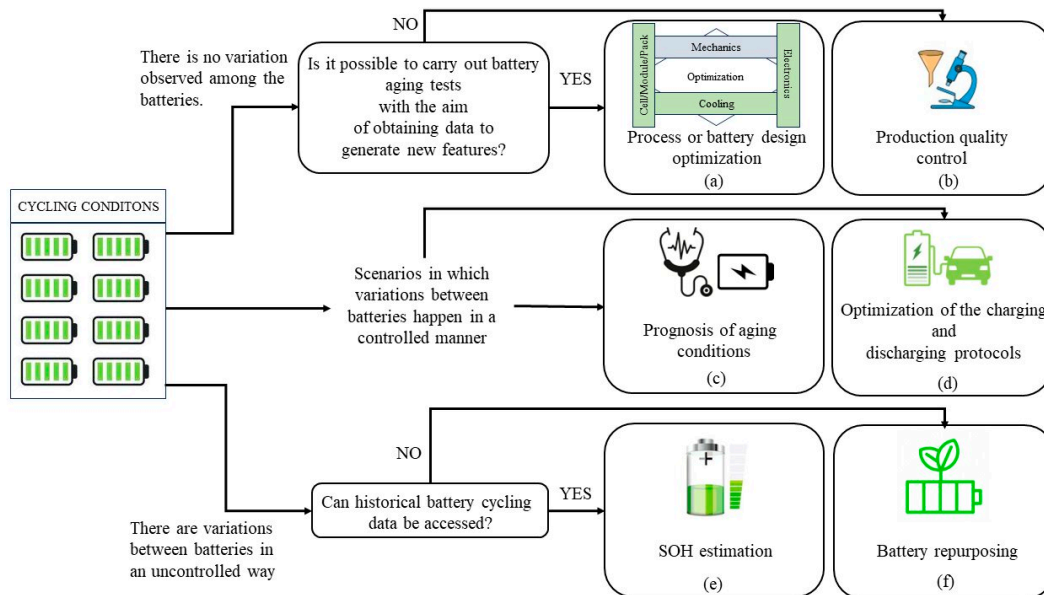
In all of these scenarios, data-driven models must be adapted to each use case's specific conditions, carefully considering data granularity, sampling period, filtering, and feature selection to maximize their accuracy and utility.

Table 7 presents some recent works published, the methods' main features and outputs, and the metrics used to evaluate the performance of the models [104].

As demonstrated in [105], features must be selected appropriately for each real use case. Inadequate feature selection can artificially inflate performance. It shows six use cases of machine-learning algorithms in batteries. Scenario (a) refers to optimizing battery design. In this scenario, the battery engineer must perform battery aging tests identically so that it is possible to compare the performance of cells designed differently. Scenario (b) refers to quality control. In scenario (b), quality control tests should be carried out with the lowest possible time and cost. In this scenario, it is desired to avoid cycling the batteries several times to prevent the data cycling process from impacting the aging of the batteries [105].

In a third scenario (see Figure 4, scenario c), the impact of usage conditions, including discharge depth and charging current, on battery life is determined by the use of machine-learning algorithms. In order to develop a prognostic model for this application, an experiment with systematically varied aging conditions is necessary. More intricate scenarios can be assessed in addition to these conditions to determine the optimal protocol parameters (refer to Figure 4, scenario d) [105].

Finally, data can be obtained from operating vehicles to estimate the batteries' health status and remaining life (see Figure 4, scenario e). Additionally, after batteries reach the end of their useful life in the vehicle, data from battery operation in vehicles can be used to predict the best scenario for reuse, repurposing, remanufacturing, or recycling (see Figure 4, scenario f) [105].



**Figure 4.** Possible scenarios for applying machine-learning algorithms to batteries. Source: Adapted with permission from ref. [105]. Copyright (2023), Elsevier.

Purely data-driven models have high accuracy but do not provide information about cycling conditions and battery aging mechanisms. As mentioned above, physics-based models are physically interpretable. However, defining the parameters of physics-based models is not trivial due to the complexity of battery aging mechanisms [106].

Therefore, models driven by interpretable data are an area of research that is still little explored. Interpretable data-driven models differ from so-called "black box" machine-learning models. Purely data-driven models offer little information about the underlying

relationships between inputs and outputs. On the other hand, interpretable data-driven models can provide clear metrics that directly reflect degradation mechanisms. This includes metrics such as capacity loss rate, internal resistance, and voltage variations, which infer the degradation progression [106].

Data-driven models become interpretable when they explicitly include characteristics that are directly related to the physical phenomena that govern the behaviour of batteries. For example, incorporating variables representing internal resistance, cell capacity, and degradation parameters allows models to provide insights into how operating conditions affect the lifespan and health of batteries [106].

This significantly contributes to battery design by enabling the optimization of components based on identified degradation patterns. Interpretable models can identify and correlate specific degradation patterns with operational parameters such as temperature and load cycles to predict RUL. This allows BMSs to have greater accuracy in estimating the remaining battery life under different usage conditions [106].

Additionally, the ability to interpret battery behaviour helps identify anomalies that may be indicative of imminent failures, improving safety. This also contributes to optimizing performance and reliability, as battery management can be adjusted based on battery health, reducing the risk of failure and improving efficiency [106].

Combining the interpretation provided by such models with physics-based electrochemical simulations and mechanistic models makes it possible to obtain a more holistic understanding of degradation phenomena. This helps predict battery life under different operating scenarios, improving the performance projections and reliability of lithium-ion batteries across a wide range of applications [106].

**Table 7.** Summary of recent work on machine learning for battery state predictions.

Reference	Method										Features						Metrics						
	Neural Network	Support-Vector Machine	Gaussian/Bayesian	Regression	Random Forest/Tree	Kalman Filter	Voltage	Current	Temperature	Cycle Number	Capacity	Power	Geometry	EIS	P2D Models Parameters	SOC	SOH	RUL	MAE [%]	MSE	RMSE [%]	R <sup>2</sup> [%]	Percentage Error
[17]				✓			✓	✓		✓	✓							✓					9.1
[107]	✓						✓		✓	✓	✓									~8 × 10 <sup>-4</sup>			6.4
[108]			✓				✓	✓		✓												97	8.7
[109]	✓							✓				✓											7
[110]	✓						✓	✓	✓		✓					✓			0.1				0.1
[111]	✓						✓	✓	✓							✓			1.1 <sup>a</sup>				2.4
[112]	✓						✓	✓	✓							✓				9.27 × 10 <sup>-7</sup>			1.3
[113]	✓	✓		✓	✓		✓											✓					3.3
[114]						✓	✓	✓	✓							✓							3
[115]	✓	✓	✓	✓			✓	✓	✓									✓			12.41		6.7
[116]	✓						✓	✓		✓							✓	✓			3.427 <sup>b</sup>		0.6
[117]			✓				✓	✓	✓							✓			0.55 <sup>c</sup>	0.28 <sup>d</sup>			0.8
[118]		✓					✓	✓	✓							✓					97		12.2
[119]	✓						✓	✓	✓							✓							3.8
[120]	✓						✓	✓		✓						✓			3 <sup>e</sup>				
[121]	✓						✓	✓								✓			5 <sup>f</sup>				1.7
[122]	✓						✓	✓	✓							✓							3
[123]	✓						✓		✓							✓			0.45 <sup>g</sup>	0.42 <sup>h</sup>			5
[124]	✓	✓					✓	✓		✓						✓					0.92		2.1

[125]	✓	✓	✓	✓	✓	✓	✓	✓	0.98 <sup>i</sup>	1.3 <sup>i</sup>	98 <sup>i</sup>	1.6	
[126]		✓		✓	✓	✓	✓	✓		4.86 <sup>j</sup>		3.2	
[127]	✓			✓		✓	✓	✓	✓			0.4 <sup>k</sup>	
[128]		✓		✓	✓	✓	✓	✓		3.93 <sup>l</sup>			
[129]			✓	✓	✓	✓		✓			0.0280 <sup>m</sup>	98.8 <sup>m</sup>	0.2
[130]	✓			✓	✓	✓		✓			0.0074 <sup>n</sup>	99.9 <sup>n</sup>	1.5
[131]	✓			✓	✓			✓					8
[132]	✓			✓	✓			✓	✓				3
[103]		✓						✓	✓		8.57	96 <sup>o</sup>	

<sup>a</sup> Mean Absolute Error (MAE) calculated for test cells at 25 °C. <sup>b</sup> Root-Mean-Squared Error (RMSE) calculated by using the Deep Neural Network (DNN). <sup>c</sup> MAE calculated for autoregressive recurrent GPR. <sup>d</sup> RMSE calculated for autoregressive recurrent GPR. <sup>e</sup> MAE calculated for of SOC estimation under ECE operation for the battery (400 aging cycles). <sup>f</sup> MAE calculated for first and seventh Federal Urban Driving Schedule (FUDS) cycle. <sup>g</sup> MAE calculated battery 5. <sup>h</sup> MSE calculated battery 5. <sup>i</sup> MAE, RMSE and R<sup>2</sup> values obtained for the model constructed differential voltage techniques using Differential Voltage (DV) curves and/or Incremental Capacity (IC) curves and the Support Vector Machine (SVM) algorithm. <sup>j</sup> End-of-Life (EoL), obtained for the model. <sup>k</sup> Absolute Error obtained for the model built with GP kernel pair Matérn 5/2 (Ma5) plus Matérn 3/2 (Ma3). <sup>l</sup> MSE computed with SVM for the UDDSHDV cycle under the 10-cycle constraint. <sup>m</sup> RMSE and R<sup>2</sup> values obtained for the Adaptive Model III (exponential). <sup>n</sup> RMSE and R<sup>2</sup> values obtained for the Adaptive Model III (exponential). <sup>o</sup> RMSE and R<sup>2</sup> values obtained for the battery cell 05 cycled at 25 °C. Source: Adapted with permission from ref. [104].

### 3. Motivation

To design more efficient, reliable, safe, and long-lasting batteries, it is fundamental to understand the mechanisms of battery degradation. Hopefully, researchers can develop new materials and technologies to mitigate these effects and enhance the performance of batteries, by analysing the causes of battery degradation. BMSs can monitor battery health in real time and adjust their operation accordingly in one method to enhance the next generation of batteries. For instance, if a battery exhibits degradation due to overcharging or high temperatures, a BMS can reduce the charge rate or decrease the operating temperature to prevent further degradation. In addition, the battery test matrix can be designed to be condensed based on the knowledge of degradation mechanisms to capture only the most essential data for validating the design parameters.

However, further investigation is needed in specific domains while the mechanisms of degradation in small cells are presently comprehended, such as the particular ageing behaviour of large cells compared to small cells. Moreover, the precise chemical and physical changes that result in electrode degradation are still not fully understood, and more research is needed to develop new materials and manufacturing techniques to mitigate this effect. Despite the studies reported in the literature, several degradation mechanisms have not yet been described clearly and comprehensively. Some concepts remain ambiguous in the literature, and an in-depth discussion is still needed. Therefore, the present systematic review revisits the main battery degradation mechanisms, avoiding ambiguity in the description of complex chemical phenomena, and, finally, we present ways to mitigate these problems in the future.

### 4. Basic Structure of LIBs

#### 4.1. General Overview of LIBs

As mentioned above, LIBs have a high energy density and low memory effect, and they are lightweight, which are benefits that have targeted LIBs as the best alternative for supplying EVs. The high energy density is critical because it enables the cell to reach a high capacity and store energy in the same cell volume. Furthermore, the low memory effect allows the cell to be recharged at any current charge level without significant loss of the maximum energy capacity [19].

The major components of LIBs comprise the positive and negative electrodes, electrolyte, current collector, separating membrane, and casing. The electrodes used in LIBs are usually fabricated by mixing binders (i.e., polymeric-based to “glue” particles) to connect materials among themselves and to the current collector [133]. The electrodes are assembled face-to-face and separated by a mesoporous membrane (i.e., separator), and the electrodes are soaked in electrolytes. Under polarisation, the ions move out from the positive electrode and into the negative electrode. Electrolytes transport  $\text{Li}^+$  and also directly influence battery electrochemistry [134]. The electrolyte’s ions move in the same direction, i.e., from the cathode to the anode, neutralising each piece of the system. The most widely used electrolytes are made up of carbonate mixtures (e.g., ethylene, dimethyl, and propylene carbonate) and dissolved salt (e.g., LITFSI and  $\text{LiPF}_6$ ) [133].

During the charging phase,  $\text{Li}^+$  migrates towards the negatively charged electrode. Concurrently, electrons are compelled to traverse from the cathode to the anode, facilitated by an external Direct Current (DC) source, thus maintaining the overall equilibrium of the electrochemical cell. Then, during the discharge cycle,  $\text{Li}^+$  returns from the electrolyte to the positive electrode, electrons are extracted spontaneously from the positive electrode to the external circuit, and the electrodes are oxidised or reduced. The positive electrode consumes electrons from the external circuit in the course of the reduction, while there is the oxidation process on the negative electrode and the liberation of electrons to the external circuit. This electron flow is essential for the battery’s operation and the storage and release of  $\text{Li}^+$  [135]. The chemical structure, lithiation/delithiation processes, and electron transfer are represented in Figure 5.

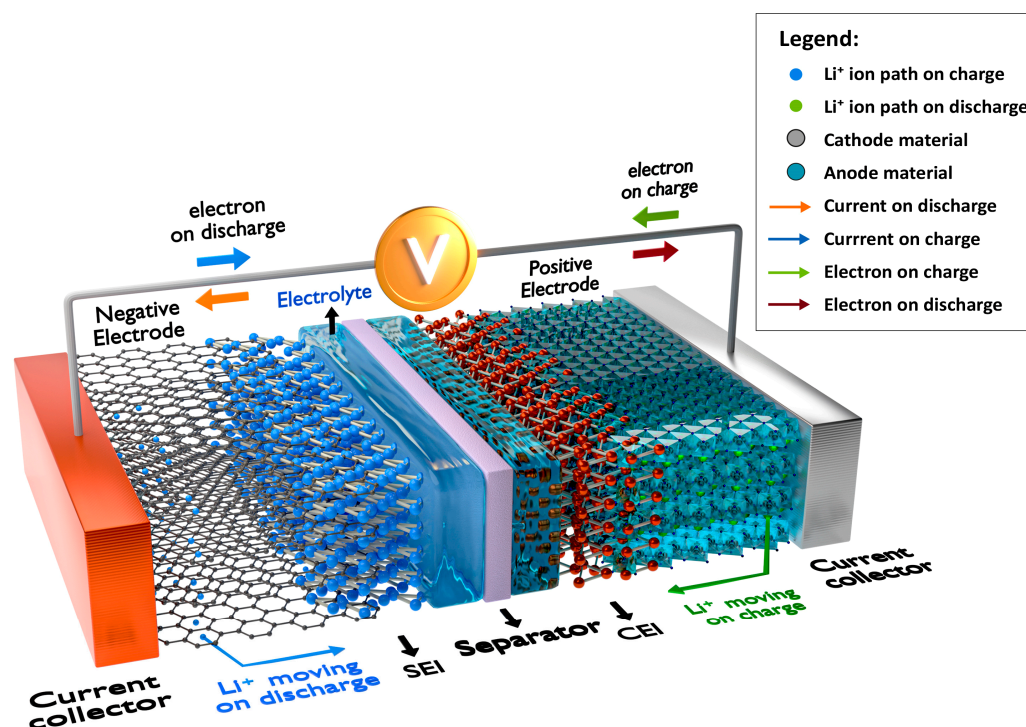


Figure 5. Technical Scheme of LIBs. Adapted from ref. [136], under terms of CC-BY license.

Regarding the battery design, according to battery manufacturers, the positive electrode should be as close as possible to the negative electrode, which will reduce the ion impedance in the electrolyte. Therefore, it is essential to have a separator to prevent proximity between the electrodes and avoid a short circuit. The separator is a permeable membrane that serves as an ionic conductor and an electrical insulator, permitting the transport of  $\text{Li}^+$  but not electrons.

Batteries applied in EVs usually have three structural shapes: pouch, prismatic, and cylindrical cells. Cylindrical cells have a lower manufacturing cost (USD/kWh) because they have been mass-manufactured for a long time, providing fast production compared to other types of cells. The assembly of cylindrical cells consists of wrapping the electrodes in a cylindrical shape encapsulated with a metal. This type of encapsulation reduces the delamination of the active material of the current collector, increasing the resistance of this type of cell to mechanical shocks, thermal charging, discharging cycles, and current collectors' mechanical expansion. Also, the temperature control of cylindrical cells is more accessible than that of prismatic cells, and they are combined into packages and modules. On the other hand, the circular cross-section of the cell does not optimally utilise the available space, which is a significant disadvantage compared to other types of shapes [137].

Furthermore, prismatic cells are more expensive and present lower energy density and mechanical stability than cylindrical batteries. However, prismatic cells can undergo swelling due to their operation, and this degradation mechanism is intensified when the cell operates outside of safe conditions, resulting from the increased pressure in the cell when the safety vent opening is obstructed, and culminating in a lower energy density than cylindrical cells [138].

Moreover, soft pouch cells have the advantage of being lightweight, presenting manufacturing with a considerably lower cost and higher density than prismatic and cylindrical cells. On the other hand, pouch cells need a robust mechanical structure for their protection; they can suffer volume expansion as they may not have a designated ventilation mechanism. The swelling effect observed in pouch cells is due to battery degradation, which is caused by the physical expansion of the battery as a consequence of gas accumulation or other factors [137]. This expansion can increase internal pressure, which can eventually cause the battery to rupture. Several technical factors influence the expansion effect, including the increased thickness and flexibility of electrodes and separators, the cell design, and the battery shape. It is essential to carefully consider and optimise these technical parameters to prevent and mitigate battery enlargement in pouch cells.

#### 4.2. Positive Electrodes of LIBs

The positive electrode presents a crystalline structure, e.g., generally made of lithium manganese oxide (LMO); lithium cobalt oxide (LCO); lithium nickel oxide, cobalt, and aluminium (NCA); and lithium oxide, nickel manganese, and cobalt (NMC). Other materials for positive electrodes comprise olivine-type materials, including lithium iron phosphate (LFP) [139]. Initially, the LIBs that dominated the battery market contained LCO as positive electrodes, which provide a working voltage window, excellent rate performance, and exceptional cycling performance. The main disadvantage of this technology is that cobalt is expensive and has a low specific capacity, and cobalt mining often takes place in precarious areas and causes severe environmental and social impacts [140–144]. Furthermore, charging LCO-based batteries at high voltages causes instability [145], and some strategies to mitigate this drawback include (i) the use of additives in electrolytes [146,147], (ii) lattice element doping [138,148], and (iii) surface coating/modification with other active/inactive materials [135,149–152].

According to Pender et al. [145], deep discharge in batteries containing LCO cathodes causes mechanical damage and a significant change in the dimension (c) of the shaft. The degradation of batteries starts in the first cycles, with a structural change of the structure that causes the increase of the grain size, reduction of the surface potential, and loss of the contact rigidity, concomitant with the irreversible fading of the capacity [145].

However, with the development of new technologies and the need to increase battery life and safety, new positive-electrode materials have been investigated, such as NMC ( $\text{LiNi}_x\text{Mn}_y\text{Co}_z\text{O}_2$ ), with the following limits:  $0 \leq x, y, z \leq 1$  [153]. The significant advantages of LIBs comprising NMC-based positive electrodes include (i) reversible capacity, (ii) low cost, and (iii) environmental friendliness. However, they may present chemical instability when exposed to air, decreasing their reversibility and restricting their use from an

industrial point of view [154], as they may present accelerated degradation processes during the lithiation/delithiation process, reducing the battery's lifespan [155–158]. The increase in nickel (Ni) content in the electrodes of battery cells provides higher extraction of  $\text{Li}^+$  at the same cut-off voltage. Therefore, it is possible to affirm that increasing the proportion of Ni in the battery cells allows one to increase their capacity [159]. Manganese (Mn) improves the battery's Depth of Discharge (DOD) [133]. The exposition of NMC-based batteries with air components (e.g.,  $\text{CO}_2$  and  $\text{H}_2\text{O}$ ) produces a reaction that forms lithium carbonate ( $\text{Li}_2\text{CO}_3$ ) and lithium hydroxide ( $\text{LiOH}$ ), considered impurities on the NCM surface. This phenomenon produces a large amount of highly reactive Li, which causes serious safety issues and reduces the electrochemical performance of the battery [140,159–165].

The main degradation mechanisms of NMC-based batteries are particle breakdown, gasification, phase transformations, and cation mixing. The breakage and deformation mechanisms within electrode particles are triggered by the voltage differentials produced by ion diffusion processes, in which concentration gradients lead to the movement of charged particles across the electrode medium [166]. These factors are mainly caused by the formation of highly reactive Ni in batteries. The main strategies adopted to reduce the instability caused by the high reactivity of Ni include (i) surface coating on the electrode of the active material, (ii) doping the electrode active material, and (iii) conversion of the NMC particles morphology from a polycrystalline to a monocrystalline structure.

In addition, LFP-based batteries are highly thermally stable and present high reversibility and power. This battery technology is also beneficial in high-power applications requiring high discharge rates. The intercalation process of LIBs can cause phase transitions in the active material, leading to volume changes and mechanical stress. Thus, some crystalline structures can effectively accommodate volume variations, reducing mechanical stress and deterioration. For instance, anisotropic structures, such as LFP (olivine), can inhibit mechanical stress during phase transitions, contributing to a longer shelf life. The primary mechanisms associated with LFP electrodes are (i) electrolyte decomposition, (ii) active material loss, (iii) formation of lithium dendrites, (iv) structural degradation of the electrodes, and (v) modification of the separator's morphology.

#### 4.3. Negative Electrodes of LIBs

Negative electrode usually consists of graphite-like materials. Graphite dominates commercial batteries because its main advantages are high cycle stability, slight voltage hysteresis, low cost, and high tap density. However, graphite anodes still provide limited power and energy densities for LIBs, affecting their application for EVs and large-scale power supplies, and it has a capacity limited to  $372 \text{ mAhg}^{-1}$ , which is considerably lower than other alternative materials, such as conversion and alloying-type anodes. Therefore, novel anode materials are being investigated to obtain alternatives that present low redox potential for high output voltage, reversibility during the intercalation process, structural stability during intercalation, high ionic and electronic conductivity, affordable cost, and environmental friendliness [167]. Graphite presents an intercalation of  $\text{Li}^+$  within its structure; it is an intercalating anode material. Intercalating-type anodes consist of crystalline materials that can store  $\text{Li}^+$  within their structure. As well as graphite, intercalating anodes include other carbonaceous materials, such as carbon nanotubes [168] and spinel lithium titanate ( $\text{Li}_4\text{Ti}_5\text{O}_{12}$ , LTO) [169].

Among the alternative anode materials, there are alloy anodes, which consist of metals with high purity, such as magnesium (Mg), aluminium (Al), tin (Sn), and silicon (Si), which present a chemical reaction with  $\text{Li}^+$ , forming  $\text{Li}_n\text{M}$  species (M consist of a metal). Alloy anodes present a theoretical capacity higher than graphite and can inhibit lithium plating, as they present a higher onset voltage above Li. However, alloy anodes present some drawbacks, such as volume expansion, irreversible capacity loss, and the evolution of an unstable SEI layer [170]. Regarding alloy anodes, Si has an extraordinarily high theoretical capacity of  $4200 \text{ mAhg}^{-1}$ , low cost, and abundancy, but it presents high volume expansion during the alloying/de-alloying process, particle cracking, delamination, an

unstable SEI layer, and significant capacity loss [171]. Therefore, significant research has been performed on overcoming the drawbacks of Si anodes, such as the polymerisation of Si particles [172] and the use of ionic liquid-based electrolytes [173,174] to provide the formation of a stable SEI layer. Furthermore, the use of Si nanoparticles [173], or the application of Si-based composite materials, such as silicon oxycarbide (SiOC) [175], can inhibit their volume expansion.

Furthermore, unlike intercalation and alloy anodes, conversion-type anodes present a redox reaction between two different materials, which can present high theoretical capacities, usually ranging from 500 to 1500 mAhg<sup>-1</sup>. Conversion-type anode materials comprise Transition Metal Oxides (TMOs), Transition Metal Dichalcogenides (TMDs), Transition Metal Phosphides (TMPs), and Transition Metal Selenides (TMSes). Otherwise, conversion-type anodes can present certain drawbacks, such as irreversible capacity fade, low conductivity, and volume expansion, culminating in a short cycling life [176]. Thus, approaches to overcome these drawbacks from conversion anodes include the design of nanostructured electrodes, which present high SSA and facilitate the diffusion of Li<sup>+</sup> [177,178].

## 5. Degradation of LIBs

LIBs are subject to the thermal runaway phenomenon when subjected to abusive conditions, such as vehicle collision, overvoltage, overcurrent, and deep discharge [179,180]. The thermal runaway is an exothermic phenomenon in which reactions inside the cell increase the temperature [181–184], leading to electrolyte decomposition, gas formation, voltage drop, and internal pressure increase. This can culminate in the cell's rupture and swell, causing electrolyte leakage, which may result in fire/flame and explosion in contact with air.

The gases inside the cell can also be produced by electrolyte reduction resulting from the decomposition reaction of electrolyte solvent and by the structural release of cathodic materials [185,186]. These released gases, such as hydrogen, organic products, and ethylene, can be toxic and flammable, which can cause severe harm to an individual's health [151,185]. These gases can also cause uncontrolled thermal runaway in the cell, which can compromise their application in EVs, as it affects the vehicle's safety [133,152]. The gas evolution inside the cell is also associated with electrolytic displacement and increased internal resistance, which reduce the battery's efficiency, the number of cycles, and the lifespan [151,185,187]. The ageing of LIBs is still the subject of research to understand and minimise electrolyte decomposition and gas evolution. Researchers can gain insights into the mechanisms that cause battery degradation by understanding the phenomena at the electrode/electrolyte interface, as this region facilitates the mobility of ions between the electrode and the electrolyte during battery operation, and any change or disruption in this interface can affect Coulombic efficiency and lead to degradation. The electrode combines Li<sup>+</sup> and electrons in the electrode/electrolyte interface. The Li<sup>+</sup> stored in the electrode can be intercalated into a host material or as an alloy or Li metal. The Li<sup>+</sup> intercalation implies electron absorption for electrode neutrality [62,149,151,188]. The charge transfer in and out of the electrode also affects the current collector, which suffers from corrosion due to cycling. This corrosion effect occurs at the negative electrode (the degradation mechanisms that occur at this electrode are discussed in more detail in Section 4.3) and causes irreversible capacity loss in the cell [152].

Gas generation is an additional form of battery deterioration that can be influenced by battery shape. Gases can be produced inside the battery due to the chemical reactions that occur during the charging and discharging process, leading to swelling, pressure build-up, and even battery rupture. The leading gases these chemical reactions produce inside the battery include H<sub>2</sub>, C<sub>2</sub>H<sub>4</sub>, CH<sub>4</sub>, CO, CO<sub>2</sub>, HF, SO<sub>2</sub>, NO<sub>2</sub>, NO, and HCl. There are several ways in which the design of the battery can affect gas production, such as flat pouch batteries that have a higher surface area/volume ratio than cylindrical batteries, which can increase gas production due to increased electrochemical reactions on the

battery's surface. Due to the design of the electrodes and separators, certain regions of pouch cells can be more susceptible to gas accumulation [137].

A study conducted by Christensen et al. [189] examined thermal runaway in LIBs under various abusive conditions and SOCs. The results showed that the first sign of thermal runaway is the ejection of white vapour, which contains a mixture of flammable and toxic gases. Intriguingly, a subset of these gaseous constituents, including the vaporised solvent specified in a work conducted by Yokoshima et al. [190], which has a relative density more significant than that of atmospheric air, naturally condense when exposed to an environment with a reduced temperature. The effects of this condensation process within a confined spatial domain are of particular interest; the condensed aerosol mixture is capable of causing a phenomenon known as a vapour cloud detonation, given an adequate oxygen concentration [189]. Extrapolating these observations necessitates additional research into the requisite safety measures and operational parameters for systems susceptible to these potentially dangerous reactions.

Furthermore, the significant SO<sub>2</sub> emission at reduced SOCs in the investigated systems has been reported elsewhere [189]. In addition, it identifies CO as the predominant gas, whose abundance is directly proportional to the SOC concentration. According to the results shown in a work conducted by Golubkov et al. [191], a comparison of the LCO and NMC chemistries reveals that both emit the same amount of CO. This similarity does not apply to the LFP-based cathodes, which exhibit a more moderate CO release than the NCA cell. These findings highlight the variation of gaseous emissions as a function of battery chemistry, SOC, and possibly other operational parameters, highlighting the complex interplay of factors contributing to LIBs' overall safety profile. This concept necessitates further investigation to better comprehend and mitigate the drawbacks associated with such energy storage systems.

Another drawback observed in LIBs is lithium plating, which is a deterioration that can occur particularly during rapid charging or at low temperatures. This occurs when metallic lithium accumulates on the anode's surface, decreasing the amount of available Li<sup>+</sup> and causing capacity loss. The geometry of the battery can influence lithium plating in several ways. For example, cylindrical batteries have a lower ratio of surface area to volume than flat pouch batteries, thereby reducing the possibility of causing lithium plating. In addition, the geometry of the anode and cathode can influence the distribution of Li<sup>+</sup> and the probability of suffering from lithium plating [192,193].

In addition, the formation of an SEI layer usually occurs during the initial discharge, when the electrode redox potential is out of the electrolyte electrochemical window. The SEI layer is formed by organic electrolytes reduced species, acting as an ionic conductor and electronic insulator, which can be observed in both the cathode and anode surfaces, but they have been significantly more investigated for anode materials, as the SEI layer formed on the anode surface used to be more unstable. The SEI layer has an important contribution to LIBs, as it provides de-solvation during the intercalating process, and the formation of an unstable SEI layer can culminate in the exfoliation of carbonaceous anodes. However, the evolution of a stable SEI layer requires an irreversible consumption of lithium and electrolyte materials, resulting in capacity fade, higher resistance, and lower power density. The approaches to provide the formation of a stable SEI layer include the use of electrolyte additives and artificial coating of electrodes [194].

Also, separator cracking is another form of battery degradation, which can occur especially in LIBs. This occurs when the separator, typically made of polymer, dissolves due to excessive heat or flame exposure and mechanical loads. The geometry of the battery can affect this process by altering the thickness and thermal conductivity of the separator, as well as the cell's design [195,196]. Generally, batteries applied to EVs can reach an energy density of nearly 300 Wh/kg [145,146], and the predominant average cost of current battery generation is approximately 100 to 200 USD/kWh [149,197]. During the phase design of LIBs, the goal is to maximise the potential difference from the positive to the negative

electrodes, minimise the active material mass and volume, and prevent the electrolyte from undergoing the oxidation/reduction process [149].

In ageing, the main problems are the effects of the cycle and the calendar, as these effects influence both the energy (capacity) and power (impedance) of the battery due to the loss of lithium and capacity decrease [62,135,140,148,159,198]. Loss of cell power happens due to loss of local contact, reduction of electrode reaction surface, structural changes in host materials and separator, changes in electrolyte properties, and corrosion on the current collector [145]. The decrease in the battery reversible capacity refers to reducing the charge that a battery can store per unit of time, usually expressed as a percentage, while the decrease in energy results from increased internal resistance [92]. In practice, the cycling and calendar effects are interrelated, especially when batteries have low cycle depth and low current rates [149,150,160–162]. The two effects coexist simultaneously, undergoing a mutual action influenced by each other [140].

The cycling effect is directly associated with battery charging and discharging and refers to the degradation mechanisms and capacity loss caused by the electrode and electrolyte decomposition [140,162]. In cycling, detecting battery degradation due to impedance increases is possible. Battery degradation can result from the formation of passivation layers in the electrode/electrolyte interfaces (i.e., SEI), mechanical stress in the electrode's active materials, or lithium coating [84,148,160,162,164]. Therefore, the cycling effect mainly impairs the reversibility of materials, and it is directly related to battery parameters, such as SOC, high/low temperature, time, charge and discharge currents, deep-of-discharge, and charge efficiency [134,162,164,165].

The calendar effect is irreversible and refers to all battery degradation mechanisms over time, regardless of the battery's charge/discharge cycle. When batteries are stored in open circuit conditions, no current flows inside the battery [84,134,148]. This effect has no linear behaviour on the SOH and can be accelerated at high temperatures that increase the dissolution of the metal and produce a reduction in the cell capacity [84,163]. Calendar ageing results from electrolyte reduction, oxidation, and surface film growth on active materials [84,149,150,163]. It is accelerated at higher SOC, longer time intervals, and/or high temperatures [134,149].

In general, some factors greatly influence the battery degradation process, such as (i) temperature, (ii) SOC variation, (iii) DOD, and (iv) voltage limits on charging and discharging. The temperature affects cell ageing because high temperatures increase the agitation of the molecules and consequently accelerate the processes of insertion and/or removal of lithium in the host network. At low temperatures, lithium metal grows due to the slow transport of lithium into and within the negative electrode host network, which increases the local lithium-ion concentration and makes the lithium metal stable. The accumulation of lithium at low temperatures is a result of the slow movement of  $\text{Li}^+$  into and within the negative electrode's host matrix [30,199–201].

The temperature affects cell ageing, as high temperatures increase the agitation of the molecules and consequently accelerate the insertion and/or removal of lithium in the host network. Furthermore, high temperatures accelerate side reactions, altering the structure and thickness of the SEI, increasing the battery's internal resistance, and enhancing the degradation process. This makes the cell more prone to thermal leakage, which can culminate in an outburst of batteries. It is also important to mention that a very thick SEI layer provides significant power loss [202–205]. Moreover, it is also important to mention that a very thick SEI layer is the main factor for the power loss in the cell. Beyond this point, low temperatures can reduce the electrolyte viscosity, decrease the lithium-ion conductivity, and cause the slow diffusion of the  $\text{Li}^+$  within the electrode, reducing the battery discharge capacity. Consequently, there is a rise in internal resistance and parasitic reactions during the battery charging process, such as the metallic lithium coating and the growth of lithium dendrite. Therefore, low temperatures can also accelerate the battery's degradation, reducing its safety [30,199–201].

The SOC indicates the quantity of lithium stored in the electrode, which means that a higher SOC implies an increase in the amount of cycling active material, culminating in a decrease of the battery capacity. Furthermore, the variation of SOC ( $\Delta$ SOC) strongly influences battery degradation, as previously detailed elsewhere [62,86,179,206], as high  $\Delta$ SOC rates culminate in a more significant degradation, which is caused by structural changes in the positive electrodes. Another study conducted by Ouyang et al. [90] showed that the imbalance of the cathode's and anode's SOC reduces the capacitance and increases the battery's internal resistance. The results were obtained by studying an LIB system by EIS for a given SOC of the electrode, which indicated that the electrodes should be designed in a way to minimise this imbalance. Moreover, another parameter widely discussed and investigated in the literature is the DOD, which is complementary to the SOC and can be further investigated, as in the work conducted by Abada et al. [207], which evidenced that high DOD rates cause a reduction in cell capacity and energy. Finally, the battery charge/discharge voltage threshold can also accelerate or reduce the degrading effects of the battery, indicating that high and low charge and discharge voltages increase its impedance and accelerate its degradation mechanisms [3,17,208,209].

Then, considering the effects of the SOC on the battery performance, it should be estimated mainly to equalise the cells and reduce the customers' range anxiety. However, collecting labelled samples for training data-driven models is expensive and time-consuming. Hopefully, it has already been investigated elsewhere [85]. This data collection can be performed by deep neural networks, which can estimate the SOC for a limited number of available labelled samples, presenting an SOC estimation error lower than 0.6%.

Also, the SEI layer can explain these effects associated with battery degradation. The SEI consists of a thin layer of electrolyte decomposition products (i.e., carbonates), as previously detailed; it is formed at the electrode/electrolyte interface if the electrode's redox potential is not within the electrolyte's Electrochemical Stability Window (ESW) [194,210,211]. The architecture of the SEI layer is still not known in detail, but it is known that this layer is composed by the decomposed products from the electrolyte, electrode, and lithium [212]. The main products reported in the literature include lithium oxide ( $\text{Li}_2\text{O}$ ), lithium carbonate ( $\text{Li}_2\text{CO}_3$ ), lithium fluoride ( $\text{LiF}$ ), lithium ethylene dicarbonate ( $\text{LiOCO}_2\text{CH}_2$ )<sub>2</sub>, and lithium methyl carbonate ( $\text{LiOCO}_2\text{CH}_3$ ) [209,213]. The reactions must take place within the electrode's ESW to provide reversibility to the rechargeable batteries [214]. This passivation layer is usually, but not exclusively, formed in the first load cycles of the LIBs, mainly at the negative electrode, as this electrode operates at voltages outside the electrolyte's ESW.

Furthermore, a passivation layer is also formed on the surface of the positive electrode at the electrode/electrolyte interface, and in such cases, is named Cathode–Electrolyte Interface (CEI). It is essential to note that one of the significant shortcomings of the literature concerns the lack of an adequate description of CEI. The CEI improves Coulombic efficiency and overall battery capacity retention [215]. The detection, measurement, and characterisation of the CEI layer are not trivial due to the high potentials in this electrode that are close to the stability window of commercial carbonate electrolytes [208,216–218]. Furthermore, the complexity of determining and understanding the formation phenomena of CEI is increased due to the numerous chemical reactions that occur near the positive electrode, including nucleophilic reactions, induced polymerisations, and dissolution of transition metals.

Moreover, the formation of SEI consumes cyclable lithium and electrolytic materials due to the irreversible electrochemical process of electrolyte decomposition. On the other hand, the SEI layer prevents further reactions between  $\text{Li}^+$  and electrolyte solvents, contributing to battery stability, and a controlled SEI formation is essential to prevent short circuits and to ensure safe battery operation. On the other hand, if the SEI layer is not formed properly or becomes unstable, it results in capacity loss, reduced cycling performance, and compromises safety issues in the battery [194,210,219].

The desolvation process of lithium ions during their incorporation into the graphite anode structure is crucial because it directly affects the performance and durability of the battery. In addition, incorporating lithium ions into graphite anodes that are still bound to solvent molecules may cause mechanical degradation or exfoliation (delamination). The SEI layer effectively removes lithium ions from their solvation shell, enabling a smooth intercalation process vital to anode integrity and performance in lithium-ion batteries. One of the most significant achievements in LIB technology was the application of carbonate solvents, including Ethylene Carbonate (EC), which contributes to the establishment of a stable SEI layer [220].

Furthermore, the SEI layer is crucial to ensure the chemical and electrochemical stability of the battery, as it allows the transportation of  $\text{Li}^+$  while blocking electrons, ensuring the continuation of the electrochemical reactions but avoiding the additional electrolyte decomposition because it is almost impenetrable by the electrolyte molecules [194,217,221,222]. In addition to these factors, the SEI stabilises the electrode, allowing a more significant number of cycles [223]. However, the SEI layer is formed by four main factors: (i) breakdown of solvents and electrolytic salts, (ii) chemical breakdown of electrode materials, (iii) consumption of lithium, and (iv) co-insertion of organic solvents in the electrodes. These effects cause battery capacity loss, reducing the energy density and increasing the cell's internal resistance and temperature. Consequently, this is going to accelerate the battery degradation mechanisms [212,224,225]. Furthermore, approaches to obtain a stable SEI layer and inhibit electrolyte and electrode material consumption include the use of electrolyte additives, the design of anode materials with high wettability, the development of an artificial SEI layer before battery assembly, and the use of binders and separators that facilitate SEI formation [220].

In addition, battery degradation can happen in two ways: decreased capacity and decreased power due to loss of inventory lithium, negative electrode capacity, and positive-electrode capacity. The decrease in battery capacity refers to the decrease in the charge that a battery can store per unit of time, usually expressed as a percentage. The energy decrease refers to reducing the ability to supply energy because of increased internal resistance [226]. Therefore, as the negative and positive electrodes are related to several battery ageing mechanisms, the following sections aim to explain in detail the degradation mechanisms that occur in the negative electrode, positive electrode, separator, and electrolyte, and, finally, a discussion is presented.

### *5.1. Degradation Process at the Negative Electrode*

Negative electrode ageing is mainly caused by lithium coating, electrolyte decomposition, solvent co-intercalation, gas evolution, decreased accessible surface area (due to the SEI layer), changes in porosity, loss of particle contact (due to changes in volume due to cycling), binder and electrolyte decomposition, and corrosion of the current collector, as detailed in Figure 6 [30].

The formation of the SEI layer can consume 10 to 15% of the battery's initial capacity, but during the operation this capacity loss is lower than when the SEI layer is formed, and this passivation layer is stable most of the time; the batteries operate within their stability window [220,227–229]. The SEI layer formation process requires controlled conditions and technical knowledge about the batteries. Furthermore, the SEI depends on the Specific Surface Area (SSA) of the graphite anode, which is related to the type and graphite morphology. On the other hand, the formation conditions of the SEI depend on the electrolyte's concentration, electrochemical conditions, and cell temperature. After long periods, corrosion of the SEI may occur, and the formation of an additional SEI produces a new capacity loss [226].

After assembly, the batteries are initially discharged because the carbon lithium is unstable in the air. Therefore,  $\text{Li}^+$  may exist only in the electrolyte or interspersed at the cathode. As mentioned above, the SEI layer is formed in the battery's initial cycle, which is a thin film formed at the anode due to the reaction of the  $\text{Li}^+$  of the cathode and the

organic compounds of the electrolyte solvent [226]. Then, battery manufacturers must conduct the first charge before releasing them on the market, aiming to prevent capacity loss on the initial charge [212]. On the other hand, despite the capacity loss from the initial cycle, batteries can be used in EVs for many years [217].

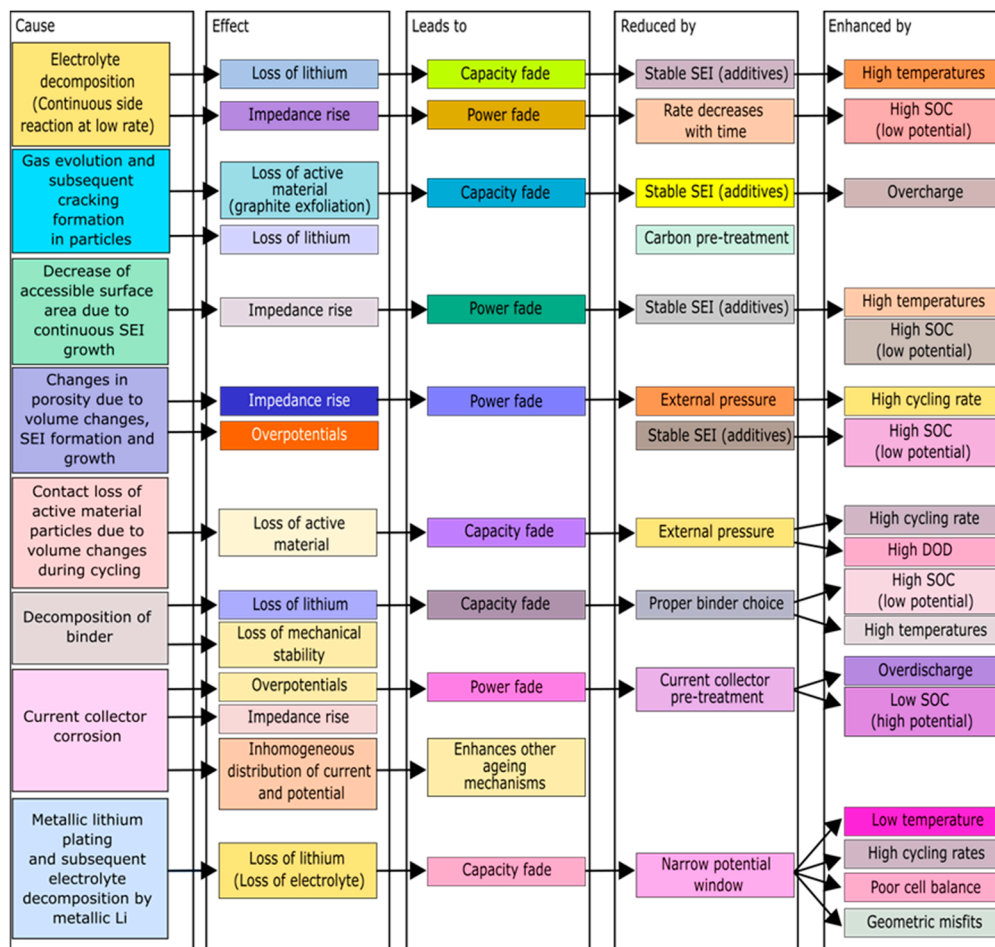


**Figure 6.** Lithium-ion negative electrode ageing: causes, effects, and influences. Adapted with permission from ref. [230]. Copyright (2004), Elsevier.

The intercalation of solvated  $\text{Li}^+$  in the graphite anode can induce graphite exfoliation, producing gases capable of cracking the SEI. Therefore, it expands, increasing the internal cell's pressure and causing mechanical stress [231]. The cycling effect increases and reduces the graphite particle diameter, which implies a variation in the cell volume, and the carbonaceous electrode is lithiated and de-lithiated in this process. This volume change causes an increase in the cell's mechanical tension, which results in graphite exfoliation by particle cracking. The reduction in the amount of active material available allows the broadening of the SEI layer in a more significant number of locations that become available at the electrode/electrolyte interface. Then, the simultaneous insertion of the electrolyte components with the insertion of lithium in the spaces available by the cracks caused by the negative electrode expansion in the SEI layer increases the thickness and the cell's resistance, consuming the cyclable lithium and reducing the system's capacity [212,226]. Moreover, the accumulation of  $\text{Li}^+$  on the SEI causes an increase in localised resistances [61]. In conjunction with the lithium plating, this factor results in non-uniform resistances and current distribution [61]. This non-uniformity contributes to the non-uniform degradation of second-life batteries.

An observed correlation exists between the SEI layer thickness broadening and the corresponding rise in the rate of battery over-discharge. The notable rise in cell

temperature as the SEI layer thickness and discharge rate increase have been evidenced in a study conducted by Andriunas et al. [232], as the capacity of batteries tends to decrease as the particle size of both electrodes increases. In addition, delamination can occur in two ways: the first occurs when the electrode volume expansion breaks the connection between the electrode and the collector. The second possible way of delamination is caused when the current collector is not able to insert lithium. In that case, the electrode does not increase in volume, but increases the surface tension of the negative electrode–current collector interface, causing the connection between the electrode and current collector, resulting in delamination. Delamination implicates higher internal resistance and current congestion at the interface, which can cause short circuits [212,226]. Current congestion at the interface can induce local lithium metal growth, which can eventually lead to dendrite formation and culminate in a short circuit.

Furthermore, a high SOC decreases the potential of the negative electrode that is highly lithiated, allowing for a thermodynamic process where lithium is deposited on the electrode instead of being intercalated during charging. To avoid this problem and to prevent the negative electrode from being fully lithiated, battery manufacturers design this electrode with 10% of the positive-electrode capacity [226,233]. In addition to the SOC, the temperature also influences the batteries' degradation; once the high temperature increases, the SEI solubility can create lithium crystals less permeable to  $\text{Li}^+$ , which increases the negative electrode impedance [226,233].

Similarly to the SEI formation, lithium coating is one of the most significant degradation mechanisms and compromises the safety of batteries. The lithium coating consists of the coating of negative electrodes with lithium, as  $\text{Li}^+$  move between the electrodes while the battery is charging and further intercalates in the active material of the negative electrode, which in most cases is graphite.

Moreover, two factors cause lithium coating, and the first one is charging batteries at low temperatures with a high C-rate and high SOC. This factor is caused by charging batteries at low temperatures, with high current rates and high SOC, limiting lithium diffusion and the transfer of charge at the interface formed by the graphite and the SEI. This causes the graphite particle surface to be saturated with  $\text{Li}^+$ , polarising the negative electrode and forcing the graphite potential to reduce under the lithium potential limit (0 V), and consequently, the negative electrode is coated by lithium [234,235]. In this context, the potential difference between  $\text{Li}^+$  intercalation in graphite and the formation of metallic Li must be lower than 90 mV if the cell is nearly fully charged [236]. Other negative electrode materials, such as LTO, are safer than graphite-like electrodes, but they provide lower cell voltage and energy density.

The second factor is an imbalance in the capacity of the cell, specifically a capacity loss of the negative electrode, which drives it below one of the positive electrodes. This can create (local) lithium plating, even at higher temperatures. The lithium coating can be responsible for serious safety failures because the lithium deposition on the anode can form dendrites or mosses, which can cause capacity loss and short circuits [234,235]. It also increases cell resistance due to the formation of thin films in the coated lithium metal and reduces electrolyte ionic conductivity [234].

Negative electrodes of batteries that have reached their full lifespan can be further recycled. However, such procedures necessitate the purification of graphite impurities and the reconstitution of particle morphology. This can be accomplished by applying acid-washing techniques for graphite decontamination and high-temperature annealing for particle structure restoration. Further research is required to address the significant initial cycle losses resulting from the graphite's increased exposure to the electrolyte during annealing and morphology restoration. Innovative, low-temperature refining techniques for electrodes are advantageous. The effectiveness of the anode recycling procedure depends on the ultimate lifecycle conditions of the electrode, which include cycle history and battery usage variation [24]. Despite its abundance and low price, graphite recycling presents

a significant challenge. However, there is still no established method for regenerating battery-recovered graphite to electrochemical grade specifications [24].

### 5.2. Degradation Process at the Positive Electrode

Positive-electrode degradation mainly results from material loss and SEI layer growth. The active material loss occurs due to the dissolution of the transition metals from the cathode, and their further reaction with the electrolyte, which is accelerated at high temperatures. The presence of water in the batteries can cause hydrolysis with the  $\text{LiPF}_6$  salt, forming hydrofluoric acid and causing the dissolution of the transition metals. Positive electrodes containing manganese (Mn) usually dissolve transition metals when the discharge is completed. Cathode transition metals that have been dissolved in the electrolyte can react with the SEI layer formed on the negative electrode's surface, increasing the conductivity, forming additional SEI and dendrites, and decreasing the quantity of active materials available in the electrode [226].

Furthermore, a reaction between the transition metal and the SEI causes the loss of inventory lithium when the cathode is exposed to the electrolyte. The SOC also influences positive-electrode degradation, considering that a low SOC can reduce the amount of lithium that can intercalate in the positive electrode, promoting structural changes in this electrode. At the positive electrode, high temperatures can culminate in the loss of oxygen from the metal oxide, and, together with the electrolytic decomposition promoted by high voltages, it can generate the cracking of particles and produce gases inside the batteries [226].

Therefore, based on the factors that affect the battery's degradation mechanisms, it is possible to state that LIBs are degraded more quickly when the cell operates outside its ESW. The ESW consists of a voltage range and temperature that the cell can safely operate with minimised degradation mechanisms. Otherwise, when the cell operates outside its ESW, effects that accelerate cell degeneration can occur, and more severe effects that degrade the cell quickly can also compromise its safety. This is why a BMS is required to control some parameters (e.g., potential, current, and temperature) to keep the cell operating within its stability window.

To summarise the degradation mechanisms, it is possible to highlight that the positive electrode degrades due to a combination of factors, which include active mass attrition, electrolyte degradation, gas generation, binder corrosion, and the formation of the SEI. The positive electrode is strongly related to SOC and temperature [217,225,237].

### 5.3. Degradation Process at the Electrolyte

Electrolytes undergo a degradation process caused by the decomposition of salts and solvents and the formation of electrolyte interphases during cycling [238]. In the initial cycles of the cell, the electrolyte comes into contact with the negative electrode, which generally operates at voltages below the electrolyte's ESW. This contact between the anode surface and the electrolyte accelerates the redox processes, causing the electrolyte's decomposition and reducing the battery's performance. In summary, it is possible to state that the decomposition of electrolyte solvents is one of the most significant degradation mechanisms that occurs in electrolytes.

Furthermore, the products formed by the reactions that result from electrolyte decomposition can be used as a marker of the health status of electrolytes in batteries [134]. In a study conducted by Weber et al. [239], the authors noted that organophosphate molecules can be a type of marker to assess the health status of lithium hexafluorophosphate ( $\text{LiPF}_6$ )-based electrolytes. However, the products of the reaction can have a variety of molecules, such as ether, organocarbonate, and organophosphate species [134]. Therefore, further studies should be performed to identify more markers that can be used to assess electrolyte health status. This will allow the possibility of assessing the need for predictive battery maintenance for the second-life battery market, developing a unique identifier, and estimating the battery safety level.

The decomposition of solvents also causes the formation of CEI and SEI, and multi-functional additives can be used to form protective films on the electrode surfaces to prevent these electrolyte decompositions. In a work conducted by Henschel et al. [240], the authors investigated the degradation mechanisms of an electrolyte containing  $\text{LiPF}_6$  dissolved in a mixture of organic carbonates. The results showed that the electrolytes undergo thermally and electrochemically induced degradation. Furthermore, high temperatures can accelerate the degradation mechanisms in certain types of batteries because it causes the formation of ethylene glycols via EC polymerisation and subsequent decarboxylation. Therefore, some ways to suppress electrolyte decomposition still need to be explored, aiming to increase batteries' thermal and electrochemical stability.

Moreover, the results discussed in a work conducted by Dose et al. [241] indicate that the performance of batteries containing nickel-rich cathodes, such as NMC811 ( $\text{LiNi}_{0.8}\text{Mn}_{0.1}\text{Co}_{0.1}\text{O}_2$ ), can be limited by the main component of conventional electrolytes, known as Ethylene Carbonate (EC). The main reason for this limitation is that, in scenarios where batteries are charged at high potentials (above 4.4 V vs.  $\text{Li}/\text{Li}^+$ ), EC can increase oxygen release, causing oxidation/breakdown of electrolytes and degradation of the cathode surface. However, this increase in oxygen release was not observed in NMC111-based batteries, independent of the electrolyte. Therefore, it is possible to observe that the development of electrodes with different chemistries has increased the useful life of the batteries and improved their performance. Otherwise, electrolytes compatible with these electrodes need to be developed to ensure battery safety. Furthermore, the degradation of NMC811-based batteries can also occur below the cutoff potential. In this case, the electrolyte over-decomposition processes are mainly caused by electrolytic oxidation of electrolytic solvents [241]. This electrolytic oxidation is caused by oxygen release, as discussed earlier.

In addition, the electrolyte degradation mechanisms in secondary lifecycle batteries have rarely been investigated. The findings delineated in a study performed by Attidekou et al. [61] elucidate the impact of electrolyte degradation on ionic mobility diffusion phenomena. The deposition of  $\text{Li}^+$  on the SEI subsequently causes an increase in local resistance, which is a phenomenon that induces lithium plating, resulting in an uneven resistance and current distribution. This results in selective conduction pathways due to the SEI thickness and the consequential loss of material conductivity.

#### 5.4. Degradation Process in the Separator

The separator has a fundamental importance in avoiding short circuits and, consequently, establishing the safety and reliability of batteries. The separators are a fundamental component for battery safety and must be disconnected in the event of an abnormal temperature increase or a thermal runaway [242]. Short circuits are responsible for serious safety failures in batteries, which can cause fire and outbursts. A brief circuit occurs when a path of minimal resistance connects both electrodes, causing a sudden current surge and accelerating the generation of ohmic heat [243]. Short circuits can be classified as external or internal. External short circuits happen while the tabs are aligned along a low-resistance path; in contrast, internal short circuits happen when there is a failure in the separator layer. Another issue that can cause a short circuit is nail penetration, when a metallic nail penetrates the separator, connecting the electrodes current collectors and resulting in an internal short circuit. Furthermore, the penetration of the separator by impurities or lithium dendrites facilitates low-resistance connections between the electrodes, and it can culminate in an internal short circuit [243]. As a result, an increase in temperature is observed, and consequently, the separator melts [179,244].

In a work conducted by Li et al. [242], the authors highlighted four main phenomena that cause separator degradation, which are (i) growth of lithium dendrites culminated by separator pores, (ii) blocking passes in the separator during cycling, and (iii) structural degradation due to high temperature or a long number of cycles. Furthermore, Internal Short Circuit (ISC) has also been investigated in a study conducted by Liu et al. [244], which investigated the Electrochemical Impedance Spectroscopy (EIS) tests of LIB cells

without  $\text{LiPF}_6$  to assess the short-circuit resistance. Additionally, accelerated calorimetry and separator oven tests were used to evaluate thermoelectric behaviours and short-circuit failure modes. The findings suggest that voltage failure occurs due to self-discharge resulting from ISC, such as those of the Al-Cu and Al-An types, at low SOC. In contrast, voltage failure occurs due to separator collapse, and at high levels of SOC, a distinct extension of the ISC region, such as the Al-An type of ISC, indicates a more significant potential hazard. The expansion behaviour of ISC affects the safety characteristics of the battery, which is significantly influenced by the separator's thermal stability. The ageing of the separators causes a reduction in the mechanical strength of the separator as the number of cycles are extended, reducing the battery's ability to withstand mechanical impact and battery safety.

However, high temperatures can overheat the cell, causing thermal shrinkage or even melting the separator, resulting in a short-circuit. The first stage of separator disintegration is dependent on the separator's constituents. The melting values of polyethylene and polypropylene are  $130\text{ }^\circ\text{C}$  and  $170\text{ }^\circ\text{C}$ , respectively, according to previous studies reported elsewhere [185,245]. Thermal shrinkage is typified by a decrement in the polymer separator's pore size, an effect induced by the separator's swelling. This, in turn, curtails the comprehensive coverage of the separator, leading to a consequential decrease in pore dimensions. This alteration precipitates a decline in the velocity at which  $\text{Li}^+$  traverses the separator, thereby impairing the battery's capacity to supply elevated current rates. Existing works in the literature also showed that increasing the number of cycles causes a reduction in pore size. The reduction of separator pores is accentuated at high temperatures, which causes an increase in battery impedance and ionic conductivity.

The electrode cycling process influences the separator; as the electrode undergoes expansion and compresses the separator, the battery charging process causes the reduction of the useful lifetime of the separator. Furthermore, the electrolyte can also influence the elasticity of the separator and, consequently, the separator's performance. Beyond this point, the presence of liquid electrolyte into the separator reduces its elasticity, which is an important indicator of the separator degradation level.

In a study conducted by Yuan et al. [246], the authors evaluated the performance of polyolefin separators in puncture, expansion, and softening tests in electrolytic solvents. The exposure of the separators to cyclic understanding caused a decrease in ionic conductivity, a decrease in the C-rate capacity, and poor electrochemical performance of the separator, which consequently reduced the battery's useful life.

### 5.5. Degradation of Large-Format LIBs

Large-format cells are designed to provide the necessary power and energy for the vehicle's operation. Increasing the size of the cells, however, causes higher energy density but vulnerability to safety-related incidents due to the more significant stored energy and cooling difficulties because of the lower surface/volume ratio [247]. The increase in battery size also leads to an increase in degradation mechanisms, causing a gradual loss of battery capacity and performance over time. The lack of uniformity or consistency within the battery pack (i.e., inhomogeneities) mainly causes the degradation processes in large-format batteries for EVs. The presence of inhomogeneities can be due to variations in cell manufacturing, differences in cell performance, or uneven distribution of electrical and thermal loads within the battery pack [248].

The presence of inhomogeneities can considerably impact the battery degradation processes, which can lead to uneven distribution of current and heat within the battery pack and accelerate degradation in specific cells or regions. Inhomogeneities can also result in variations in the cells' current density, voltage, SOC, temperature, and SOH, further contributing to degradation [249]. Furthermore, the degradation process involves the initiation of lithium deposits in regions with high current density, which then propagate and cause pore closure in the separator. A peak height from a differential voltage curve can be used as an indicator to detect inhomogeneity and guide the development of large-format cells [250].

Temperature variations across the cell accelerate degradation in hot spots, and they can cause inhomogeneous temperature ranges, influencing degradation behaviour. High temperatures accelerate side reactions, altering SEI layer composition and increasing internal resistance. In a study conducted by Xie et al. [250], it was confirmed that homogeneities affect battery degradation by observing battery degradation that first occurred in regions close to the battery tabs, which consisted of the initial degradation effects before spreading to the central regions of the battery. Furthermore, the authors employed Scanning Electron Microscopy (SEM) and Nuclear Magnetic Resonance (NMR) techniques to provide evidence that lithium plating was the primary side reaction that caused non-uniform degradation. Furthermore, it was concluded that lithium plating caused the deformation of the battery during the ageing process. Finally, the results have shown that the region with a high current density, which is the area where the most degradation occurs, shifted towards the battery centre after sheltering the tab-near regions with deposited lithium. Then, this shift in the high-current-density areas supports the idea that the degradation starts in the tab-near regions and spreads to the central areas.

The current inhomogeneities in large-format cells are discussed in many papers in the literature. Another important factor refers to the required distance for the ions to move within the battery during electrochemical reactions. In a study conducted by Zhou et al. [251], the uneven distribution of the degree of lithiation/delithiation within the cathode material has been observed. According to the authors, this distribution is generally uneven and causes particle damage, such as cracks and spraying. The authors also identified that the effect of degradation was more severe in regions close to the near flap and the bottom of the electrode, similar to the study conducted by Xie et al. [250].

Furthermore, in a work conducted by Li et al. [252], the authors investigated degradation in large-format prismatic LIBs at a preload force of 2.5 kN at 25 °C while charged and discharged, observing that degradation occurs in two stages. The first one is characterised by linear degradation, meaning that the degradation occurs at a constant rate. The second stage is characterised by a non-linear degradation, meaning the degradation rate varies, which is also referred to as rollover failure. The term “rollover” is used to describe the phenomenon where the degradation rate of the batteries increases significantly after a certain point, leading to a rapid decline in their performance. The postmortem analysis revealed that in the arched regions of the jelly roll, there were instances of lithium plating, which consists of the emergence of metallic lithium on the electrode surface.

Additionally, the cathode materials were found to be delaminated, meaning that they were separated or detached from the electrode structure. Furthermore, the SEM images showed that the graphite particles in the arched regions of the jelly roll were deformed and cracked. Moreover, it was observed that their cycle life, which is associated with the number of cycles the batteries can undergo before their performance significantly deteriorates, was reduced when the LIBs were subjected to a preloading force of 5.5 kN, evidencing that mechanical force contributes to the rollover failure. Moreover, the Shift Voltage-Resistance Voltage (SV-RV) analysis indicated that the formation of lithium plating on the electrodes typically occurs after approximately 300 charge–discharge cycles. The results showed that battery degradation in the non-linear stage is attributed to two factors: loss of active materials, which refers to the degradation or depletion of the electrode materials, and Li inventory loss. Finally, lithium inventory and active material losses comprise the primary degradation mechanisms in this stage, as these factors contribute to the increase in resistance within the battery.

In large-format cells, the non-uniform distribution of the SOC leads to local degradation, necessitating a deeper understanding to improve battery management systems. The non-uniform distribution of SOC in large-format cells mainly results from the non-uniform distribution of current during charge and discharge cycles, temperature differences that cause side reactions, and change in the voltage window within which a battery operates due to side reactions, such as passivation film formation. Side reactions can lead to an incompatibility in lithiation levels between the electrodes, increasing the risk of thermal

runaway. Furthermore, SOC window slippage is the primary reason for irreversible capacity loss in NCA-type large-format battery cells [253].

The ageing of large-format cells should be investigated under fast-charging conditions. In a study conducted by Sieg et al. [254], the authors investigated the ageing of large format cells under fast-charging conditions, showing that cell ageing is mainly due to electrolyte consumption in fast-charging scenarios. The cell's charging capacity was lost due to the metallic Li deposition and its further reaction with the electrolyte. According to the authors, the electrodes did not significantly impact the batteries' fast charging capacity. Furthermore, the authors found that battery ageing caused a significant loss of accessible cathode material, which has not been observed for anode material. These results are important for optimising the BMS design to adjust the charging currents based on the battery's health status. Furthermore, controlling the amount of electrolyte contributes to extending the useful life of the batteries.

The battery's internal impedance is also an important parameter for evaluating battery degradation. In a study conducted by Li et al. [255], the authors observed a significant degradation in pouch cells that were cycled under a high-pressure level. Furthermore, the authors reported that cell heterogeneity increases as cells age. This result is important for the second-life scenario, in which many cells with high heterogeneity are expected. Thus, BMSs for these applications must be designed to deal with these degrees of heterogeneity [22].

For small-scale LIBs, the macroscopic parameters, including material thicknesses, current collector, and separator, have not played a significant role. However, when the cells are upscaled, these dimensional parameters gain importance and cannot be neglected anymore [249]. Because of the size, inhomogeneities are also more noticeable than in small format Li-Ion cells [256].

Moreover, higher effects of inhomogeneous current distribution result when increasing the size of the cells [189,249,255,257]. Inhomogeneities in the discharge currents become apparent, particularly in the case of higher discharge rates. Especially in the cell tabs, the discharge currents are notably greater than in the surrounding area. This also results in an inhomogeneous discharge of different cell areas [258], and inhomogeneous temperature ranges across the cell co-occur with unevenly distributed discharge currents [249].

The temperature gradients within large-format battery cells profoundly impact their degradation mechanisms. The surface-to-volume ratio is reduced when the cell size increases, reducing heat dissipation efficiency, which is a phenomenon that results in elevated heat flux within the cell. Concurrently, the reduced cooling surface relative to volumetric heat generation reduces the cell's overall cooling capacity. Furthermore, the more considerable heat diffusion distances in such cells increase thermal resistance, further complicating heat removal efficiency. These factors contribute to developing temperature inhomogeneities within the cell, accelerating ageing processes such as electrolyte oxidation, SEI layer formation, and lithium plating [247]. Finally, elevated cycling temperatures facilitate local overload reactions, accelerating degradation [253].

Moreover, localised hotspots can initiate a thermal runaway, potentially due to internal short circuits, which is particularly hazardous in large format cells because of their substantial energy content. It can lead to uneven ageing across the cell, causing capacity to fade and impedance to rise, ultimately reducing the cell's lifespan and operational safety. Mitigating these thermal effects through advanced thermal management systems and cell design optimisation is essential for extending longevity and providing safety for large-format battery cells [247].

During their service life, LIBs undergo various forms of deformation, and a distinction can be made between reversible and irreversible deformation. In this context, reversible deformation is defined as the deformation during the cycling process [259], while irreversible deformation is due to degradation processes [260]. At higher levels of deformation, this can also negatively affect further degradation behaviour. Increasing deformation may cause significant mechanical stress on the cell, which can further expand the porosity of the relatively weak separators and thus accelerate degradation [261].

The study presented by Chen et al. [262] investigated the deformation behaviour of an LIB, in particular a 100 Ah prismatic cell, which indicated that the deformation over the battery is inhomogeneous. The main reasons for this were local differences in the SOC, temperature variations, and variations in stiffness between the central and border areas of the battery.

The irreversible deformation can exceed 45% of the total thickness of new cells, and aged cells can, therefore, have significant internal forces, which particularly stress the separator. These effects can thus lead to severe cell degradation, and intense deformation can be reduced by using spacers within the cell [261].

Over time, the previously described inhomogeneities in large-format Li-Ion cells can lead to localised cell ageing. This results in creating more robust and weaker regions in the cell. This leads to faster ageing compared to smaller cells, especially for large-format cells [249]. The individual packs of LIBs often have a different orientation, which results in some cell areas being wetter than others due to gravity force. It also leads to local temperature differences, which, in the long term, result in inhomogeneities in ageing. Orientation should thus also be considered in second-life application.

## 6. Discussion

### 6.1. Main Findings

Concerns regarding batteries, particularly those utilised in EVs, focus on the potential mechanical pressures induced by incidents such as vehicle collisions. Such pressures may exert force on the electrodes, resulting in their breaking or shredding across the separator. This may culminate in a short circuit within the cell, compromising its functionality. The cell short-circuit can also be caused by the separator break because of the formation of dendrites on the electrode surface, as previously detailed. Therefore, battery manufacturers design electronic circuits to control the voltage so that its value is not reduced below the cut-off voltage, so as not to make the negative electrode decompose, ensure safety, protect the cell, and increase the RUL [154].

Furthermore, a battery module in field deployments typically comprises electrochemical cells connected in series, parallel, or hybrid configurations. Different degradation rates among cells are possible in this context, and due to the degradation differences, cells in the same module may have heterogeneous SOC. Furthermore, manufacturing errors, material defects and contamination, cell architecture, and the susceptibility of large-format ion cells to mechanical, thermal, and chemical stresses can also cause variability. Generally, individual cells show performance variations depending on the operational conditions, and a battery module imbalance can result in an unequal distribution of current levels among the cells due to differences in the SOC. Then, cells that are not in synchrony with one another could experience deep discharges or operational overloads as a result of this less-than-ideal current distribution [186]. To minimise this problem, batteries are equipped with an energy management circuit that seeks to maintain the charge state of the cells uniformly. To balance the SOC of each cell, the BMS seeks to transfer the charge from the most charged cell to a less charged cell to balance the entire battery module [212].

The BMS should monitor and estimate the parameters cell by cell because a defect in only one cell compromises the performance of the entire package, jeopardising its entire package security, as the cells have different degradation levels, capacities, and loading and unloading times. Then, a cell with low capacity reaches full charge in a shorter time than non-degraded cells with nominal capacity. If there is a heterogeneous pack, i.e., composed of cells with different levels of degradation and, consequently, different capacities, the battery that has the lowest capacity achieves the state of full charge in a shorter time, and its voltage will increase beyond the limit of the cell, causing an overvoltage, and presenting a poorer performance, as degraded cells present a capacity lower than non-degraded cells and discharge faster. A protection circuit is necessary to prevent the cells from exhausting their voltage or reducing their voltage to a value lower than their threshold [263].

Thus, understanding the causes and mechanisms of degradation and how they relate to degradation modes to produce effects on batteries is fundamental for batteries utilised in EVs to be safely reused. The battery capacity reduction depends on the lithium inventory and active material losses of both electrodes, as detailed in Figure 7. Furthermore, irreversible chemical reactions cause the loss of lithium inventory in LIBs, and these reactions result in the reduction of cyclable  $\text{Li}^+$  by decreasing the number of locations available for lithium intercalation. This reduction is accompanied by the loss of active material from the electrodes, resulting in a decrease in the capacity and energy of the battery electrodes. The decrease in the number of locations available for intercalation results in a decrease in the capacity and energy of battery electrodes [226]. It is essential to observe that the loss of capacity and energy can happen side-by-side [226].

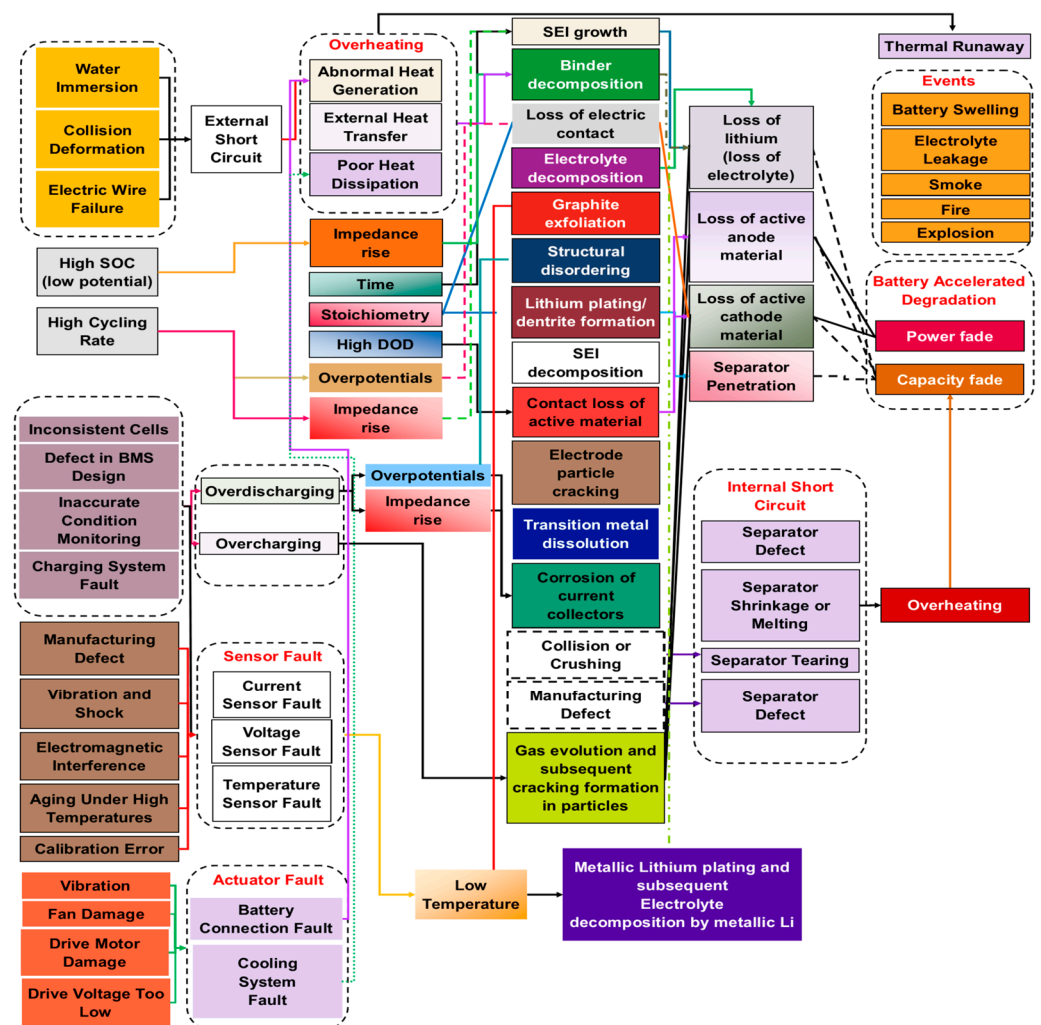


**Figure 7.** Cause and effect of lithium-ion battery degradation mechanisms related to degradation modes. Adapted with permission from ref. [97]. Copyright (2020), IEEE Xplore.

Moreover, the leading causes of battery degradation are time, high and low temperatures, high charge current, mechanical stress, and the high and low association of the cell voltage with the SOC [154]. The parameters that influence heat generation include electrolyte volume fraction, resistance, and capacity [257]. These factors should be considered to optimise the design and control of the thermal management system.

The ageing process of the cells during operation in EVs is not uniform, so the cells degrade individually. After reaching 70 to 80% of the remaining charge, some cells may suffer an abrupt fall in health when they reach 60% of SOH, causing their sudden death and making it impossible to reuse, while other cells may continue to work beyond that

limit. However, this fact is not yet clearly explained in the literature and requires future studies to explain this phenomenon [225,264,265].

Furthermore, battery manufacturers recommend discharging batteries to a cut-off voltage level to preserve the device, minimise degradation effects, reduce battery stress, preserve some energy for maintenance, and prevent self-discharge. Then, users should also follow some recommendations while charging batteries, such as charging them at a constant voltage for a specific period, allowing enough lithium amount to intercalate at the negative electrode [212].

Battery storage must also follow safety standards and protocols to prevent fires and explosions in these locations, and it is recommended that batteries are stored at low temperatures when not in operation [266]. In summary, it can be noted that batteries can age in EVs due to three main factors related to operating conditions [267]:

- Battery charging type: slower battery charging provides a lower rate of battery degradation.
- Battery composition and chemical properties: battery characteristics such as voltage level, chemistry, performance, and efficiency can influence the battery's degradation process.
- Climate: when exposed to low or high temperatures, batteries degrade quickly.

Figure 7 shows an overview of different ageing mechanisms and how they are inter-linked, evidencing the complex ageing behaviour of LIB cells and pointing out investigations that need to be performed before using second-life LIB cells. This overview helps to determine the state of used cells/batteries and distinguish which second-life application the cells can be used in. After understanding the degradation mechanisms in second-life batteries, it is plausible to understand the reuse process of this type of battery. Regarding large-format Li-Ion cells, as is often the case with EVs, it must be noted that ageing can be faster than in small cells and locally different due to inhomogeneity. Other factors, including the original orientation in the vehicle, should also be considered, as these also influence ageing behaviour.

## 6.2. Comparison with Other Studies

There is great interest in describing, understanding, and modelling battery degradation. Numerous reviews are available in the literature that discuss battery diagnosis, SOH prediction [268,269], SOX estimation [270,271], RUL estimation [272–282], battery charging, and fault prognostic methods. However, most models described in the literature are not chemical-agnostic and only extrapolate from cell to pack level. In the review study reported by Li et al. [268], the authors divided the degradation modes of batteries into loss of lithium stock, active electrode material loss, and increase in resistance. The authors also presented a short discussion on the main degradation mechanisms but approached the subject in sufficient depth to explain all the phenomena, the causes, and the forms of mitigation. Furthermore, the authors presented an interesting discussion about the techniques for establishing the SOH and the useful life of batteries.

Some reviews previously reported elsewhere [283] have presented a description of battery diagnostic methods that were categorised into empirical, model-based, data-driven, and hybrid methods. These reviews also present an excellent discussion of promising techniques for diagnosing batteries and future opportunities and challenges. However, these studies have not profoundly investigated battery degradation mechanisms, SOH estimation methods, and short-circuit diagnostic methods.

Moreover, the degradation effects of LFP-based batteries have been previously reviewed elsewhere [133], and these studies related degradation effects to the formation of cracks that increase surface roughness. These cracks are mainly formed in the first charge and discharge cycles and are accelerated at high rates of SOC and depth of discharge. These reviews have also stated that the loss of cell capacity is directly related to the degradation mechanisms at the anode.

Briefly, there are excellent review articles [217,284,285] that try to explain battery degradation phenomena. The main internal factors highlighted in the literature are (i) the loss of inventory lithium, (ii) electrode active material loss, and (iii) electrolyte conductivity decrease, resulting in capacity and power loss. The main causes reported are (i) high temperatures, (ii) high battery charge and discharge rates, and (iii) cycles with high discharge depth, voltage, and current.

### 6.3. Implication and Explanation of Findings

In general, studies are still needed to improve existing battery self-diagnosis methods. Diagnostic methods that use non-destructive techniques to avoid the need to disassemble or destroy batteries tend to be faster and cheaper and, therefore, more promising [90]. In addition, ideal batteries should be able to self-diagnose and reduce testing time and cost.

According to a work conducted by Preger et al. [286], NMC- and NCA-based cells have accelerated degradation mechanisms at high discharge depth rates, while LFP-based cells are more stable. The authors showed that cells with different chemistry are influenced by temperature in different ways. LFP cells suffer a more significant capacity loss than NMC and NCA cells when exposed to high or low temperatures. Therefore, efficient thermal management is essential to extend the useful life of batteries and ensure that the cells will have the ideal conditions for a second use.

Understanding the ageing mechanisms of batteries becomes easier with understanding the factors that cause the establishment of the SEI. The existing works in the literature [286] report that the change of positive potential in the anode causes an overload in the cathode material, accelerating its degradation. The loss of capacity of LIBs is related to the loss of oxygen and the loss of free Li in the SEI. Hopefully, these phenomena can be mitigated with the use of solid electrolytes.

Data extracted from the literature have shown that battery control systems must be appropriately designed to guarantee that the batteries will operate within the appropriate temperature, voltage, current, and SOC limits. In this way, it is possible to avoid overload, over-discharge, short circuits, electrolyte leakage, thermal runaway, and accelerated degradation [97]. However, battery modelling is challenging because (i) the degradation mechanisms are non-linear and the parameters are time-varying, (ii) the internal states of the battery can only be measured indirectly, and (iii) the high variability of cells and constant change of technology make it challenging to extrapolate the model from the cell level to the pack level [32]. Furthermore, different LIB operating scenarios produce different degradation phenomena and must be carefully described, as each application has different protocols for loading, unloading (direction), and resting time [198].

In the case of EVs, parameters such as driving habits, driving frequency, ambient temperature, charging habits, road conditions, and terrain conditions can influence LIBs' degradation mechanisms [198]. Commercial chargers generally use the CCCV protocol to charge batteries. According to recent studies [287], the utilisation of pulse current for battery charging and discharging has enhanced the safety and stability of the batteries. Furthermore, pulse currents have advantages over existing charging protocols because they balance charge diffusion and electron transfer rates. Pulse charging can effectively prevent the formation of dendrites, which are known to form during charging and can cause short circuits that may result in thermal runaway, which occurs due to the deposition of  $\text{Li}^+$  on the anode, creating an uneven surface and forming dendrites. Pulse charging mitigates this issue by limiting the number of  $\text{Li}^+$  deposited on the anode at any given time, thereby reducing the likelihood of dendrite formation. Pulse protocols can also regulate the temperature of the battery, which is a critical factor that can impact the battery's safety and stability. Pulse protocols can help to reduce the heat generated by the battery, and prevent temperature spikes that can result in thermal runaway, by limiting the amount of charge or discharge that occurs at any given time [287].

Furthermore, pulse protocols can optimise the charging and discharging rates and patterns to improve the efficiency and performance of the battery. Pulse protocols can also increase the overall efficiency of the battery, resulting in a longer battery life and improved performance, by reducing energy losses during charge–discharge cycles. In brief, pulse current charging and discharging protocols offer several advantages over existing battery charge–discharge protocols, including mitigating dendrite formation, regulating battery temperature, and optimising battery efficiency and performance. However, new loading protocols have been investigated to mitigate degradation mechanisms and reduce loading time. Despite the efforts of the scientific community to unravel the degradation mechanisms of batteries, further studies must be conducted to better comprehend the degradation mechanisms in fast-charging scenarios.

In summary, stationary applications may experience less frequent and less severe temperature fluctuations compared to EVs, potentially leading to slower SEI degradation. EV applications involve more dynamic operating conditions, including variable loads and temperatures, which can accelerate SEI degradation. Low-range vehicles may have shorter and less intense usage cycles, possibly resulting in a different SEI degradation pattern compared to EVs.

#### 6.4. Strengths and Limitations

This systematic review comprehensively describes the main phenomena that cause battery degradation, focusing on LIBs. This paper also discusses the main differences between the degradation of batteries applied for EVs and other applications, such as portable electronics. This systematic review does not discuss the degradation mechanisms that occur in solid-state batteries. However, the authors encourage the development of new studies that seek to understand and describe the phenomena that occur at the electrolyte–electrode interface of this category of battery.

The diversity of battery chemistry, format, and application poses several challenges in describing battery degradation phenomena which can affect the safety and reliability of these ESSs. Moreover, new studies must be carried out to describe battery degradation phenomena and produce high-fidelity models agnostic to chemistry. Diagnosis and self-diagnosis of battery health status in real-time are still limited due to a lack of quality data and the low processing capacity of current computers.

Additional research is needed to investigate how smart sensors can contribute to data acquisition capable of updating real-time battery models. These models can be robust and consider the uncertainties of electronic and battery components. Furthermore, machine-learning algorithms are an alternative to estimate battery health and system confidence levels, predict severe failures, and provide predictive maintenance services.

#### 6.5. Current Problems and Future Research Directions

Due to the numerous battery deterioration mechanisms that influence the modules, it is still difficult to establish the SOH of batteries at the pack level. The degradation of batteries is not uniform, resulting in an electrical imbalance between cells [24].

These factors assume more significant concern in rapid charging settings, characterised by increased battery charging rates, a trend that is expected to become increasingly prevalent. The precise prediction of battery health state is of utmost importance to mitigate the necessity of costly, time-consuming, and hazardous battery disassembly procedures. This necessitates the development of robust battery-aging models [24].

Battery degradation is a complex phenomenon that arises due to several parameters, including temperature, SOC, cycling frequency, and chemical reactions within the battery. The most promising research problems in this area include the following:

- Elucidating the degradation mechanisms: battery degradation mechanisms are still not fully understood. Developing accurate models and simulation tools that can

explain the physical and chemical processes responsible for degradation is a crucial research problem.

- Developing advanced battery materials: novel materials with high stability and degradation resistance are required to enhance battery performance and durability. Advanced cathode materials and solid-state electrolytes are currently being studied for this purpose.
- Developing effective BMSs: BMSs are crucial to ensure safe and optimal battery operation. Developing new algorithms and control strategies to optimise battery performance and mitigate degradation is a pressing research problem.
- Developing reliable testing methodologies: accurate measurement of battery degradation is critical to developing effective strategies to combat it. Developing testing methods that provide accurate and dependable battery performance and degradation measurements is a critical research problem.
- Developing predictive models: predictive models anticipating battery performance and degradation are needed to create effective maintenance and replacement strategies. Developing models that can account for various parameters that influence battery degradation, such as temperature, cycling frequency, and SOC, is an essential research problem.

In recent years, several new research topics have emerged that seek to deepen our understanding of battery degradation and develop strategies to mitigate its effects. Some of the newest issues related to battery degradation include the following:

- Studying the effects of fast charging: fast charging is becoming increasingly popular, but it can also accelerate battery degradation. Researchers are investigating the influence of fast charging on different types of batteries and analysing how it affects battery degradation. Researchers aim to develop new charging strategies to minimise battery degradation by studying the fundamental mechanisms of fast charging.
- Investigating the effects of ageing on batteries: researchers have explored advanced characterisation techniques to gain more precise insights into the formation and composition of the SEI layer, co-intercalation phenomena and  $\text{Li}^+$  diffusion from the electrolyte to graphite bulk, and principles for designing anode materials, electrolytes, and cellular structure. Researchers are exploring the mechanisms behind ageing and developing models to predict how batteries degrade over time. Then, researchers can develop strategies to extend battery life by understanding the factors that contribute to battery ageing.
- Developing recycling and second-life strategies: battery recycling is an important issue, as batteries contain valuable materials that can be reused [22]. However, the degradation of these materials can make recycling difficult. Researchers are developing new recycling strategies that can recover valuable materials from degraded batteries and are exploring second-life strategies that can extend the batteries lifespan.
- Investigating the effects of extreme temperatures: temperature significantly impacts battery degradation, and extreme temperatures can accelerate the degradation process. Researchers are studying the mechanisms behind temperature-induced battery degradation and developing strategies to mitigate its effects. Researchers can develop new battery materials and cooling strategies to minimise temperature-related degradation by analysing how temperature affects the chemical reactions within batteries.
- Developing machine-learning models for predicting battery degradation: machine-learning models are an alternative to predicting battery degradation and optimising battery performance. Researchers are developing new machine-learning models that can account for various factors contributing to battery degradation, such as temperature, cycling frequency, and SOC. Researchers can develop effective maintenance and replacement strategies by accurately predicting battery degradation.

## 7. Conclusions

Hopefully, LIBs can be used in EVs and stationary applications, such as microgrids, power tools, short-range vehicles, ships, and grid-connected applications. The degradation mechanisms that occur in batteries can be accelerated depending on the application. The accelerated degradation of batteries can lead to severe safety failures, cause accidents, and increase the safety risk of people and equipment. Therefore, understanding battery degradation mechanisms is critical to increasing safety and reliability and extending battery life.

However, mitigating the effects of battery degradation is challenging. Despite the relevance of this subject to the scientific community and industry, a review of recent discoveries in this field was needed. Therefore, this paper provides a comprehensive and didactic review of battery degradation mechanisms. The systematic review also provides some recommendations for EV owners, and it highlights the factors that affect these equipments' health, aiming to minimise battery degradation mechanisms and reduce damage. In addition, we hope it can support companies interested in improving existing BMS and user manuals. Updating user manuals is essential to avoid contradictory information incompatible with battery behaviour, preserving your customer's life.

The results of the work highlight an increased understanding of how battery degradation mechanisms influences each other and occur on a microscopic scale. Some phenomena that occur mainly in the SEI or CEI layers are poorly understood and need further investigation. The results show that several factors can accelerate battery degradation, including operating conditions, temperature, SOC, DOD, voltage, and current. All battery components are affected by calendar ageing and cyclic ageing.

Knowledge of battery degradation mechanisms helps to understand batteries' behaviour when operating on EVs and a second application. From this, it is possible to control the conditions of use and the parameters of the batteries to minimise the mechanisms of battery degradation, maximising and predicting their helpful life in both the first life (for EVs) and the second life (for secondary applications).

Extending the life of EV batteries enables company revenue because the longer the batteries operate on EVs, the greater the product's added value and the lower the recycling costs. It is also possible to generate value for the environment by reducing the number of batteries that will achieve their end of life and will be discarded in the environment or recycled.

This systematic review aims to stimulate future studies investigating the degradation mechanisms, particularly the SEI and CEI layers, describing each phenomenon more reliably. The results show the need to understand battery degradation mechanisms for developing new BMS that are battery agnostic and easily adaptable to second-life batteries. There are still many gaps to be filled, and more studies are needed to clarify the mechanisms of battery degradation and how to manage them for companies and users. In this way, it will be possible for companies to improve the existing manuals and devise new materials to instruct EV owners on how to operate the vehicle or system to maximise its use and avoid accidents.

**Author Contributions:** H.Z., E.R.S., P.G. and H.-G.S. proposed the concept and were the supervisors of the work. They were responsible for project administration and funding acquisition. C.A.R.J. wrote the first draft of this manuscript. E.R.S., P.G., D.K., H.-G.S. and H.Z. co-wrote the manuscript. All authors participated in data analysis and manuscript discussion. All authors have read and agreed to the published version of the manuscript.

**Funding:** C.A.R.J. and H.Z. would like to thank financial CNPq (159332/2019-2). M.M.A. and H.Z. would like to acknowledge the financial support from the Sao Paulo Research Foundation (FAPESP, grant number: 2021/09387-1). H.Z. would like to thank the Total Energies company through ANP (Brazil's National Oil, Natural Gas, and Biofuels Agency), who funded part of this research. E.R.S. and P.G. would like to thank the BloRin Project—"Blockchain for renewables decentralized management", PO FESR Sicilia 2014/2020—Action 1.1.5—identification code: SI\_1\_23074 CUP: G79J18000680007 for all the support given to the authors. C.A.R.J. and H.-G.S. would like to thank the financial support from the Bavarian Ministry of Economic Affairs, Regional Development, and Energy in the program BayVFP Digitalisierung, grant number DIK0384/02.

**Conflicts of Interest:** The authors declare no conflicts of interest.

## References

1. Sun, C.; Negro, E.; Vezzù, K.; Pagot, G.; Cavinato, G.; Nale, A.; Herve Bang, Y.; Di Noto, V. Hybrid Inorganic-Organic Proton-Conducting Membranes Based on SPEEK Doped with WO<sub>3</sub> Nanoparticles for Application in Vanadium Redox Flow Batteries. *Electrochim. Acta* **2019**, *309*, 311–325.
2. Song, K.; Lan, Y.; Zhang, X.; Jiang, J.; Sun, C.; Yang, G.; Yang, F.; Lan, H. A Review on Interoperability of Wireless Charging Systems for Electric Vehicles. *Energies* **2023**, *16*, 1653.
3. Yang, F.; Xie, Y.; Deng, Y.; Yuan, C. Predictive Modeling of Battery Degradation and Greenhouse Gas Emissions from U.S. State-Level Electric Vehicle Operation. *Nat. Commun.* **2018**, *9*, 2429.
4. Glaeser, E.L.; Kahn, M.E. The Greenness of Cities: Carbon Dioxide Emissions and Urban Development. *J. Urban Econ.* **2010**, *67*, 404–418.
5. Chu, S.; Majumdar, A. Opportunities and Challenges for a Sustainable Energy Future. *Nature* **2012**, *488*, 294–303.
6. Wanitschke, A.; Hoffmann, S. Are Battery Electric Vehicles the Future? An Uncertainty Comparison with Hydrogen and Combustion Engines. *Environ. Innov. Soc. Transit.* **2020**, *35*, 509–523.
7. Zhou, W.; Cleaver, C.J.; Dunant, C.F.; Allwood, J.M.; Lin, J. Cost, Range Anxiety and Future Electricity Supply: A Review of How Today's Technology Trends May Influence the Future Uptake of BEVs. *Renew. Sustain. Energy Rev.* **2023**, *173*, 113074.
8. EC Regulation (EU) 2019/631 of the 2019/631 of the European Parliament and of the Council of 17 April 2019 Setting CO<sub>2</sub> Emission Performance Standards for New Passenger Cars and for New Light Commercial Vehicles, and Repealing Regulations (EC) No 443/2009 and (EU) No 510/2011. *Off. J. Eur. Union L* **2021**, *111*, 13.
9. Greene, D.L.; Park, S.; Liu, C. Public Policy and the Transition to Electric Drive Vehicles in the U.S.: The Role of the Zero Emission Vehicles Mandates. *Energy Strat. Rev.* **2014**, *5*, 66–77.
10. Li, C.; Negnevitsky, M.; Wang, X.; Yue, W.L.; Zou, X. Multi-Criteria Analysis of Policies for Implementing Clean Energy Vehicles in China. *Energy Policy* **2019**, *129*, 826–840.
11. Åhman, M. Government Policy and the Development of Electric Vehicles in Japan. *Energy Policy* **2006**, *34*, 433–443.
12. Liu, Z.; Qian, Q.; Hu, B.; Shang, W.-L.; Li, L.; Zhao, Y.; Zhao, Z.; Han, C. Government Regulation to Promote Coordinated Emission Reduction among Enterprises in the Green Supply Chain Based on Evolutionary Game Analysis. *Resour. Conserv. Recycl.* **2022**, *182*, 106290.
13. Yu, H.; Jiang, Y.; Zhang, Z.; Shang, W.-L.; Han, C.; Zhao, Y. The Impact of Carbon Emission Trading Policy on Firms' Green Innovation in China. *Financ. Innov.* **2022**, *8*, 55. <https://doi.org/10.1186/s40854-022-00359-0>.
14. Dunn, B.; Kamath, H.; Tarascon, J.-M. Electrical Energy Storage for the Grid: A Battery of Choices. *Science* **2011**, *334*, 928–935.
15. Nykvist, B.; Nilsson, M. Rapidly Falling Costs of Battery Packs for Electric Vehicles. *Nat. Clim. Change* **2015**, *5*, 329–332.
16. Schmich, R.; Wagner, R.; Hörpel, G.; Placke, T.; Winter, M. Performance and Cost of Materials for Lithium-Based Rechargeable Automotive Batteries. *Nat. Energy* **2018**, *3*, 267–278.
17. Severson, K.A.; Attia, P.M.; Jin, N.; Perkins, N.; Jiang, B.; Yang, Z.; Chen, M.H.; Aykol, M.; Herring, P.K.; Fraggedakis, D.; et al. Data-Driven Prediction of Battery Cycle Life before Capacity Degradation. *Nat. Energy* **2019**, *4*, 383–391.
18. Guo, J.; Yang, J.; Cao, W.; Serrano, C. Evaluation of EV Battery Degradation under Different Charging Strategies and V2G Schemes. In Proceedings of the 8th Renewable Power Generation Conference (RPG 2019), Institution of Engineering and Technology, Shanghai, China, 24–25 October 2019.
19. Chen, H.; Shen, J. A Degradation-Based Sorting Method for Lithium-Ion Battery Reuse. *PLoS ONE* **2017**, *12*, e0185922.
20. Lucu, M.; Martinez-Laserna, E.; Gandiaga, I.; Camblong, H. A Critical Review on Self-Adaptive Li-Ion Battery Ageing Models. *J. Power Sources* **2018**, *401*, 85–101.
21. Rufino Júnior, C.A.; Riva Sanseverino, E.; Gallo, P.; Koch, D.; Kotak, Y.; Schweiger, H.-G.; Zanin, H. Towards a Business Model for Second-Life Batteries—Barriers, Opportunities, Uncertainties, and Technologies. *J. Energy Chem.* **2023**, *78*, 507–525.
22. Rufino Júnior, C.A.; Riva Sanseverino, E.; Gallo, P.; Koch, D.; Diel, S.; Walter, G.; Trilla, L.; Ferreira, V.J.; Pérez, G.B.; Kotak, Y.; et al. Towards to Battery Digital Passport: Reviewing Regulations and Standards for Second-Life Batteries. *Batteries* **2024**, *10*, 115.
23. Naseri, F.; Schaltz, E.; Stroe, D.-I.; Gismero, A.; Farjah, E. An Enhanced Equivalent Circuit Model with Real-Time Parameter Identification for Battery State-of-Charge Estimation. *IEEE Trans. Ind. Electron.* **2022**, *69*, 3743–3751.
24. Harper, G.D.J.; Kendrick, E.; Anderson, P.A.; Mroziak, W.; Christensen, P.; Lambert, S.; Greenwood, D.; Das, P.K.; Ahmeid, M.; Milojevic, Z.; et al. Roadmap for a Sustainable Circular Economy in Lithium-Ion and Future Battery Technologies. *J. Phys. Energy* **2023**, *5*, 021501.
25. Júnior, C.A.R.; Sanseverino, E.R.; Gallo, P.; Koch, D.; Schweiger, H.G.; Zanin, H. Blockchain Review for Battery Supply Chain Monitoring and Battery Trading. *Renew. Sustain. Energy Rev.* **2022**, *157*, 112078.
26. Rauhala, T. *Electrochemical Studies on Degradation Mechanisms of Electrode Materials in Lithium-Ion Batteries*, School of Chemical Technology, Aalto University: Espoo, Finland, 2020.
27. Liu, D.; Shadike, Z.; Lin, R.; Qian, K.; Li, H.; Li, K.; Wang, S.; Yu, Q.; Liu, M.; Ganapathy, S.; et al. Review of Recent Development of in Situ/Operando Characterization Techniques for Lithium Battery Research. *Adv. Mater.* **2019**, *31*, e1806620.
28. Braithwaite, J.W. Corrosion of Lithium-Ion Battery Current Collectors. *J. Electrochem. Soc.* **1999**, *146*, 448.
29. Christensen, J.; Newman, J. Cyclable Lithium and Capacity Loss in Li-Ion Cells. *J. Electrochem. Soc.* **2005**, *152*, A818.

30. Vetter, J.; Novák, P.; Wagner, M.R.; Veit, C.; Möller, K.-C.; Besenhard, J.O.; Winter, M.; Wohlfahrt-Mehrens, M.; Vogler, C.; Hammouche, A. Ageing Mechanisms in Lithium-Ion Batteries. *J. Power Sources* **2005**, *147*, 269–281.
31. Singh, S.; Weeber, M.; Birke, K.P. Implementation of Battery Digital Twin: Approach, Functionalities and Benefits. *Batteries* **2021**, *7*, 78.
32. Wang, Y.; Tian, J.; Sun, Z.; Wang, L.; Xu, R.; Li, M.; Chen, Z. A Comprehensive Review of Battery Modeling and State Estimation Approaches for Advanced Battery Management Systems. *Renew. Sustain. Energy Rev.* **2020**, *131*, 110015.
33. Meng, J.; Luo, G.; Ricco, M.; Swierczynski, M.; Stroe, D.-I.; Teodorescu, R. Overview of Lithium-Ion Battery Modeling Methods for State-of-Charge Estimation in Electrical Vehicles. *Appl. Sci.* **2018**, *8*, 659.
34. Falconi, A. Electrochemical Li-Ion Battery Modeling for Electric Vehicles. Doctoral Dissertation, Communauté Université Grenoble Alpes, Saint-Martin-d'Hères, France, 2017.
35. Wu, L.; Pang, H.; Geng, Y.; Liu, X.; Liu, J.; Liu, K. Low-complexity State of Charge and Anode Potential Prediction for Lithium-Ion Batteries Using a Simplified Electrochemical Model-based Observer under Variable Load Condition. *Int. J. Energy Res.* **2022**, *46*, 11834–11848.
36. Yu, H.; Zhang, L.; Wang, W.; Yang, K.; Zhang, Z.; Liang, X.; Chen, S.; Yang, S.; Li, J.; Liu, X. Lithium-Ion Battery Multi-Scale Modeling Coupled with Simplified Electrochemical Model and Kinetic Monte Carlo Model. *iScience* **2023**, *26*, 107661.
37. Louis, S.-Y.; Siriwardane, E.M.D.; Joshi, R.P.; Omeel, S.S.; Kumar, N.; Hu, J. Accurate Prediction of Voltage of Battery Electrode Materials Using Attention-Based Graph Neural Networks. *ACS Appl. Mater. Interfaces* **2022**, *14*, 26587–26594.
38. Trembacki, B.L.; Vadakkepatt, A.; Roberts, S.A.; Murthy, J.Y. Volume-Averaged Electrochemical Performance Modeling of 3D Interpenetrating Battery Electrode Architectures. *J. Electrochem. Soc.* **2020**, *167*, 013507.
39. Chen, Z.; Danilov, D.L.; Eichel, R.-A.; Notten, P.H.L. Porous Electrode Modeling and Its Applications to Li-ion Batteries. *Adv. Energy Mater.* **2022**, *12*, 2201506.
40. Zhu, G.; Wu, Z.; Ren, X.; Wang, J.V.; Kang, J.; Wang, Q.; Deng, X. A Self-Correction Single Particle Model of Lithium-Ion Battery Based on Multi-Population Genetic Algorithm. *J. Energy Storage* **2023**, *71*, 108005.
41. Wett, C.; Ganuza, C.; Ayerbe, E.; Turan, B.; Schwunk, S. Method of Lines for Flexible Coupling of the Single Particle Model for Lithium-Ion Batteries Demonstrated by Thermal Modelling. *J. Energy Storage* **2023**, *68*, 107459.
42. Trivella, A.; Corno, M.; Radrizzani, S.; Savaresi, S.M. Non-Invasive Experimental Identification of a Single Particle Model for LiFePO<sub>4</sub> Cells. *arXiv* **2023**, arXiv:2306.14195.
43. Chundru, V.R.; Downing, W.D.; Sarlashkar, J.; Surampudi, B. Extension of Single Particle Model with Electrolyte and Temperature (SPMeT) for Real-Time Performance and Safety Monitoring of Battery Energy Storage Systems (BESS) in Grid Service. In Proceedings of the 2023 IEEE International Systems Conference (SysCon), Vancouver, BC, Canada, 17–20 April 2023; IEEE: Piscataway, NJ, USA, 2023.
44. Elmahallawy, M.; Elfouly, T.; Alouani, A.; Massoud, A.M. A Comprehensive Review of Lithium-Ion Batteries Modeling, and State of Health and Remaining Useful Lifetime Prediction. *IEEE Access* **2022**, *10*, 119040–119070.
45. Xu, B.; Oudalov, A.; Ulbig, A.; Andersson, G.; Kirschen, D.S. Modeling of Lithium-Ion Battery Degradation for Cell Life Assessment. *IEEE Trans. Smart Grid* **2018**, *9*, 1131–1140.
46. Zheng, Y.; Qin, C.; Lai, X.; Han, X.; Xie, Y. A Novel Capacity Estimation Method for Lithium-Ion Batteries Using Fusion Estimation of Charging Curve Sections and Discrete Arrhenius Aging Model. *Appl. Energy* **2019**, *251*, 113327.
47. Moore, S.; Eshani, M. An Empirically Based Electrode Horizon Lead-Acid Battery Model. In *Proceedings of the SAE Technical Paper Series*; SAE International: Warrendale, PA, USA, 1996.
48. Manwell, J.; McGowan, J.G. Extension of the Kinetic Battery Model for Wind/Hybrid Power Systems. *Proc. EWEC* **1994**, *3*, 284–289.
49. Unnewehr, L.E.; Nasar, S.A. *Electric Vehicle Technology*; Wiley: Hoboken, NJ, USA, 1982; ISBN 9780471083788.
50. Fang, H.; Zhao, X.; Wang, Y.; Sahinoglu, Z.; Wada, T.; Hara, S.; de Callafon, R.A. State-of-Charge Estimation for Batteries: A Multi-Model Approach. In Proceedings of the 2014 American Control Conference, Portland, OR, USA, 4–6 June 2014; IEEE: Piscataway, NJ, USA, 2014.
51. Manwell, J.F.; McGowan, J.G. Lead Acid Battery Storage Model for Hybrid Energy Systems. *Sol. Energy* **1993**, *50*, 399–405.
52. Tremblay, O.; Dessaint, L.-A. Experimental Validation of a Battery Dynamic Model for EV Applications. *World Electric Veh. J.* **2009**, *3*, 289–298.
53. Tremblay, O.; Dessaint, L.-A.; Dekkiche, A.-I. A Generic Battery Model for the Dynamic Simulation of Hybrid Electric Vehicles. In Proceedings of the 2007 IEEE Vehicle Power and Propulsion Conference, Arlington, TX, USA, 9–12 September 2007; IEEE: Piscataway, NJ, USA, 2007.
54. Zhang, Y.; Lyden, S.; de la Barra, B.A.L.; Haque, M.E. Optimization of Tremblay's Battery Model Parameters for Plug-in Hybrid Electric Vehicle Applications. In Proceedings of the 2017 Australasian Universities Power Engineering Conference (AUPEC), Melbourne, VIC, Australia, 19–22 November 2017; IEEE: Piscataway, NJ, USA, 2017.
55. Hu, X.; Sun, F.; Zou, Y.; Peng, H. Online Estimation of an Electric Vehicle Lithium-Ion Battery Using Recursive Least Squares with Forgetting. In Proceedings of the 2011 American Control Conference, San Francisco, CA, USA, 29 June–1 July 2011; IEEE: Piscataway, NJ, USA, 2011.
56. Plett, G. *Battery Management Systems, Volume I: Battery Modeling*; Artech: Norwood, MA, USA, 2015.

57. Seidl, C.; Kathan, J.; Lauss, G.; Lehfuss, F. Power Hardware-in-the-Loop Implementation and Verification of a Real Time Capable Battery Model. In Proceedings of the 2014 IEEE 23rd International Symposium on Industrial Electronics (ISIE), Istanbul, Turkey, 1–4 June 2014; IEEE: Piscataway, NJ, USA, 2014.
58. Seidl, C.; Kathan, J.; Lauss, G.; Lehfuss, F. Selection and Implementation of a Generic Battery Model for PHIL Applications. In Proceedings of the IECON 2013—39th Annual Conference of the IEEE Industrial Electronics Society, Vienna, Austria, 10–13 November 2013; IEEE: Piscataway, NJ, USA, 2013.
59. Plett, G.L. Extended Kalman Filtering for Battery Management Systems of LiPB-Based HEV Battery Packs. *J. Power Sources* **2004**, *134*, 262–276.
60. Ecker, M.; Gerschler, J.B.; Vogel, J.; Käbitz, S.; Hust, F.; Dechent, P.; Sauer, D.U. Development of a Lifetime Prediction Model for Lithium-Ion Batteries Based on Extended Accelerated Aging Test Data. *J. Power Sources* **2012**, *215*, 248–257.
61. Attidekou, P.S.; Milojevic, Z.; Muhammad, M.; Ahmeid, M.; Lambert, S.; Das, P.K. Methodologies for Large-Size Pouch Lithium-Ion Batteries End-of-Life Gateway Detection in the Second-Life Application. *J. Electrochem. Soc.* **2020**, *167*, 160534.
62. Guo, J.; Che, Y.; Pedersen, K.; Stroe, D.-I. Battery Impedance Spectrum Prediction from Partial Charging Voltage Curve by Machine Learning. *J. Energy Chem.* **2023**, *79*, 211–221.
63. Hosen, M.S.; Pirooz, A.; Kalogiannis, T.; He, J.; Van Mierlo, J.; Berecibar, M. A Strategic Pathway from Cell to Pack-Level Battery Lifetime Model Development. *Appl. Sci.* **2022**, *12*, 4781.
64. Wu, G.; Lu, R.; Zhu, C.; Chan, C.C. An Improved Ampere-Hour Method for Battery State of Charge Estimation Based on Temperature, Coulomb Efficiency Model and Capacity Loss Model. In Proceedings of the 2010 IEEE Vehicle Power and Propulsion Conference, Lille, France, 1–3 September 2010; IEEE: Piscataway, NJ, USA, 2010.
65. Zhang, X.; Hou, J.; Wang, Z.; Jiang, Y. Study of SOC Estimation by the Ampere-Hour Integral Method with Capacity Correction Based on LSTM. *Batteries* **2022**, *8*, 170.
66. Xiao, F.; Li, C.; Fan, Y.; Yang, G.; Tang, X. State of Charge Estimation for Lithium-Ion Battery Based on Gaussian Process Regression with Deep Recurrent Kernel. *Int. J. Electr. Power Energy Syst.* **2021**, *124*, 106369.
67. Ren, X.; Liu, S.; Yu, X.; Dong, X. A Method for State-of-Charge Estimation of Lithium-Ion Batteries Based on PSO-LSTM. *Energy* **2021**, *234*, 121236.
68. Liu, Z.; Zhe, L.; Zhang, J. Alternate Adaptive Extended Kalman Filter and Ampere-Hour Counting Method to Estimate the State of Charge. In Proceedings of the 2018 IEEE International Power Electronics and Application Conference and Exposition (PEAC), Shenzhen, China, 4–7 November 2018; IEEE: Piscataway, NJ, USA, 2018.
69. Huang, C.-S. A Lithium-Ion Batteries Fault Diagnosis Method for Accurate Coulomb Counting State-of-Charge Estimation. *J. Electr. Eng. Technol.* **2024**, *19*, 433–442. <https://doi.org/10.1007/s42835-023-01533-9>.
70. Zine, B.; Bia, H.; Benmouna, A.; Becherif, M.; Iqbal, M. Experimentally Validated Coulomb Counting Method for Battery State-of-Charge Estimation under Variable Current Profiles. *Energies* **2022**, *15*, 8172.
71. Zine, B.; Marouani, K.; Becherif, M.; Yahmedi, S. Estimation of Battery Soc for Hybrid Electric Vehicle Using Coulomb Counting Method. *Int. J. Emerg. Electr. Power Syst.* **2018**, *19*, 20170181. <https://doi.org/10.1515/ijeeps-2017-0181>.
72. Movassagh, K.; Raihan, A.; Balasingam, B.; Pattipati, K. A Critical Look at Coulomb Counting Approach for State of Charge Estimation in Batteries. *Energies* **2021**, *14*, 4074.
73. Wang, S.; Fernandez, C.; Yu, C.; Fan, Y.; Cao, W.; Stroe, D.-I. A Novel Charged State Prediction Method of the Lithium Ion Battery Packs Based on the Composite Equivalent Modeling and Improved Splice Kalman Filtering Algorithm. *J. Power Sources* **2020**, *471*, 228450.
74. Feng, X.; Weng, C.; He, X.; Wang, L.; Ren, D.; Lu, L.; Han, X.; Ouyang, M. Incremental Capacity Analysis on Commercial Lithium-Ion Batteries Using Support Vector Regression: A Parametric Study. *Energies* **2018**, *11*, 2323.
75. Tang, X.; Liu, K.; Lu, J.; Liu, B.; Wang, X.; Gao, F. Battery Incremental Capacity Curve Extraction by a Two-Dimensional Luenberger–Gaussian-Moving-Average Filter. *Appl. Energy* **2020**, *280*, 115895.
76. Kato, H.; Kobayashi, Y.; Miyashiro, H. Differential Voltage Curve Analysis of a Lithium-Ion Battery during Discharge. *J. Power Sources* **2018**, *398*, 49–54.
77. Lewerenz, M.; Marongiu, A.; Warnecke, A.; Sauer, D.U. Differential Voltage Analysis as a Tool for Analyzing Inhomogeneous Aging: A Case Study for LiFePO<sub>4</sub>|Graphite Cylindrical Cells. *J. Power Sources* **2017**, *368*, 57–67.
78. Sihvo, J.; Roinila, T.; Stroe, D.-I. Novel Fitting Algorithm for Parametrization of Equivalent Circuit Model of Li-Ion Battery from Broadband Impedance Measurements. *IEEE Trans. Ind. Electron.* **2021**, *68*, 4916–4926.
79. Sui, X.; He, S.; Stroe, D.-I.; Huang, X.; Meng, J.; Teodorescu, R. A Review of Sliding Mode Observers Based on Equivalent Circuit Model for Battery SoC Estimation. In Proceedings of the 2019 IEEE 28th International Symposium on Industrial Electronics (ISIE), Vancouver, BC, Canada, 12–14 June 2019; IEEE: Piscataway, NJ, USA, 2019.
80. Guo, R.; Shen, W. A Review of Equivalent Circuit Model Based Online State of Power Estimation for Lithium-Ion Batteries in Electric Vehicles. *Vehicles* **2021**, *4*, 1–31.
81. Brosa Planella, F.; Ai, W.; Boyce, A.M.; Ghosh, A.; Korotkin, I.; Sahu, S.; Sulzer, V.; Timms, R.; Tranter, T.G.; Zyskin, M.; et al. A Continuum of Physics-Based Lithium-Ion Battery Models Reviewed. *Prog. Energy* **2022**, *4*, 042003.
82. Mckay, M.B.; Wetton, B.; Gopaluni, R.B. Learning Physics Based Models of Lithium-Ion Batteries. *IFAC-PapersOnLine* **2021**, *54*, 97–102.
83. Pozzato, G.; Onori, S. Combining Physics-Based and Machine Learning Methods to Accelerate Innovation in Sustainable Transportation and beyond: A Control Perspective. *arXiv* **2023**, arXiv:2305.04840.

84. Liu, X.; Zhang, X.-Q.; Chen, X.; Zhu, G.-L.; Yan, C.; Huang, J.-Q.; Peng, H.-J. A Generalizable, Data-Driven Online Approach to Forecast Capacity Degradation Trajectory of Lithium Batteries. *J. Energy Chem.* **2022**, *68*, 548–555.
85. Ma, L.; Zhang, T. Deep Learning-Based Battery State of Charge Estimation: Enhancing Estimation Performance with Unlabelled Training Samples. *J. Energy Chem.* **2023**, *80*, 48–57.
86. Xiong, R.; Tian, J.; Shen, W.; Lu, J.; Sun, F. Semi-Supervised Estimation of Capacity Degradation for Lithium Ion Batteries with Electrochemical Impedance Spectroscopy. *J. Energy Chem.* **2023**, *76*, 404–413.
87. Chen, C.; Xiong, R.; Yang, R.; Li, H. A Novel Data-Driven Method for Mining Battery Open-Circuit Voltage Characterization. *Green Energy Intell. Transp.* **2022**, *1*, 100001.
88. Liu, M.; Xu, J.; Jiang, Y.; Mei, X. Multi-Dimensional Features Based Data-Driven State of Charge Estimation Method for LiFePO<sub>4</sub> Batteries. *Energy* **2023**, *274*, 127407.
89. Seh, Z.W. Interpretable Hybrid Machine Learning Demystifies the Degradation of Practical Lithium–Sulfur Batteries. *J. Energy Chem.* **2023**, *79*, 54–55.
90. Ando, K.; Matsuda, T.; Imamura, D. Degradation Diagnosis of Lithium-Ion Batteries Using AC Impedance Technique in Fixing the State of Charge of an Electrode. *J. Energy Chem.* **2021**, *53*, 285–289.
91. Ji, S.; Zhu, J.; Lyu, Z.; You, H.; Zhou, Y.; Gu, L.; Qu, J.; Xia, Z.; Zhang, Z.; Dai, H. Deep Learning Enhanced Lithium-Ion Battery Nonlinear Fading Prognosis. *J. Energy Chem.* **2023**, *78*, 565–573.
92. Galatro, D.; Silva, C.D.; Romero, D.A.; Trescases, O.; Amon, C.H. Challenges in Data-based Degradation Models for Lithium-ion Batteries. *Int. J. Energy Res.* **2020**, *44*, 3954–3975.
93. Zhou, Y.; Huang, M. Lithium-Ion Batteries Remaining Useful Life Prediction Based on a Mixture of Empirical Mode Decomposition and ARIMA Model. *Microelectron. Reliab.* **2016**, *65*, 265–273.
94. Cao, L.; Xu, R.; Bi, Y. Research on Life Prediction of Lithium-Ion Battery Based on WEMD-ARIMA Model. In Proceedings of the 2022 34th Chinese Control and Decision Conference (CCDC), Hefei, China, 15–17 August 2022; IEEE: Piscataway, NJ, USA, 2022.
95. Che, Y.; Zheng, Y.; Wu, Y.; Sui, X.; Bharadwaj, P.; Stroe, D.-I.; Yang, Y.; Hu, X.; Teodorescu, R. Data Efficient Health Prognostic for Batteries Based on Sequential Information-Driven Probabilistic Neural Network. *Appl. Energy* **2022**, *323*, 119663.
96. Zhang, L.; Li, K.; Du, D.; Zhu, C.; Zheng, M. A Sparse Least Squares Support Vector Machine Used for SOC Estimation of Li-Ion Batteries. *IFAC-PapersOnLine* **2019**, *52*, 256–261.
97. Hu, X.; Zhang, K.; Liu, K.; Lin, X.; Dey, S.; Onori, S. Advanced Fault Diagnosis for Lithium-Ion Battery Systems: A review of fault mechanisms, fault features, and diagnosis procedures. *IEEE Ind. Electron. Mag.* **2020**, *14*, 65–91.
98. Guo, W.; He, M. An Optimal Relevance Vector Machine with a Modified Degradation Model for Remaining Useful Lifetime Prediction of Lithium-Ion Batteries. *Appl. Soft Comput.* **2022**, *124*, 108967.
99. Qin, X.; Zhao, Q.; Zhao, H.; Feng, W.; Guan, X. Prognostics of Remaining Useful Life for Lithium-Ion Batteries Based on a Feature Vector Selection and Relevance Vector Machine Approach. In Proceedings of the 2017 IEEE International Conference on Prognostics and Health Management (ICPHM), Dallas, TX, USA, 19–21 June 2017; IEEE: Piscataway, NJ, USA, 2017.
100. Hassini, M.; Redondo-Iglesias, E.; Venet, P. Lithium–Ion Battery Data: From Production to Prediction. *Batteries* **2023**, *9*, 385.
101. Tang, R.; Dore, J.; Ma, J.; Leong, P.H.W. Interpolating High Granularity Solar Generation and Load Consumption Data Using Super Resolution Generative Adversarial Network. *Appl. Energy* **2021**, *299*, 117297.
102. Hauck, B.; Wang, W.; Xue, Y. On the Model Granularity and Temporal Resolution of Residential PV-Battery System Simulation. *Dev. Built Environ.* **2021**, *6*, 100046.
103. Zhang, Y.; Tang, Q.; Zhang, Y.; Wang, J.; Stimming, U.; Lee, A.A. Identifying Degradation Patterns of Lithium Ion Batteries from Impedance Spectroscopy Using Machine Learning. *Nat. Commun.* **2020**, *11*, 1706.
104. Ng, M.-F.; Zhao, J.; Yan, Q.; Conduit, G.J.; Seh, Z.W. Predicting the State of Charge and Health of Batteries Using Data-Driven Machine Learning. *Nat. Mach. Intell.* **2020**, *2*, 161–170.
105. Geslin, A.; van Vlijmen, B.; Cui, X.; Bhargava, A.; Asinger, P.A.; Braatz, R.D.; Chueh, W.C. Selecting the Appropriate Features in Battery Lifetime Predictions. *Joule* **2023**, *7*, 1956–1965. <https://doi.org/10.1016/j.joule.2023.07.021>.
106. van Vlijmen, B.; Asinger, P.A.; Lam, V.; Cui, X.; Ganapathi, D.; Sun, S.; Herring, P.K.; Gopal, C.B.; Geise, N.; Deng, H.D.; et al. Interpretable Data-Driven Modeling Reveals Complexity of Battery Aging. *ChemRxiv* **2023**. <https://doi.org/10.1234/chemrxiv.2023.123456>.
107. Nuhic, A.; Terzimehic, T.; Soczka-Guth, T.; Buchholz, M.; Dietmayer, K. Health Diagnosis and Remaining Useful Life Prognostics of Lithium-Ion Batteries Using Data-Driven Methods. *J. Power Sources* **2013**, *239*, 680–688.
108. Guo, J.; Li, Z.; Pecht, M. A Bayesian Approach for Li-Ion Battery Capacity Fade Modeling and Cycles to Failure Prognostics. *J. Power Sources* **2015**, *281*, 173–184.
109. Wu, B.; Han, S.; Shin, K.G.; Lu, W. Application of Artificial Neural Networks in Design of Lithium-Ion Batteries. *J. Power Sources* **2018**, *395*, 128–136.
110. Zahid, T.; Xu, K.; Li, W.; Li, C.; Li, H. State of Charge Estimation for Electric Vehicle Power Battery Using Advanced Machine Learning Algorithm under Diversified Drive Cycles. *Energy* **2018**, *162*, 871–882.
111. Chemali, E.; Kollmeyer, P.J.; Preindl, M.; Emadi, A. State-of-Charge Estimation of Li-Ion Batteries Using Deep Neural Networks: A Machine Learning Approach. *J. Power Sources* **2018**, *400*, 242–255.
112. Jiménez-Bermejo, D.; Fraile-Ardanuy, J.; Castaño-Solis, S.; Merino, J.; Álvaro-Hermana, R. Using Dynamic Neural Networks for Battery State of Charge Estimation in Electric Vehicles. *Procedia Comput. Sci.* **2018**, *130*, 533–540.

113. Mansouri, S.S.; Karvelis, P.; Georgoulas, G.; Nikolakopoulos, G. Remaining Useful Battery Life Prediction for UAVs Based on Machine Learning. *IFAC-PapersOnLine* **2017**, *50*, 4727–4732.
114. Huang, C.; Wang, Z.; Zhao, Z.; Wang, L.; Lai, C.S.; Wang, D. Robustness Evaluation of Extended and Unscented Kalman Filter for Battery State of Charge Estimation. *IEEE Access* **2018**, *6*, 27617–27628.
115. Ren, L.; Zhao, L.; Hong, S.; Zhao, S.; Wang, H.; Zhang, L. Remaining Useful Life Prediction for Lithium-Ion Battery: A Deep Learning Approach. *IEEE Access* **2018**, *6*, 50587–50598.
116. Khumprom, P.; Yodo, N. A Data-Driven Predictive Prognostic Model for Lithium-Ion Batteries Based on a Deep Learning Algorithm. *Energies* **2019**, *12*, 660.
117. Sahinoglu, G.O.; Pajovic, M.; Sahinoglu, Z.; Wang, Y.; Orlik, P.V.; Wada, T. Battery State-of-Charge Estimation Based on Regular/Recurrent Gaussian Process Regression. *IEEE Trans. Ind. Electron.* **2018**, *65*, 4311–4321.
118. Álvarez Antón, J.C.; García Nieto, P.J.; de Cos Juez, F.J.; Sánchez Lasheras, F.; González Vega, M.; Roqueñí Gutiérrez, M.N. Battery State-of-Charge Estimator Using the SVM Technique. *Appl. Math. Model.* **2013**, *37*, 6244–6253.
119. Tong, S.; Lacap, J.H.; Park, J.W. Battery State of Charge Estimation Using a Load-Classifying Neural Network. *J. Energy Storage* **2016**, *7*, 236–243.
120. Kang, L.; Zhao, X.; Ma, J. A New Neural Network Model for the State-of-Charge Estimation in the Battery Degradation Process. *Appl. Energy* **2014**, *121*, 20–27.
121. Hu, X.; Li, S.E.; Yang, Y. Advanced Machine Learning Approach for Lithium-Ion Battery State Estimation in Electric Vehicles. *IEEE Trans. Transp. Electrification* **2016**, *2*, 140–149.
122. Wu, T.; Wang, M.; Xiao, Q.; Wang, X. The SOC Estimation of Power Li-Ion Battery Based on ANFIS Model. *Smart Grid Renew. Energy* **2012**, *03*, 51–55.
123. Wu, J.; Wang, Y.; Zhang, X.; Chen, Z. A Novel State of Health Estimation Method of Li-Ion Battery Using Group Method of Data Handling. *J. Power Sources* **2016**, *327*, 457–464.
124. Hu, C.; Jain, G.; Schmidt, C.; Strief, C.; Sullivan, M. Online Estimation of Lithium-Ion Battery Capacity Using Sparse Bayesian Learning. *J. Power Sources* **2015**, *289*, 105–113.
125. Berecibar, M.; Devriendt, F.; Dubarry, M.; Villarreal, I.; Omar, N.; Verbeke, W.; Van Mierlo, J. Online State of Health Estimation on NMC Cells Based on Predictive Analytics. *J. Power Sources* **2016**, *320*, 239–250.
126. Richardson, R.R.; Osborne, M.A.; Howey, D.A. Gaussian Process Regression for Forecasting Battery State of Health. *J. Power Sources* **2017**, *357*, 209–219.
127. Zhang, Y.; Xiong, R.; He, H.; Liu, Z. A LSTM-RNN Method for the Lithium-Ion Battery Remaining Useful Life Prediction. In Proceedings of the 2017 Prognostics and System Health Management Conference (PHM-Harbin), Harbin, China, 9–12 July 2017; IEEE: Piscataway, NJ, USA, 2017.
128. Hu, J.N.; Hu, J.J.; Lin, H.B.; Li, X.P.; Jiang, C.L.; Qiu, X.H.; Li, W.S. State-of-Charge Estimation for Battery Management System Using Optimized Support Vector Machine for Regression. *J. Power Sources* **2014**, *269*, 682–693.
129. Tseng, K.-H.; Liang, J.-W.; Chang, W.; Huang, S.-C. Regression Models Using Fully Discharged Voltage and Internal Resistance for State of Health Estimation of Lithium-Ion Batteries. *Energies* **2015**, *8*, 2889–2907.
130. Hussein, A.A. Kalman Filters versus Neural Networks in Battery State-of-Charge Estimation: A Comparative Study. *Int. J. Mod. Nonlinear Theory Appl.* **2014**, *03*, 199–209.
131. Yang, D.; Wang, Y.; Pan, R.; Chen, R.; Chen, Z. A Neural Network Based State-of-Health Estimation of Lithium-Ion Battery in Electric Vehicles. *Energy Procedia* **2017**, *105*, 2059–2064.
132. Sin, S.; Cho, S.; Lee, P.; Abbas, M.; Lee, S.; Kim, J. Data-Driven Prediction of Battery Degradation Using EIS-Based Robust Features. In Proceedings of the 2022 IEEE Energy Conversion Congress and Exposition (ECCE), Detroit, MI, USA, 9–13 October 2022; IEEE: Piscataway, NJ, USA, 2022.
133. Li, Y.; Sogaard, A.J.; Sorensen, J.I.; Guo, J.; Stroe, D.-I.; Pedersen, K.; Gurevich, L. Aging Mechanisms of Electrodes in LiFePO<sub>4</sub>/Graphite Batteries. In Proceedings of the 2022 IEEE Energy Conversion Congress and Exposition (ECCE), Detroit, MI, USA, 9–13 October 2022; IEEE: Piscataway, NJ, USA, 2022.
134. Fang, C.; Tran, T.-N.; Zhao, Y.; Liu, G. Electrolyte Decomposition and Solid Electrolyte Interphase Revealed by Mass Spectrometry. *Electrochim. Acta* **2021**, *399*, 139362.
135. Zhou, A.; Wang, W.; Liu, Q.; Wang, Y.; Yao, X.; Qing, F.; Li, E.; Yang, T.; Zhang, L.; Li, J. Stable, Fast and High-Energy-Density LiCoO<sub>2</sub> Cathode at High Operation Voltage Enabled by Glassy B<sub>2</sub>O<sub>3</sub> Modification. *J. Power Sources* **2017**, *362*, 131–139.
136. Stenzel, Y.; Horsthemke, F.; Winter, M.; Nowak, S. Chromatographic Techniques in the Research Area of Lithium Ion Batteries: Current State-of-the-Art. *Separations* **2019**, *6*, 26.
137. Aalund, R.; Endreddy, B.; Pecht, M. How Gas Generates in Pouch Cells and Affects Consumer Products. *Front. Chem. Eng.* **2022**, *4*, 828375. <https://doi.org/10.3389/fceng.2022.828375>.
138. Kim, S.; Choi, S.; Lee, K.; Yang, G.J.; Lee, S.S.; Kim, Y. Self-Assembly of Core-Shell Structures Driven by Low Doping Limit of Ti in LiCoO<sub>2</sub>: First-Principles Thermodynamic and Experimental Investigation. *Phys. Chem. Chem. Phys.* **2017**, *19*, 4104–4113.
139. Ruiz, V.; Pfrang, A.; Kriston, A.; Omar, N.; Van den Bossche, P.; Boon-Brett, L. A Review of International Abuse Testing Standards and Regulations for Lithium Ion Batteries in Electric and Hybrid Electric Vehicles. *Renew. Sustain. Energy Rev.* **2018**, *81*, 1427–1452.

140. Chen, Z.; Wang, J.; Huang, J.; Fu, T.; Sun, G.; Lai, S.; Zhou, R.; Li, K.; Zhao, J. The High-Temperature and High-Humidity Storage Behaviors and Electrochemical Degradation Mechanism of  $\text{LiNi}_{0.6}\text{Co}_{0.2}\text{Mn}_{0.2}\text{O}_2$  Cathode Material for Lithium Ion Batteries. *J. Power Sources* **2017**, *363*, 168–176.
141. Sun, Y.-K.; Kim, D.-H.; Yoon, C.S.; Myung, S.-T.; Prakash, J.; Amine, K. A Novel Cathode Material with a Concentration-Gradient for High-Energy and Safe Lithium-Ion Batteries. *Adv. Funct. Mater.* **2010**, *20*, 485–491.
142. Liu, S.; Xiong, L.; He, C. Long Cycle Life Lithium Ion Battery with Lithium Nickel Cobalt Manganese Oxide (NCM) Cathode. *J. Power Sources* **2014**, *261*, 285–291.
143. Kong, J.-Z.; Zhai, H.-F.; Ren, C.; Gao, M.-Y.; Zhang, X.; Li, H.; Li, J.-X.; Tang, Z.; Zhou, F. Synthesis and Electrochemical Performance of Macroporous  $\text{LiNi}_{0.5}\text{Co}_{0.2}\text{Mn}_{0.3}\text{O}_2$  by a Modified Sol–Gel Method. *J. Alloys Compd.* **2013**, *577*, 507–510.
144. Hsieh, C.-T.; Chen, Y.-F.; Pai, C.-T.; Mo, C.-Y. Synthesis of Lithium Nickel Cobalt Manganese Oxide Cathode Materials by Infrared Induction Heating. *J. Power Sources* **2014**, *269*, 31–36.
145. Pender, J.P.; Jha, G.; Youn, D.H.; Ziegler, J.M.; Andoni, I.; Choi, E.J.; Heller, A.; Dunn, B.S.; Weiss, P.S.; Penner, R.M.; et al. Electrode Degradation in Lithium-Ion Batteries. *ACS Nano* **2020**, *14*, 1243–1295.
146. Zhu, Y.; Luo, X.; Zhi, H.; Yang, X.; Xing, L.; Liao, Y.; Xu, M.; Li, W. Structural Exfoliation of Layered Cathode under High Voltage and Its Suppression by Interface Film Derived from Electrolyte Additive. *ACS Appl. Mater. Interfaces* **2017**, *9*, 12021–12034.
147. Zhou, M.; Qin, C.; Liu, Z.; Feng, L.; Su, X.; Chen, Y.; Xia, L.; Xia, Y.; Liu, Z. Enhanced High Voltage Cyclability of  $\text{LiCoO}_2$  Cathode by Adopting Poly[Bis-(Ethoxyethoxyethoxy)Phosphazene] with Flame-Retardant Property as an Electrolyte Additive for Lithium-Ion Batteries. *Appl. Surf. Sci.* **2017**, *403*, 260–266.
148. Yu, J.; Han, Z.; Hu, X.; Zhan, H.; Zhou, Y.; Liu, X. Solid-State Synthesis of  $\text{LiCoO}_2/\text{LiCo}_{0.99}\text{Ti}_{0.01}\text{O}_2$  Composite as Cathode Material for Lithium Ion Batteries. *J. Power Sources* **2013**, *225*, 34–39.
149. Kalluri, S.; Yoon, M.; Jo, M.; Park, S.; Myeong, S.; Kim, J.; Dou, S.X.; Guo, Z.; Cho, J. Li-Ion Cells: Surface Engineering Strategies of Layered  $\text{LiCoO}_2$  Cathode Material to Realize High-Energy and High-Voltage Li-Ion Cells (Adv. Energy Mater. 1/2017). *Adv. Energy Mater.* **2017**, *7*, 170006. <https://doi.org/10.1002/aenm.201770006>.
150. Kalluri, S.; Yoon, M.; Jo, M.; Liu, H.K.; Dou, S.X.; Cho, J.; Guo, Z. Feasibility of Cathode Surface Coating Technology for High-energy Lithium-ion and Beyond-lithium-ion Batteries. *Adv. Mater.* **2017**, *29*, 1605807.
151. Lee, K.T.; Jeong, S.; Cho, J. Roles of Surface Chemistry on Safety and Electrochemistry in Lithium Ion Batteries. *Acc. Chem. Res.* **2013**, *46*, 1161–1170.
152. Fu, L.J.; Liu, H.; Li, C.; Wu, Y.P.; Rahm, E.; Holze, R.; Wu, H.Q. Surface Modifications of Electrode Materials for Lithium Ion Batteries. *Solid State Sci.* **2006**, *8*, 113–128.
153. Keil, P. Aging of Lithium-Ion Batteries in Electric Vehicles. Ph.D. Thesis, Technische Universität München, Munich, Germany, 2017.
154. Birkl, C.R.; Roberts, M.R.; McTurk, E.; Bruce, P.G.; Howey, D.A. Degradation Diagnostics for Lithium Ion Cells. *J. Power Sources* **2017**, *341*, 373–386.
155. Whittingham, M.S. Lithium Batteries and Cathode Materials. *Chem. Rev.* **2004**, *104*, 4271–4301.
156. Winter, M.; Besenhard, J.O.; Spahr, M.E.; Novák, P. Insertion Electrode Materials for Rechargeable Lithium Batteries. *Adv. Mater.* **1998**, *10*, 725–763.
157. Liu, C.; Neale, Z.G.; Cao, G. Understanding Electrochemical Potentials of Cathode Materials in Rechargeable Batteries. *Mater. Today* **2016**, *19*, 109–123.
158. Rowden, B.; Garcia-Araez, N. A Review of Gas Evolution in Lithium Ion Batteries. *Energy Rep.* **2020**, *6*, 10–18.
159. Teichert, P.; Jahnke, H.; Figgemeier, E. Degradation Mechanism of Monocrystalline Ni-Rich  $\text{Li}[\text{Ni}_x\text{Mn}_y\text{Co}_z]\text{O}_2$  (NMC) Active Material in Lithium Ion Batteries. *J. Electrochem. Soc.* **2021**, *168*, 090532.
160. Zhuang, G.V.; Chen, G.; Shim, J.; Song, X.; Ross, P.N.; Richardson, T.J.  $\text{Li}_2\text{CO}_3$  in  $\text{LiNi}_{0.8}\text{Co}_{0.15}\text{Al}_{0.05}\text{O}_2$  Cathodes and Its Effects on Capacity and Power. *J. Power Sources* **2004**, *134*, 293–297.
161. Oh, P.; Song, B.; Li, W.; Manthiram, A. Overcoming the Chemical Instability on Exposure to Air of Ni-Rich Layered Oxide Cathodes by Coating with Spinel  $\text{LiMn}_{1.9}\text{Al}_{0.1}\text{O}_4$ . *J. Mater. Chem. A Mater. Energy Sustain.* **2016**, *4*, 5839–5841.
162. Shizuka, K.; Kiyohara, C.; Shima, K.; Takeda, Y. Effect of  $\text{CO}_2$  on Layered  $\text{Li}_{1+z}\text{Ni}_{1-x-y}\text{Co}_x\text{Mn}_y\text{O}_2$  (M=Al, Mn) Cathode Materials for Lithium Ion Batteries. *J. Power Sources* **2007**, *166*, 233–238.
163. Liu, W.; Hu, G.; Du, K.; Peng, Z.; Cao, Y. Enhanced Storage Property of  $\text{LiNi}_{0.8}\text{Co}_{0.15}\text{Al}_{0.05}\text{O}_2$  Coated with  $\text{LiCoO}_2$ . *J. Power Sources* **2013**, *230*, 201–206.
164. Eom, J.; Kim, M.G.; Cho, J. Storage Characteristics of  $\text{LiNi}_{0.8}\text{Co}_{0.1+x}\text{Mn}_{0.1-x}\text{O}_2$  (X=0, 0.03, and 0.06) Cathode Materials for Lithium Batteries. *J. Electrochem. Soc.* **2008**, *155*, A239.
165. Li, J.; Zheng, J.M.; Yang, Y. Studies on Storage Characteristics of  $\text{LiNi}_{0.4}\text{Co}_{0.2}\text{Mn}_{0.4}\text{O}_2$  as Cathode Materials in Lithium-Ion Batteries. *J. Electrochem. Soc.* **2007**, *154*, A427.
166. Zhou, W.; Hao, F.; Fang, D. The Effects of Elastic Stiffening on the Evolution of the Stress Field within a Spherical Electrode Particle of Lithium-Ion Batteries. *Int. J. Appl. Mech.* **2013**, *05*, 1350040.
167. Zhang, L.; Zhu, C.; Yu, S.; Ge, D.; Zhou, H. Status and Challenges Facing Representative Anode Materials for Rechargeable Lithium Batteries. *J. Energy Chem.* **2022**, *66*, 260–294.
168. Wu, Y.P.; Rahm, E.; Holze, R. Carbon Anode Materials for Lithium Ion Batteries. *J. Power Sources* **2003**, *114*, 228–236.
169. Yoo, H.D.; Markevich, E.; Salitra, G.; Sharon, D.; Aurbach, D. On the Challenge of Developing Advanced Technologies for Electrochemical Energy Storage and Conversion. *Mater. Today* **2014**, *17*, 110–121.

170. Asenbauer, J.; Eisenmann, T.; Kuenzel, M.; Kazzazi, A.; Chen, Z.; Bresser, D. The Success Story of Graphite as a Lithium-Ion Anode Material—Fundamentals, Remaining Challenges, and Recent Developments Including Silicon (Oxide) Composites. *Sustain. Energy Fuels* **2020**, *4*, 5387–5416.
171. Nzereogu, P.U.; Omah, A.D.; Ezema, F.I.; Iwuoha, E.I.; Nwanya, A.C. Anode Materials for Lithium-Ion Batteries: A Review. *Appl. Surf. Sci. Adv.* **2022**, *9*, 100233.
172. Piper, D.M.; Yersak, T.A.; Son, S.-B.; Kim, S.C.; Kang, C.S.; Oh, K.H.; Ban, C.; Dillon, A.C.; Lee, S.-H. Conformal Coatings of Cyclized-PAN for Mechanically Resilient Si Nano-composite Anodes. *Adv. Energy Mater.* **2013**, *3*, 697–702.
173. Sánchez-Ramírez, N.; Monje, I.E.; Bélanger, D.; Camargo, P.H.C.; Torresi, R.M. High Rate and Long-Term Cycling of Silicon Anodes with Phosphonium-Based Ionic Liquids as Electrolytes for Lithium-Ion Batteries. *Electrochim. Acta* **2023**, *439*, 141680.
174. Araño, K.; Mazouzi, D.; Kerr, R.; Lestriez, B.; Le Bideau, J.; Howlett, P.C.; Dupré, N.; Forsyth, M.; Guyomard, D. Editors' Choice—Understanding the Superior Cycling Performance of Si Anode in Highly Concentrated Phosphonium-Based Ionic Liquid Electrolyte. *J. Electrochem. Soc.* **2020**, *167*, 120520.
175. Sujith, R.; Gangadhar, J.; Greenough, M.; Bordia, R.K.; Panda, D.K. A Review of Silicon Oxycarbide Ceramics as next Generation Anode Materials for Lithium-Ion Batteries and Other Electrochemical Applications. *J. Mater. Chem. A Mater. Energy Sustain.* **2023**, *11*, 20324–20348.
176. Xu, H.; Li, H.; Wang, X. The Anode Materials for Lithium-ion and Sodium-ion Batteries Based on Conversion Reactions: A Review. *ChemElectroChem* **2023**, *10*, e202201151. <https://doi.org/10.1002/celec.202201151>.
177. Zhang, N.; Liu, E.; Chen, H.; Hou, J.; Li, C.; Wan, H. High-Performance of LaCoO<sub>3</sub>/Co<sub>3</sub>O<sub>4</sub> Nanocrystal as Anode for Lithium-Ion Batteries. *Colloids Surf. A Physicochem. Eng. Asp.* **2021**, *628*, 127265.
178. Liu, S.; Sun, Y.-H.; Dong, P.-P.; Nan, J.-M. Conversion of  $\alpha$ -Fe<sub>2</sub>O<sub>3</sub> from Spindle Nanorods to Nanotubes, and Their Lithium-Storage Performance. *Mater. Sci. Eng. B Solid State Mater. Adv. Technol.* **2015**, *202*, 15–24.
179. Xiong, R.; Ma, S.; Li, H.; Sun, F.; Li, J. Toward a Safer Battery Management System: A Critical Review on Diagnosis and Prognosis of Battery Short Circuit. *iScience* **2020**, *23*, 101010.
180. Wang, Z.; Yuan, J.; Zhu, X.; Wang, H.; Huang, L.; Wang, Y.; Xu, S. Overcharge-to-Thermal-Runaway Behavior and Safety Assessment of Commercial Lithium-Ion Cells with Different Cathode Materials: A Comparison Study. *J. Energy Chem.* **2021**, *55*, 484–498.
181. Liu, J.; Wang, Z.; Bai, J. Influences of Multi Factors on Thermal Runaway Induced by Overcharging of Lithium-Ion Battery. *J. Energy Chem.* **2022**, *70*, 531–541.
182. Liu, S.; Ma, T.; Wei, Z.; Bai, G.; Liu, H.; Xu, D.; Shan, Z.; Wang, F. Study about Thermal Runaway Behavior of High Specific Energy Density Li-Ion Batteries in a Low State of Charge. *J. Energy Chem.* **2021**, *52*, 20–27.
183. Yun, F.; Liu, S.; Gao, M.; Bi, X.; Zhao, W.; Chang, Z.; Yuan, M.; Li, J.; Shen, X.; Qi, X.; et al. Investigation on Step Overcharge to Self-Heating Behavior and Mechanism Analysis of Lithium Ion Batteries. *J. Energy Chem.* **2023**, *79*, 301–311. <https://doi.org/10.1016/j.jechem.2022.12.033>.
184. Ouyang, D.; Chen, M.; Weng, J.; Wang, K.; Wang, J.; Wang, Z. Exploring the Thermal Stability of Lithium-Ion Cells via Accelerating Rate Calorimetry: A Review. *J. Energy Chem.* **2023**, *81*, 543–573. <https://doi.org/10.1016/j.jechem.2023.02.030>.
185. Wang, Q.; Mao, B.; Stoliarov, S.I.; Sun, J. A Review of Lithium Ion Battery Failure Mechanisms and Fire Prevention Strategies. *Prog. Energy Combust. Sci.* **2019**, *73*, 95–131.
186. Zhou, H.; Fear, C.; Jeevarajan, J.A.; Mukherjee, P.P. State-of-Electrode (SOE) Analytics of Lithium-Ion Cells under Overdischarge Extremes. *Energy Storage Mater.* **2023**, *54*, 60–74.
187. Zhitao, E.; Guo, H.; Yan, G.; Wang, J.; Feng, R.; Wang, Z.; Li, X. Evolution of the Morphology, Structural and Thermal Stability of LiCoO<sub>2</sub> during Overcharge. *J. Energy Chem.* **2021**, *55*, 524–532.
188. Wang, L.; Chen, B.; Ma, J.; Cui, G.; Chen, L. Reviving Lithium Cobalt Oxide-Based Lithium Secondary Batteries-toward a Higher Energy Density. *Chem. Soc. Rev.* **2018**, *47*, 6505–6602. <https://doi.org/10.1039/c8cs00322j>.
189. Christensen, P.A.; Milojevic, Z.; Wise, M.S.; Ahmeid, M.; Attidekou, P.S.; Mroziak, W.; Dickmann, N.A.; Restuccia, F.; Lambert, S.M.; Das, P.K. Thermal and Mechanical Abuse of Electric Vehicle Pouch Cell Modules. *Appl. Therm. Eng.* **2021**, *189*, 116623.
190. Yokoshima, T.; Mukoyama, D.; Maeda, F.; Osaka, T.; Takazawa, K.; Egusa, S.; Naoi, S.; Ishikura, S.; Yamamoto, K. Direct Observation of Internal State of Thermal Runaway in Lithium Ion Battery during Nail-Penetration Test. *J. Power Sources* **2018**, *393*, 67–74.
191. Golubkov, A.W.; Scheikl, S.; Planteu, R.; Voitic, G.; Wiltische, H.; Stangl, C.; Fauler, G.; Thaler, A.; Hacker, V. Thermal Runaway of Commercial 18650 Li-Ion Batteries with LFP and NCA Cathodes—Impact of State of Charge and Overcharge. *RSC Adv.* **2015**, *5*, 57171–57186.
192. Chang, H.; Wu, Y.-R.; Han, X.; Yi, T.-F. Recent Developments in Advanced Anode Materials for Lithium-Ion Batteries. *Energy Mater* **2022**, *1*, 100003.
193. Chen, Y.; Sun, H.; Guo, J.; Zhao, Y.; Yang, H.; Li, H.; Li, W.-J.; Chou, S.; Jiang, Y.; Zhang, Z. Research on Carbon-Based and Metal-Based Negative Electrode Materials via DFT Calculation for High Potassium Storage Performance: A Review. *Energymater* **2023**, *3*, 300044.
194. Wang, A.; Kadam, S.; Li, H.; Shi, S.; Qi, Y. Review on Modeling of the Anode Solid Electrolyte Interphase (SEI) for Lithium-Ion Batteries. *NPJ Comput. Mater.* **2018**, *4*, 15. <https://doi.org/10.1038/s41524-018-0064-0>.
195. Majasan, J.O.; Robinson, J.B.; Owen, R.E.; Maier, M.; Radhakrishnan, A.N.P.; Pham, M.; Tranter, T.G.; Zhang, Y.; Shearing, P.R.; Brett, D.J.L. Recent Advances in Acoustic Diagnostics for Electrochemical Power Systems. *J. Phys. Energy* **2021**, *3*, 032011.

196. Bulla, M.; Schmandt, C.; Kolling, S.; Kisters, T.; Sahraei, E. An Experimental and Numerical Study on Charged 21700 Lithium-Ion Battery Cells under Dynamic and High Mechanical Loads. *Energies* **2022**, *16*, 211.
197. Yu, Y.; Cui, C.; Qian, W.; Xie, Q.; Zheng, C.; Kong, C.; Wei, F. Carbon Nanotube Production and Application in Energy Storage. *Asia-Pac. J. Chem. Eng.* **2013**, *8*, 234–245.
198. Guo, J.; Li, Y.; Pedersen, K.; Stroe, D.-I. Lithium-Ion Battery Operation, Degradation, and Aging Mechanism in Electric Vehicles: An Overview. *Energies* **2021**, *14*, 5220.
199. Ma, S.; Jiang, M.; Tao, P.; Song, C.; Wu, J.; Wang, J.; Deng, T.; Shang, W. Temperature Effect and Thermal Impact in Lithium-Ion Batteries: A Review. *Prog. Nat. Sci.* **2018**, *28*, 653–666.
200. Mizushima, K.; Jones, P.C.; Wiseman, P.J.; Goodenough, J.B.M. *Advances in Lithium-Ion Batteries*; van Schalkwijk, W., Scrosati, B., Eds.; Springer: New York, NY, USA, 2007; Volume 1; ISBN 9780306475085.
201. Danzer, M.A.; Liebau, V.; Maglia, F. Aging of Lithium-Ion Batteries for Electric Vehicles. In *Advances in Battery Technologies for Electric Vehicles*; Elsevier: Amsterdam, The Netherlands, 2015; pp. 359–387, ISBN 9781782423775.
202. Wiemers-Meyer, S.; Winter, M.; Nowak, S. Mechanistic Insights into Lithium Ion Battery Electrolyte Degradation—A Quantitative NMR Study. *Phys. Chem. Chem. Phys.* **2016**, *18*, 26595–26601.
203. Ouyang, D.; Weng, J.; Chen, M.; Wang, J. Impact of High-Temperature Environment on the Optimal Cycle Rate of Lithium-Ion Battery. *J. Energy Storage* **2020**, *28*, 101242.
204. Stroe, D.-I.; Swierczynski, M.; Kar, S.K.; Teodorescu, R. Degradation Behavior of Lithium-Ion Batteries during Calendar Ageing—The Case of the Internal Resistance Increase. *IEEE Trans. Ind. Appl.* **2018**, *54*, 517–525.
205. Gao, T.; Bai, J.; Ouyang, D.; Wang, Z.; Bai, W.; Mao, N.; Zhu, Y. Effect of Aging Temperature on Thermal Stability of Lithium-Ion Batteries: Part A—High-Temperature Aging. *Renew. Energy* **2023**, *203*, 592–600.
206. Aiken, C.P.; Self, J.; Petibon, R.; Xia, X.; Paulsen, J.M.; Dahn, J.R. A Survey of in Situ Gas Evolution during High Voltage Formation in Li-Ion Pouch Cells. *J. Electrochem. Soc.* **2015**, *162*, A760–A767.
207. Abada, S.; Marlair, G.; Lecocq, A.; Petit, M.; Sauvant-Moynot, V.; Huet, F. Safety Focused Modeling of Lithium-Ion Batteries: A Review. *J. Power Sources* **2016**, *306*, 178–192.
208. Zhang, Z.; Yang, J.; Huang, W.; Wang, H.; Zhou, W.; Li, Y.; Li, Y.; Xu, J.; Huang, W.; Chiu, W.; et al. Cathode-Electrolyte Interphase in Lithium Batteries Revealed by Cryogenic Electron Microscopy. *Matter* **2021**, *4*, 302–312.
209. Liu, T.; Lin, L.; Bi, X.; Tian, L.; Yang, K.; Liu, J.; Li, M.; Chen, Z.; Lu, J.; Amine, K.; et al. In Situ Quantification of Interphasial Chemistry in Li-Ion Battery. *Nat. Nanotechnol.* **2019**, *14*, 50–56.
210. Goodenough, J.B. Challenges for Rechargeable Li Batteries. *Chem. Mater.* **2010**, *22*, 587–603.
211. Pinson, M.B.; Bazant, M.Z. Theory of SEI Formation in Rechargeable Batteries: Capacity Fade, Accelerated Aging and Lifetime Prediction. *arXiv* **2012**, arXiv:1210.3672.
212. Williard, N.D. Degradation Analysis and Health Monitoring of Lithium-Ion Batteries. Master's Thesis, University of Maryland, College Park, MD, USA, 2011.
213. Edge, J.S.; O'Kane, S.; Prosser, R.; Kirkaldy, N.D.; Patel, A.N.; Hales, A.; Ghosh, A.; Ai, W.; Chen, J.; Yang, J.; et al. Lithium Ion Battery Degradation: What You Need to Know. *Phys. Chem. Chem. Phys.* **2021**, *23*, 8200–8221.
214. Xu, K.; Wang, C. Batteries: Widening Voltage Windows. *Nat. Energy* **2016**, *1*, 16161.
215. Da Silva, L.M.; Cesar, R.; Moreira, C.M.R.; Santos, J.H.M.; De Souza, L.G.; Pires, B.M.; Vicentini, R.; Nunes, W.; Zanin, H. Reviewing the Fundamentals of Supercapacitors and the Difficulties Involving the Analysis of the Electrochemical Findings Obtained for Porous Electrode Materials. *Energy Storage Mater.* **2020**, *27*, 555–590.
216. Hendricks, C.; Williard, N.; Mathew, S.; Pecht, M. A Failure Modes, Mechanisms, and Effects Analysis (FMMEA) of Lithium-Ion Batteries. *J. Power Sources* **2015**, *297*, 113–120.
217. Barré, A.; Deguilhem, B.; Grolleau, S.; Gérard, M.; Suard, F.; Riu, D. A Review on Lithium-Ion Battery Ageing Mechanisms and Estimations for Automotive Applications. *J. Power Sources* **2013**, *241*, 680–689.
218. Koltypin, M.; Aurbach, D.; Nazar, L.; Ellis, B. More on the Performance of LiFePO<sub>4</sub> Electrodes—The Effect of Synthesis Route, Solution Composition, Aging, and Temperature. *J. Power Sources* **2007**, *174*, 1241–1250.
219. Horstmann, B.; Single, F.; Latz, A. Review on Multi-Scale Models of Solid-Electrolyte Interphase Formation. *Curr. Opin. Electrochem.* **2019**, *13*, 61–69.
220. An, S.J.; Li, J.; Daniel, C.; Mohanty, D.; Nagpure, S.; Wood, D.L., III. The State of Understanding of the Lithium-Ion-Battery Graphite Solid Electrolyte Interphase (SEI) and Its Relationship to Formation Cycling. *Carbon* **2016**, *105*, 52–76.
221. Zhang, S.S. A Review on Electrolyte Additives for Lithium-Ion Batteries. *J. Power Sources* **2006**, *162*, 1379–1394.
222. Ogumi, Z.; Wang, H. Carbon Anode Materials. In *Lithium-Ion Batteries*; Yoshio, M., Brodd, R.J., Kozawa, A., Eds.; Springer: New York, NY, USA, 2009; Volume 1, pp. 49–73, ISBN 9780387344447.
223. Ramanujapuram, A.; Gordon, D.; Magasinski, A.; Ward, B.; Nitta, N.; Huang, C.; Yushin, G. Degradation and Stabilization of Lithium Cobalt Oxide in Aqueous Electrolytes. *Energy Environ. Sci.* **2016**, *9*, 1841–1848.
224. Ahmadi, L.; Young, S.B.; Fowler, M.; Fraser, R.A.; Achachlouei, M.A. A Cascaded Life Cycle: Reuse of Electric Vehicle Lithium-Ion Battery Packs in Energy Storage Systems. *Int. J. Life Cycle Assess.* **2017**, *22*, 111–124.
225. Casals, L.C.; Amante García, B.; Canal, C. Second Life Batteries Lifespan: Rest of Useful Life and Environmental Analysis. *J. Environ. Manag.* **2019**, *232*, 354–363.
226. Woody, M.; Arbabzadeh, M.; Lewis, G.M.; Keoleian, G.A.; Stefanopoulou, A. Strategies to Limit Degradation and Maximize Lithium-Ion Battery Service Lifetime—Critical Review and Guidance for Stakeholders. *J. Energy Storage* **2020**, *28*, 101231.

227. Wissler, M. Graphite and Carbon Powders for Electrochemical Applications. *J. Power Sources* **2006**, *156*, 142–150.
228. Ng, S.H.; Vix-Guterl, C.; Bernardo, P.; Tran, N.; Ufheil, J.; Buqa, H.; Dentzer, J.; Gadiou, R.; Spahr, M.E.; Goers, D.; et al. Correlations between Surface Properties of Graphite and the First Cycle Specific Charge Loss in Lithium-Ion Batteries. *Carbon* **2009**, *47*, 705–712.
229. Lin, Y.-X.; Liu, Z.; Leung, K.; Chen, L.-Q.; Lu, P.; Qi, Y. Connecting the Irreversible Capacity Loss in Li-Ion Batteries with the Electronic Insulating Properties of Solid Electrolyte Interphase (SEI) Components. *J. Power Sources* **2016**, *309*, 221–230.
230. Wohlfahrt-Mehrens, M.; Vogler, C.; Garche, J. Aging Mechanisms of Lithium Cathode Materials. *J. Power Sources* **2004**, *127*, 58–64.
231. Dai, K.; Wang, Z.; Ai, G.; Zhao, H.; Yuan, W.; Song, X.; Battaglia, V.; Sun, C.; Wu, K.; Liu, G. The Transformation of Graphite Electrode Materials in Lithium-Ion Batteries after Cycling. *J. Power Sources* **2015**, *298*, 349–354.
232. Andriunas, I.; Milojevic, Z.; Wade, N.; Das, P.K. Impact of Solid-Electrolyte Interphase Layer Thickness on Lithium-Ion Battery Cell Surface Temperature. *J. Power Sources* **2022**, *525*, 231126.
233. Waldmann, T.; Hogg, B.-I.; Wohlfahrt-Mehrens, M. Li Plating as Unwanted Side Reaction in Commercial Li-Ion Cells—A Review. *J. Power Sources* **2018**, *384*, 107–124.
234. Petzl, M.; Kasper, M.; Danzer, M.A. Lithium Plating in a Commercial Lithium-Ion Battery—A Low-Temperature Aging Study. *J. Power Sources* **2015**, *275*, 799–807.
235. Liu, Q.; Du, C.; Shen, B.; Zuo, P.; Cheng, X.; Ma, Y.; Yin, G.; Gao, Y. Understanding Undesirable Anode Lithium Plating Issues in Lithium-Ion Batteries. *RSC Adv.* **2016**, *6*, 88683–88700.
236. Collins, G.A.; Geaney, H.; Ryan, K.M. Alternative Anodes for Low Temperature Lithium-Ion Batteries. *J. Mater. Chem. A Mater. Energy Sustain.* **2021**, *9*, 14172–14213. <https://doi.org/10.1039/d1ta00998b>.
237. Broussely, M.; Biensan, P.; Bonhomme, F.; Blanchard, P.; Herreyre, S.; Nechev, K.; Staniewicz, R.J. Main Aging Mechanisms in Li Ion Batteries. *J. Power Sources* **2005**, *146*, 90–96.
238. Zhang, C. Deciphering Electrolyte Degradation. *Nat. Energy* **2019**, *4*, 1006.
239. Weber, W.; Kraft, V.; Grütze, M.; Wagner, R.; Winter, M.; Nowak, S. Identification of Alkylated Phosphates by Gas Chromatography-Mass Spectrometric Investigations with Different Ionization Principles of a Thermally Aged Commercial Lithium Ion Battery Electrolyte. *J. Chromatogr. A* **2015**, *1394*, 128–136.
240. Henschel, J.; Peschel, C.; Klein, S.; Horsthemke, F.; Winter, M.; Nowak, S. Clarification of Decomposition Pathways in a State-of-the-Art Lithium Ion Battery Electrolyte through <sup>13</sup>C-Labeling of Electrolyte Components. *Angew. Chem. Int. Ed.* **2020**, *59*, 6128–6137.
241. Dose, W.M.; Li, W.; Temprano, I.; O’Keefe, C.A.; Mehdi, B.L.; De Volder, M.F.L.; Grey, C.P. Onset Potential for Electrolyte Oxidation and Ni-Rich Cathode Degradation in Lithium-Ion Batteries. *ChemRxiv* **2022**, *7*, 3524–3530, <https://doi.org/10.1021/acseenergylett.2c01722>.
242. Li, A.; Yuen, A.C.Y.; Wang, W.; De Cacho Cordeiro, I.M.; Wang, C.; Chen, T.B.Y.; Zhang, J.; Chan, Q.N.; Yeoh, G.H. A Review on Lithium-Ion Battery Separators towards Enhanced Safety Performances and Modelling Approaches. *Molecules* **2021**, *26*, 478.
243. Abaza, A.; Ferrari, S.; Wong, H.K.; Lyness, C.; Moore, A.; Weaving, J.; Blanco-Martin, M.; Dashwood, R.; Bhagat, R. Experimental Study of Internal and External Short Circuits of Commercial Automotive Pouch Lithium-Ion Cells. *J. Energy Storage* **2018**, *16*, 211–217.
244. Liu, L.; Feng, X.; Rahe, C.; Li, W.; Lu, L.; He, X.; Sauer, D.U.; Ouyang, M. Internal Short Circuit Evaluation and Corresponding Failure Mode Analysis for Lithium-Ion Batteries. *J. Energy Chem.* **2021**, *61*, 269–280.
245. Feng, X.; Ouyang, M.; Liu, X.; Lu, L.; Xia, Y.; He, X. Thermal Runaway Mechanism of Lithium Ion Battery for Electric Vehicles: A Review. *Energy Storage Mater.* **2018**, *10*, 246–267.
246. Yuan, Z.; Xue, N.; Xie, J.; Xu, R.; Lei, C. Separator Aging and Performance Degradation Caused by Battery Expansion: Cyclic Compression Test Simulation of Polypropylene Separator. *J. Electrochem. Soc.* **2021**, *168*, 030506.
247. Kim, G.-H.; Pesaran, A.; Spontnitz, R. A Three-Dimensional Thermal Abuse Model for Lithium-Ion Cells. *J. Power Sources* **2007**, *170*, 476–489.
248. Kim, H.-K.; Kim, C.-J.; Kim, C.-W.; Lee, K.-J. Numerical Analysis of Accelerated Degradation in Large Lithium-Ion Batteries. *Comput. Chem. Eng.* **2018**, *112*, 82–91.
249. Arunachala, R.; Parthasarathy, C.; Jossen, A.; Garche, J. Inhomogeneities in Large Format Lithium Ion Cells: A Study by Battery Modelling Approach. *ECS Trans.* **2016**, *73*, 201–212.
250. Xie, Y.; Wang, S.; Li, R.; Ren, D.; Yi, M.; Xu, C.; Han, X.; Lu, L.; Friess, B.; Offer, G.; et al. Inhomogeneous Degradation Induced by Lithium Plating in a Large-Format Lithium-Ion Battery. *J. Power Sources* **2022**, *542*, 231753.
251. Zhou, S.; Zhang, X.; Chen, C.; Chen, M.; Kong, F.; Qiao, Y.; Wang, J. Uncovering the Degradation Mechanism Induced by Ion-Diffusion Kinetics in Large-Format Lithium-Ion Pouch Cells. *J. Energy Chem.* **2023**, *83*, 98–105.
252. Li, X.; Zeng, T.; Qin, H.; Huo, R.; Liu, Y.; Wei, D.; Ding, X. Investigation of Inhomogeneous Degradation in Large-Format Lithium-Ion Batteries. *J. Energy Storage* **2021**, *42*, 103113.
253. Zhu, X.; Revilla, R.I.; Jaguemont, J.; Van Mierlo, J.; Hubin, A. Insights into Cycling Aging of LiNi<sub>0.80</sub>Co<sub>0.15</sub>Al<sub>0.05</sub>O<sub>2</sub> Cathode Induced by Surface Inhomogeneity: A Post-Mortem Analysis. *J. Phys. Chem. C Nanomater. Interfaces* **2019**, *123*, 30046–30058.
254. Sieg, J.; Schmid, A.U.; Rau, L.; Gesterkamp, A.; Storch, M.; Spier, B.; Birke, K.P.; Sauer, D.U. Fast-Charging Capability of Lithium-Ion Cells: Influence of Electrode Aging and Electrolyte Consumption. *Appl. Energy* **2022**, *305*, 117747.

255. Li, R.; Ren, D.; Wang, S.; Xie, Y.; Hou, Z.; Lu, L.; Ouyang, M. Non-Destructive Local Degradation Detection in Large Format Lithium-Ion Battery Cells Using Reversible Strain Heterogeneity. *J. Energy Storage* **2021**, *40*, 102788.
256. Hou, M.; Hu, Y.; Zhang, J.; Cao, H.; Wang, Z. Development of Electrochemical-Thermal Modelling for Large-Format Li-Ion Battery. *Electrochim. Acta* **2020**, *347*, 136280.
257. Song, M.; Hu, Y.; Choe, S.-Y.; Garrick, T.R. Modeling and Analysis of Heat Generation Rate of a Large Format Pouch-Type Lithium-Ion Battery Considering Degradation. *J. Electrochem. Soc.* **2022**, *169*, 070502.
258. Kim, G.-H.; Smith, K.; Lee, K.-J.; Santhanagopalan, S.; Pesaran, A. Multi-Domain Modeling of Lithium-Ion Batteries Encompassing Multi-Physics in Varied Length Scales. *J. Electrochem. Soc.* **2011**, *158*, A955.
259. Sturm, J.; Spingler, F.B.; Rieger, B.; Rheinfeld, A.; Jossen, A. Non-Destructive Detection of Local Aging in Lithium-Ion Pouch Cells by Multi-Directional Laser Scanning. *J. Electrochem. Soc.* **2017**, *164*, A1342–A1351.
260. Sauerteig, D.; Ivanov, S.; Reinshagen, H.; Bund, A. Reversible and Irreversible Dilatation of Lithium-Ion Battery Electrodes Investigated by in-Situ Dilatometry. *J. Power Sources* **2017**, *342*, 939–946.
261. Li, R.; Ren, D.; Guo, D.; Xu, C.; Fan, X.; Hou, Z.; Lu, L.; Feng, X.; Han, X.; Ouyang, M. Volume Deformation of Large-Format Lithium Ion Batteries under Different Degradation Paths. *J. Electrochem. Soc.* **2019**, *166*, A4106–A4114.
262. Chen, H.; Fan, J.; Zhang, M.; Feng, X.; Zhong, X.; He, J.; Ai, S. Mechanism of Inhomogeneous Deformation and Equal-Stiffness Design of Large-Format Prismatic Lithium-Ion Batteries. *Appl. Energy* **2023**, *332*, 120494.
263. Truchot, C.A. Study of State-Of-Charge and Degradation in Lithium Ion Battery Pack. Ph.D. Thesis, University of Hawaii at Manoa, Honolulu, HI, USA, 2012.
264. Martinez-Laserna, E.; Sarasketa-Zabala, E.; Stroe, D.-I.; Swierczynski, M.; Warnecke, A.; Timmermans, J.M.; Goutam, S.; Rodriguez, P. Evaluation of Lithium-Ion Battery Second Life Performance and Degradation. In Proceedings of the 2016 IEEE Energy Conversion Congress and Exposition (ECCE), Milwaukee, WI, USA, 18–22 September 2016; pp. 1–7.
265. Martinez-Laserna, E.; Sarasketa-Zabala, E.; Villarreal Sarria, I.; Stroe, D.-I.; Swierczynski, M.; Warnecke, A.; Timmermans, J.-M.; Goutam, S.; Omar, N.; Rodriguez, P. Technical Viability of Battery Second Life: A Study from the Ageing Perspective. *IEEE Trans. Ind. Appl.* **2018**, *54*, 2703–2713.
266. Sarasketa-Zabala, E.; Gandiaga, I.; Rodriguez-Martinez, L.M.; Villarreal, I. Calendar Ageing Analysis of a LiFePO<sub>4</sub>/Graphite Cell with Dynamic Model Validations: Towards Realistic Lifetime Predictions. *J. Power Sources* **2014**, *272*, 45–57.
267. Olsson, L.; Fallahi, S.; Schnurr, M.; Diener, D.; Van Loon, P. Circular Business Models for Extended EV Battery Life. *Batteries* **2018**, *4*, 57.
268. Li, Y.; Liu, K.; Foley, A.M.; Zülke, A.; Berecibar, M.; Nanini-Maury, E.; Van Mierlo, J.; Hoster, H.E. Data-Driven Health Estimation and Lifetime Prediction of Lithium-Ion Batteries: A Review. *Renew. Sustain. Energy Rev.* **2019**, *113*, 109254.
269. Bonfitto, A.; Ezemobi, E.; Amati, N.; Feraco, S.; Tonoli, A.; Hegde, S. State of Health Estimation of Lithium Batteries for Automotive Applications with Artificial Neural Networks. In Proceedings of the 2019 AEIT International Conference of Electrical and Electronic Technologies for Automotive (AEIT AUTOMOTIVE), Turin, Italy, 2–4 July 2019; IEEE: Piscataway, NJ, USA, 2019.
270. Hossain Lipu, M.; Karim, T.; Ansari, S.; Miah, M.; Rahman, M.; Meraj, S.; Elavarasan, R.; Vijayaraghavan, R. Intelligent SOX Estimation for Automotive Battery Management Systems: State-of-the-Art Deep Learning Approaches, Open Issues, and Future Research Opportunities. *Energies* **2022**, *16*, 23.
271. Shrivastava, P.; Soon, T.K.; Idris, M.Y.I.B.; Mekhilef, S.; Adnan, S.B.R.S. Model-based State of X Estimation of Lithium-ion Battery for Electric Vehicle Applications. *Int. J. Energy Res.* **2022**, *46*, 10704–10723.
272. Li, S.; Fang, H.; Shi, B. Remaining Useful Life Estimation of Lithium-Ion Battery Based on Interacting Multiple Model Particle Filter and Support Vector Regression. *Reliab. Eng. Syst. Saf.* **2021**, *210*, 107542.
273. Gao, D.; Zhou, Y.; Wang, T.; Wang, Y. A Method for Predicting the Remaining Useful Life of Lithium-Ion Batteries Based on Particle Filter Using Kendall Rank Correlation Coefficient. *Energies* **2020**, *13*, 4183.
274. Hell, S.M.; Kim, C.D. Development of a Data-Driven Method for Online Battery Remaining-Useful-Life Prediction. *Batteries* **2022**, *8*, 192.
275. Gao, K.; Xu, J.; Li, Z.; Cai, Z.; Jiang, D.; Zeng, A. A Novel Remaining Useful Life Prediction Method for Capacity Diving Lithium-Ion Batteries. *ACS Omega* **2022**, *7*, 26701–26714.
276. Chen, L.; An, J.; Wang, H.; Zhang, M.; Pan, H. Remaining Useful Life Prediction for Lithium-Ion Battery by Combining an Improved Particle Filter with Sliding-Window Gray Model. *Energy Rep.* **2020**, *6*, 2086–2093.
277. Zhang, D.; Dey, S.; Perez, H.E.; Moura, S.J. Remaining Useful Life Estimation of Lithium-Ion Batteries Based on Thermal Dynamics. In Proceedings of the 2017 American Control Conference (ACC), Seattle, WA, USA, 24–26 May 2017; IEEE: Piscataway, NJ, USA, 2017.
278. Wu, Y.; Li, W.; Wang, Y.; Zhang, K. Remaining Useful Life Prediction of Lithium-Ion Batteries Using Neural Network and Bat-Based Particle Filter. *IEEE Access* **2019**, *7*, 54843–54854.
279. Su, C.; Chen, H.J. A Review on Prognostics Approaches for Remaining Useful Life of Lithium-Ion Battery. *IOP Conf. Ser. Earth Environ. Sci.* **2017**, *93*, 012040.
280. Chen, L.; Xu, L.; Zhou, Y. Novel Approach for Lithium-Ion Battery on-Line Remaining Useful Life Prediction Based on Permutation Entropy. *Energies* **2018**, *11*, 820.
281. Pan, C.; Huang, A.; He, Z.; Lin, C.; Sun, Y.; Zhao, S.; Wang, L. Prediction of Remaining Useful Life for Lithium-ion Battery Based on Particle Filter with Residual Resampling. *Energy Sci. Eng.* **2021**, *9*, 1115–1133.

282. Wang, S.; Jin, S.; Deng, D.; Fernandez, C. A Critical Review of Online Battery Remaining Useful Lifetime Prediction Methods. *Front. Mech. Eng.* **2021**, *7*, 719718. <https://doi.org/10.3389/fmech.2021.719718>.
283. Hu, X.; Xu, L.; Lin, X.; Pecht, M. Battery Lifetime Prognostics. *Joule* **2020**, *4*, 310–346.
284. Matsuda, T.; Ando, K.; Myojin, M.; Matsumoto, M.; Sanada, T.; Takao, N.; Imai, H.; Imamura, D. Investigation of the Influence of Temperature on the Degradation Mechanism of Commercial Nickel Manganese Cobalt Oxide-Type Lithium-Ion Cells during Long-Term Cycle Tests. *J. Energy Storage* **2019**, *21*, 665–671.
285. Pelletier, S.; Jabali, O.; Laporte, G.; Veneroni, M. Battery Degradation and Behaviour for Electric Vehicles: Review and Numerical Analyses of Several Models. *Trans. Res. Part B Methodol.* **2017**, *103*, 158–187.
286. Preger, Y.; Barkholtz, H.M.; Fresquez, A.; Campbell, D.L.; Juba, B.W.; Romàn-Kustas, J.; Ferreira, S.R.; Chalamala, B. Degradation of Commercial Lithium-Ion Cells as a Function of Chemistry and Cycling Conditions. *J. Electrochem. Soc.* **2020**, *167*, 120532.
287. Zhu, S.; Hu, C.; Xu, Y.; Jin, Y.; Shui, J. Performance Improvement of Lithium-Ion Battery by Pulse Current. *J. Energy Chem.* **2020**, *46*, 208–214.

**Disclaimer/Publisher’s Note:** The statements, opinions and data contained in all publications are solely those of the individual author(s) and contributor(s) and not of MDPI and/or the editor(s). MDPI and/or the editor(s) disclaim responsibility for any injury to people or property resulting from any ideas, methods, instructions or products referred to in the content.